

Reeja Johnson “Structural, corrosion inhibition and biological investigations of schiff bases containing sulphur and their metal chelates.” Thesis. Research and postgraduate department of chemistry, St. Thomas’ college (autonomous), University of Calicut, 2021.

*PART I*

*SYNTHESIS AND  
CHARACTERIZATION*

## CHAPTER 1

### INTRODUCTION AND REVIEW

Sulphur, is a nonmetal and one of the first ten most abundant elements in universe. There are not much compounds which got a mention in the Bible. Of the fifteen compounds which were established during that time, sulphur, is clearly mentioned in the the context of the destruction of Sodom and Gomorrah.

*"On the wicked he will rain fiery coals and burning sulfur; a scorching wind will be their lot."* – Genesis 19:24

This again establishes the significance of the element sulphur. Sulphur's natural occurrence is often associated with hot springs or volcanoes as a stinky yellow material which relates it to hellfire and wrath. The element was isolated in its pure form in 1809 by Louis-Joseph Gay-Lussac and Louis-Jacques Thénard. There exists several allotropes of sulphur and most common form appears as yellow powder or even crystals. It is considered to be one of the most important inorganic element; it is incorporated into proteins, enzymes, vitamins, amino acids, and other crucial biomolecules. It is used as a fungicide, fumigant, in the vulcanization of rubber and in explosives. Most of the element produced goes into the production of sulfuric acid.

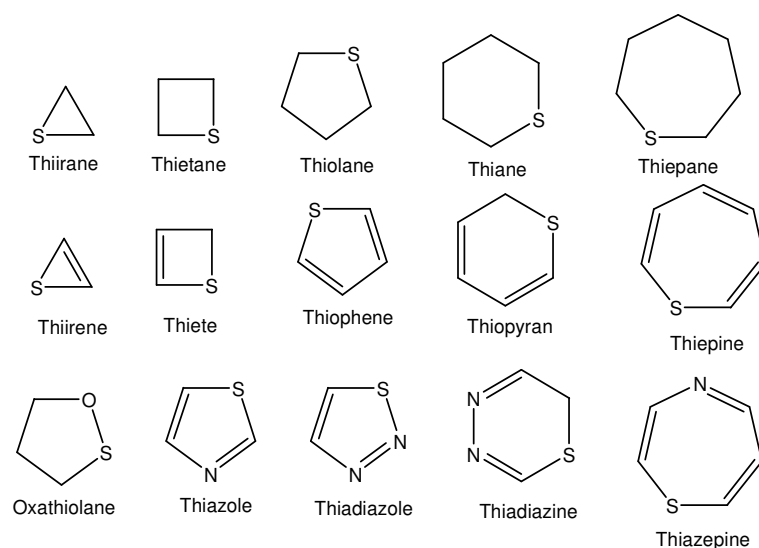
#### **Sulphur Compounds- An Outlook**

In all living things, sulphur compounds are present and they can be divided into two groups: the essential primary metabolites and the non-essential secondary metabolites. A wide variety of compounds, ranging from simple gases to complex polycyclic aromatics, constitute the family of sulfur compounds, both of biogenic and anthropogenic origin. These compounds can be observed in numerous, typically complex matrices, such as air (gas), water (aqueous systems), different fractions of petroleum

(gas, liquid and solid), beverages, foodstuffs and pharmaceutical formulations. Gas fumigants used as insecticides are sulfur-containing compounds such as carbonyl sulphide and sulfuryl fluoride. They have been developed to substitute methyl bromide, the ozone-depleting insecticide. Vikane, Zythor, Termafume, sulfuryl fluoride fumigant, sulfuryl fluoride (Master fume) and Dow AgroSciences/Profume gas fumigants include sulfuryl fluoride (CAS no.2699-79-8) as the active ingredient. The reduction of sulfoxides into their corresponding sulfides utilizes a variety of Sulfur-containing compounds.

### Sulphur Heterocycles

Heterocycles constitute a vast area of research in both organic and inorganic chemistry. They play a key role in biochemical processes since the side groups and active sites of many living cells comprise of aromatic heterocycles, eg: DNA, RNA and various enzymes [1]. Literature survey reveal that if sulphur containing heterocyclic molecules act as ligands, they are well known for its pharmacological actions include anticancer, antimicrobial, antiviral, antitubercular anti-inflammatory etc. and the most commonly found motifs in sulfur containing drugs are thiadiazole, thiazole, isothiazole, thiophene, thiopyran, thiazepine and thiazolidine.

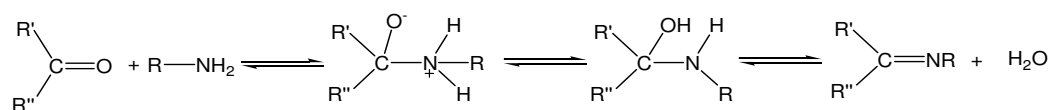


These S-heterocycles, compared to the N-heterocycles, are less reported but have enhanced prospects in pharmaceutical industry due to their superior therapeutic potential. This is also as a result of the improvements in the feasible synthesis reported recently. The field of S-heterocyclic demands much higher attention to counteract the issues of toxicity and various pathological targets.

### Schiff Base Ligands

Schiff bases are named after Hugo Schiff, and is a nitrogen analogue of carbonyl compounds like aldehydes or ketones in which carbonyl (C=O) is replaced by an azomethine or imine group. Schiff base (SB) ligands are one of the most commonly used ligands because of their ease of formation and remarkable flexibility. Schiff bases, the versatile pioneer for organic synthesis and later researches proved that it has wide variety of applications in pharmaceutical fields and that was due to the biological activities expressed. Aromatic Schiff bases have shown more potential in activity due to free electron delocalization within the ring structure. Likewise Schiff base derived from heterocyclic ring containing sulphur atom also showed more advantage in this regard.

The general synthetic method involves the condensation of primary amines with a carbonyl precursor usually in an alcoholic medium or on reflux conditions. This reversible reaction proceeds via a carbinolamine intermediate produces water as an additional product and provides excellent yield. The reaction is acid catalyzed and the products resulting from these reactions features an imine or an azomethine group (C=N) and is commonly called a Schiff base.



The majority of the heterocyclic SB ligands comprise N, O, P and S. Heterocyclic Schiff base containing sulphur atom shows impressive biological activities due to the

presence of aromatic ring containing the highly polarisable sulphur atom. Various publications had covered the antibacterial, anticancer, antifungal, anti-inflammatory and antiviral properties, hence researches had proved that Schiff bases containing heteroatoms especially sulphur atoms are highly potential drugs [2]. Making certain modification in the structure of Schiff base by thiadiazole and thiazole moieties, its would influence on biological activity may be improved. A versatile moiety, thiadiazole attracted as a privileged scaffold because of its potential therapeutic significance [3]. Superior liposolubility and mesoionic character of thiadiazole moiety are due to the presence of sulphur in the thiadiazole ring that allows them to move across the cell membrane and facilitating the interaction with biological targets. Diverse applications of thiadiazole derivatives and their varying pharmacological activities like antidepressants [4], anticancer [5], antidiabetic [6], antianxiety [7], antiviral [8], antifungal [9], antimicrobial [10], anti-inflammatory [11], anticonvulsant [12], anti-tubercular [13] etc., have attracted widespread attention in the recent years. Many drugs containing thiadiazole derivatives such as sulphamethoxazole, acetazolamide, cefazoline and methazolamide are available in the market [14]. Previous studies indicate that the biological activity exhibited by the thiadiazole ring system is due to the presence of N=C-S bonding where the sulphur atom acts as hydrogen binding domain and two nitrogen atoms are electron donors [15].

It is interesting to investigate sulphur containing Schiff bases which have broad applications in pharmaceutical fields. Computer-based drug discovery is the most appreciable method in the field of pharmaceuticals. More efficient approach in drug discovery is examining the effectiveness of the drug for a specific disease by studying the type of interactions between the target protein and the drug at its molecular level.

Accurate fast docking protocol and visualizing ability of the binding geometries

and drug-protein interactions increases the systematic understanding of ligand-receptor complex strength, bond length and structural principles. Proteins associated with specific diseases are identified by understanding the mechanistic aspects of causing diseases. For a systematic understanding of the structural principles that establish the strength of a ligand/protein complex both, an accurate and fast docking protocol and the ability to visualize binding geometries and interactions are mandatory. Here we present an interface between the popular molecular graphics system PyMOL and the molecular docking suites Autodock and Vina and demonstrate how the combination of docking and visualization can aid structure-based drug design efforts [16].

One of the most outstanding applications of Schiff bases are their use as an efficient corrosion inhibitor and it is mainly based on its ability to get adsorbed on the surface to be protected spontaneously to form a monolayer. Organic molecules having electron lone pairs on the heteroatoms such as P, S, N and O atoms have proved, both theoretically and practically, that they can perform as admirable corrosion inhibitors in aggressive solutions by improved adsorption on the metal surface [17]. Different Schiff base ligands have been used as carriers of cation in potentiometric sensors because they have exhibits excellent sensitivity, stability and selectivity for specific metal ions [18–21].

### **Transition Metal Complexes**

The modern studies of metal complexes begin with the work of Werner and Jorgenson. In 1893, Werner put forward his famous theory of coordination to explain the formation and structures of complex compounds. In recognition of his work in this field; he was awarded the Nobel Prize in 1913 in chemistry. Werner is rightly called the father of coordination chemistry. Sixty years later in 1973, E.O. Fischer and G. Wilkinson shared the Nobel Prize for their work on Ferrocene. As more complexes were discovered

in the 19<sup>th</sup> century, numerous theories were arised to account the formation of metal complexes and its properties. Later, more reliable explanation regarding the structure, formation and stability of complexes was given by valence bond theory (VBT), crystal field theory (CFT), ligand field theory (LFT) and molecular orbital theory (MOT). A sudden change in solubility, drop in conductivity or colour change indicates the formation of complex between a metal ion and ligand. According to Werner a metal ion tries to satisfy both its primary and secondary valencies. The secondary valencies are directed towards fixed positions in space so that each complex possesses a definite stereochemistry. Now majority of research papers being published every year in inorganic chemistry are on coordination chemistry. The scope of the subject is due to the various applications of coordination compounds in science and industry.

The use of coordination compounds in medicinal field is inevitable. Complexes of transition metals can be used in MRI scan. Cis platinum complexes for the treatment of cancer and gold complexes are used for the treatment of arthritis. Barium sulphate and triiodobenzene moiety can be applied in gastrointestinal tract imaging. Many catalytic enzymes in living systems are coordination compounds. Coordination compounds are involved in processes like photosynthesis, nitrogen fixation, oxygen transport etc.

### **Schiff Base Complexes**

They played an important role in the development of coordination chemistry. Free Schiff base have heteroatom show biological activity whereas in metal complexes with such ligands show better activity than free ligand because of chelation. With majority of transition metals, they readily form stable complexes. Bioinorganic chemistry, catalysis, and magnetochemistry are potential interdisciplinary avenues including their applications. Synthetic models for the metal-containing sites in metalloproteins and enzymes are often provided by the metal complexes supported by



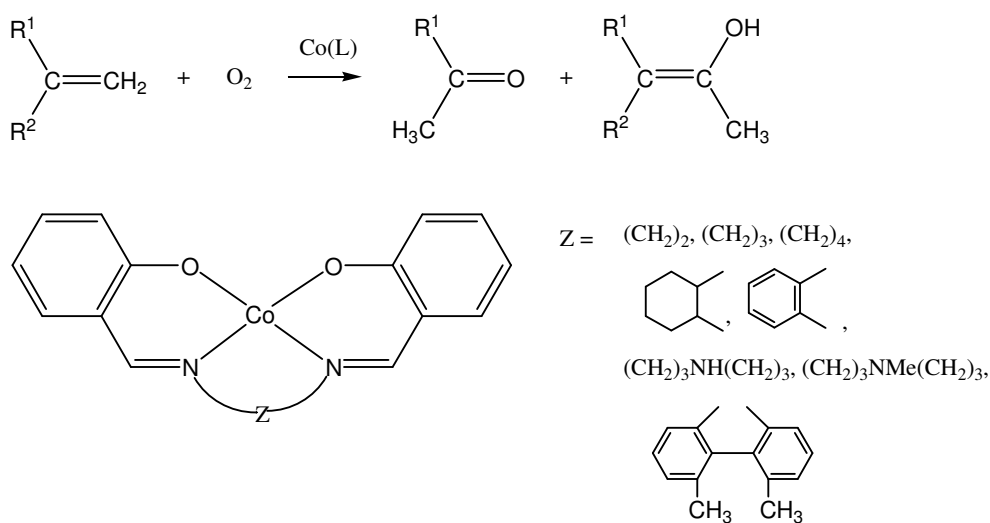
SB ligands. Yamanda *et al.* has reviewed the developments in stereochemistry of metal complexes prepared by Schiff base ligands [22]. A number of Schiff base macrocycles have been utilized as metal containing liquid crystal polymers. They are also used as odouring agents, superconductors and for the formulation of semiconductors. Currently several Schiff-base complexes have been explored as effective scavengers of reactive oxygen species (ROS) and they act as efficient antioxidants [23].

Metal complexes are important constituents of industrial processes in pharma, industrial and agricultural chemistry. Schiff bases by virtue of their lone pairs and azomethine moieties are capable of coordinating to metals and form complexes. These complexes find use in many fields including catalysis, industrial processes and various biological uses as antimicrobial, antifungal, antibacterial, insecticidal, anti-inflammatory, antitumor and cytotoxic agents. They are also useful as dyes and enzymatic regulatory agents.

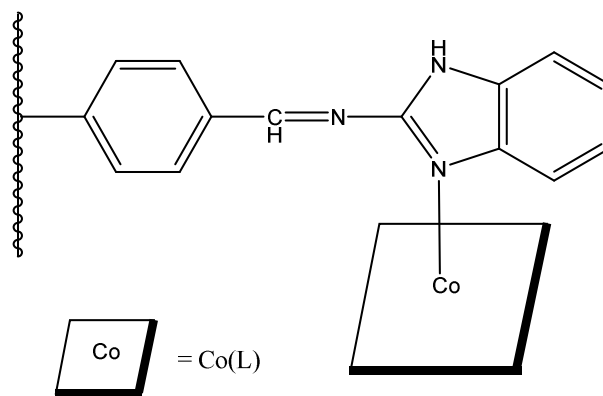
The chelating properties of ligands are used to transport across membranes or to attach to specific site, thus it can hinder the growth of the organism. The antibacterial activity is based on the selective toxicity of agents on the microbial cells. In transition metal complexes with ligand Schiff base i.e., azomethine group possess (C=N) bond, positive charge of metal ion is partially shared among hetero atoms (S, N and O) present in the Schiff base ligand. Due to the presence of lone pair of electrons in it cause delocalization of  $\pi$ -electrons over the whole chelating system. Hence this increase the lipophilic character of metal complexes which favours its permeation through the lipid layer of the bacterial membrane and inhibiting metal binding sites in enzymes of that organism and finally, inhibit its growth.

Due to synthetic flexibility and relative easiness in synthesis, Schiff base complexes are very much interesting in the field of fundamental and applied research. In

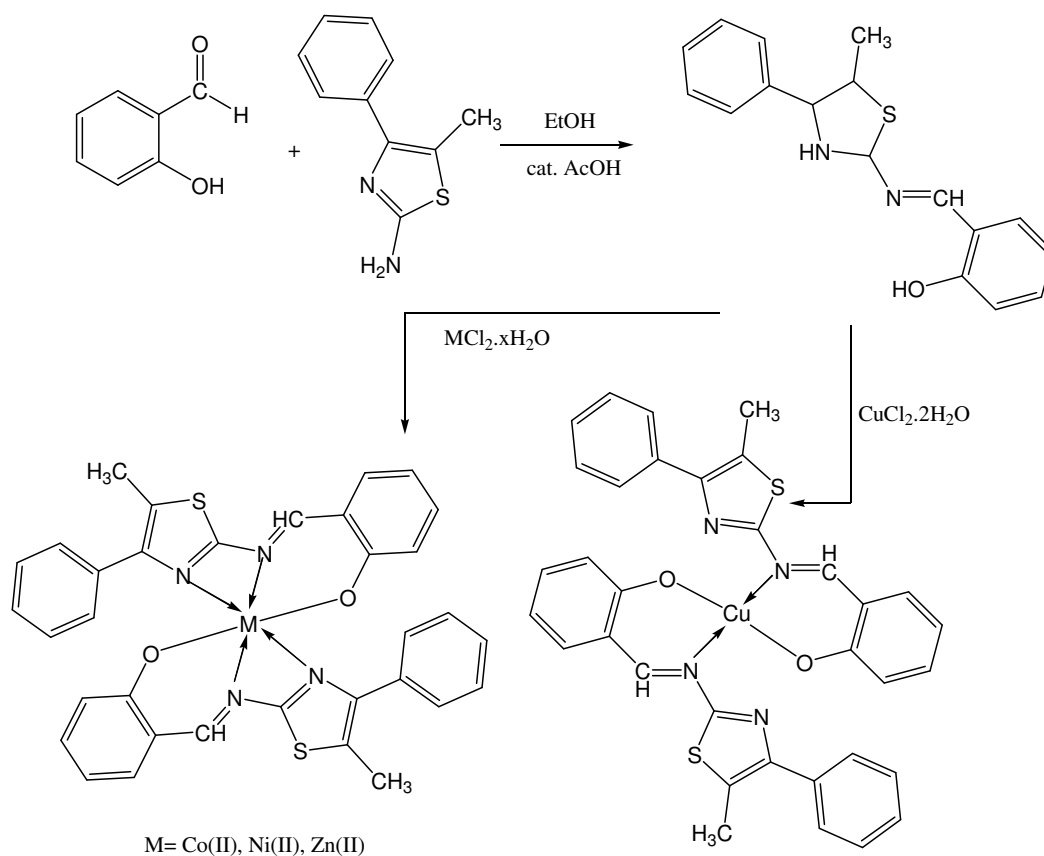
magnetochemistry, dinuclear SB complexes demonstrate and facilitate the study of the exchange coupling process between two metal ions. Chiral SB complexes have also been shown to be excellent catalysts for certain organic reactions. They have also been used as catalysts for small molecules activation. Tetra coordinate cobalt(II) Schiff base complexes can catalyze mono oxygenation of alkenes in primary or secondary alcohols under atmospheric oxygen pressure at 60°C, without a carbon-carbon bond cleavage. This happens via proposed mechanism which involves the decomposition of a benzylalcoholato cobalt(III) complex [24].



Low spin cobalt(II) square pyramidal complexes were reported from a polymer based Schiff base ligand derived from crosslinked polystyrene bound benzaldehyde and 2-aminobenzimidazole coordinated to a [Co(TPP)] (TPP= *meso*-tetraphenylporphyrin) and tetrahedral complexes of cobalt. The resulted complexes all exhibited square pyramidal structures irrespective of square planar or tetrahedral structure of starting material [25].



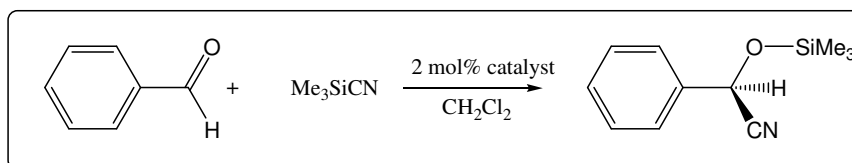
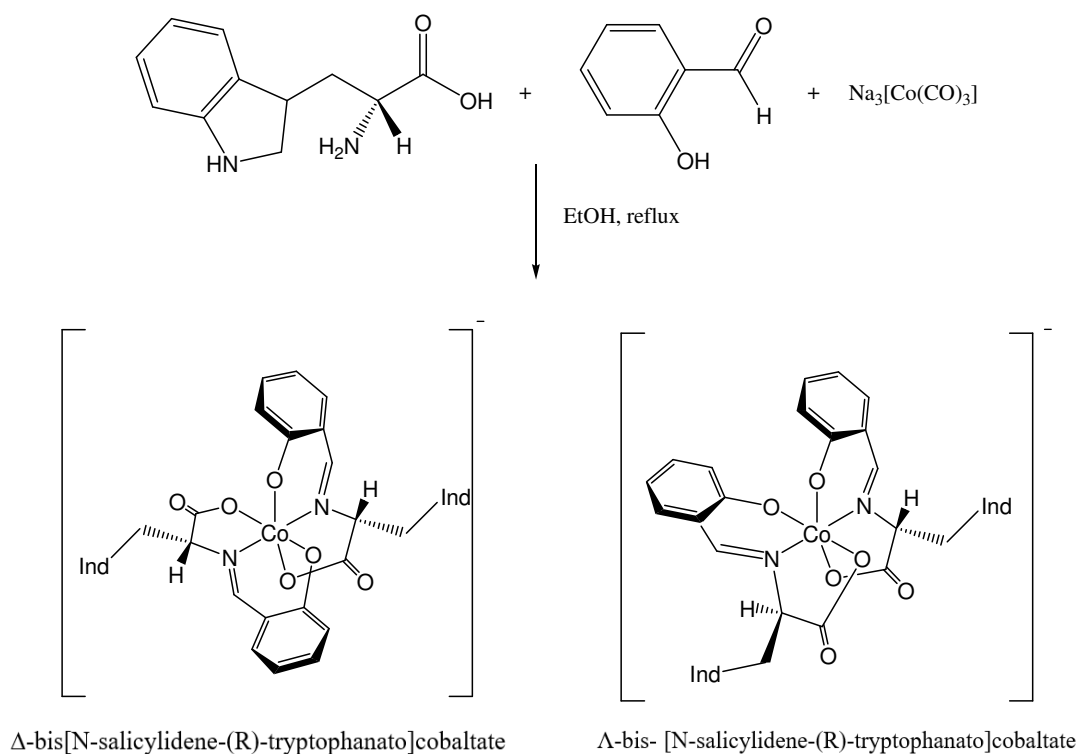
Salicylaldehyde and 2-amino-4-phenyl-5-methyl thiazole was subjected to a condensation reaction in ethanol solution in presence of a few drops of glacial acetic acid resulting in the formation of a Schiff base ligand.



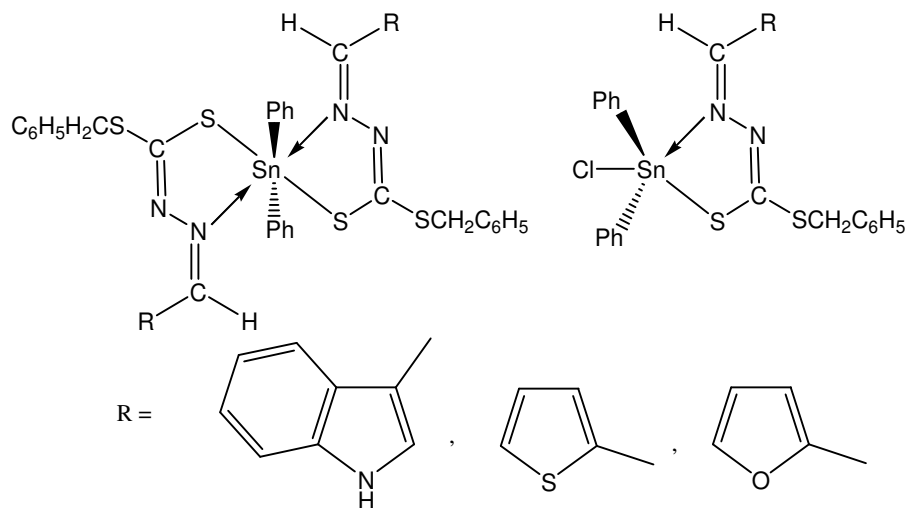
This ligand was in turn utilized to synthesize Cu, Ni, Co, Zn(II) complexes via reactions of  $\text{CuCl}_2 \cdot 2\text{H}_2\text{O}$ ,  $\text{NiCl}_2 \cdot 6\text{H}_2\text{O}$ ,  $\text{CoCl}_2 \cdot 6\text{H}_2\text{O}$ , and  $\text{ZnCl}_2$  in ethanol-reflux

conditions. Zn(II) complex exhibited anticancer activity against MCF-7, HepG2, A549 and HCT116 cell lines. Molecular docking studies were also conducted against tyrosine kinases receptor (PDB1t46) [26].

A Co(III) chiral complex supported by a Schiff base comprised from tryptophan and salicylaldehyde was reported to catalyze the trimethylsilylcynylation of benzaldehyde. (R)-tryptophan was used in the synthesis of ligand. The reaction of this ligand with  $\text{Na}_3[\text{Co}(\text{CO})_3]$  yielded a mixture of diastereomeric complexes  $\Delta$ -bis-[N-salicylidene-(R)-tryptophanato]cobaltate sodium and  $\Delta$ -bis[N-salicylidene-(R)-tryptophanato]cobaltate sodium. The counter cations were substituted by other metal ions and the complexes exhibited catalytic activity [27].



Bidentate Schiff base ligands with sulphur and nitrogen donors were synthesized via condensation of heterocyclic aldehydes with S-benzylthiocarbazate. These ligands on reaction with diphenyltin dichloride afforded Sn(IV) organometallic complexes.



The anti-bacterial and anti-fungal properties were screened for both the complexes and free ligands in which the complexes showed higher inhibitory action. This was proposed due to the metal chelation and solubility [28].

### Transition Metal Complexes of Schiff Bases –A Review

The versatile compounds, Schiff bases and their complexes exhibit a broad range of catalytical activities, corrosion inhibition activities and pharmaceutical activities including anticancer, antimalarial, antibacterial, antifungal, antiproliferative, antipyretic antiviral, anti-inflammatory properties. The influence of metals on their intrinsic chemical interest as multidentate ligands and the biological activity of these compounds has encouraged a considerable increase in their coordination behaviour investigations.

In 1990, N. K. Rao and M. R. Reddy synthesized Co(II), Ni(II) and Zn(II) complexes with indane-1,3-dione-2-imine-N-acetic acid, an intermediate Schiff base obtained by the condensation of glycine and ninhydrin [29]. IR, NMR, electronic spectrum, magnetic susceptibility, elemental analysis, thermogravimetric

analyses/differential thermal analysis and molar conductivity studies evaluated these coloured complexes and put forward a mechanism for their formation. The nature of Schiff base as a monobasic tridentate ligand whereas its complexes possess octahedral stereochemistry in this case. A comparative antimicrobial study was done with the complexes and ninhydrin against *Staphylococcus aureus*, *Streptococcus faecalis*, *Escherichia coli* and *Proteus mirabilis*.

In 2007, N. Raman, et al. synthesized transition metal complexes of Hg(II), Mn(II), Cu(II), VO(IV), Zn(II), Co(II), Cd(II) and Ni(II) from Schiff base derivative of 3-hydroxy-4-nitrobenzaldehyde, 4-aminoantipyrine and o-phenylenediamine [30]. Structural features of these complexes were studied from their IR, UV-Vis, <sup>1</sup>H NMR, elementary analyses, ESR spectrum and magnetic susceptibility. Cyclic voltammetry studies explained the redox behaviour of vanadyl and copper complexes and these complexes showed good results in antimicrobial screening tests. From the nuclease activity study of these complexes reveals that Ni(II), Cu(II) and Co(II) complexes cleave DNA by redox chemistry whereas others not.

In 2008, Monica Soni and A. P. Mishra synthesized new bidentate/tridentate Schiff bases and their Co(II) and VO(II) complexes by the condensation reaction of 2-hydroxyacetophenone with nicotinamide (han)/isoniazide (hai) and methyl isobutyl ketone with nicotinamide (mna)/2-amino-4-chlorophenol (map). Structure of the complexes were determined by physicochemical studies [31]. From the thermal data and FAB mass, degradation pattern of the complexes were obtained. XRD analysis showed the results that these complexes crystallized as a tetragonal crystal system. Well diffusion technique is used to evaluate antimicrobial activity of the complex using DMSO as a solvent on different bacteria/fungi *A. niger*, *E. coli*, *S. fecalis*, *T. polysporum* and

*S. aureus*. The studies concluded that metal chelation affects the antimicrobial activity of all complexes and they have better antimicrobial activity than free ligands

In 2009, R.D. Deshmukh, et al. synthesized novel Schiff base from glycine and 2-hydroxy-5-methyl acetophenone and its coordination with metals like Cd(II), Mn(II), Co(II), Zn(II), Fe(II), Ni(II), UO<sub>2</sub>(VI), Cu(II) results a series of new transition metal complexes [32]. Characterization of the ligand and complexes done on the basis of magnetic susceptibility measurements, electrical conductance, analytical measurements, ESR, IR, electronic spectra and thermogravimetric analysis. In all the complexes, ligand behaves as a dibasic tridentate –ONO- donor, but in Zn(II) complex, the ligand behaves as monobasic bidentate –OO- donor. In the range, 313–398 K, DC electrical conductivity of ligand and its complexes the solid state have been measured and found that complexes were semiconducting. Various Gram (+) and Gram (–) bacterial strains are used for screening studies of the ligand and complexes.

In 2011, Mehmet Tümer, et al. synthesized Pd(II), Cu(II), Ni(II), Co(II) and Ru(III) metal complexes with two Schiff base ligands (HL<sub>1</sub> and HL<sub>2</sub>). By analytical and spectroscopic methods these complexes were characterized [33]. Using cyclohexane as substrate, metal complexes alkane oxidation activities were studied. These complexes were checked for their antimicrobial performance against *Bacillus cereus*, *Micrococcus luteus*, *Bacillus brevis*, *Bacillus megaterium*, *Staphylococcus aureus*, *Enterococcus faecalis*, *Corynebacterium xerosis* and *Mycobacterium smegmatis* (Gram-positive bacterias) and *Saccharomyces cerevisiae*, *Pseudomonas aeruginosa*, *Yersinia enterocolitica*, *Klebsiella fragilis*, *Escherichia coli*, *Candida albicans* and *Klebsiella pneumonia* (Gram-negative bacterias). Thermal and electrochemical properties of these complexes are also studied. By using reducing power action of superoxide anion radical

generated in non-enzymatic systems and free radical scavenging by DPPH (1,1-diphenyl-2-picrylhydrazyl), the antioxidant properties of Schiff base ligands were also evaluated.

In 2012, Zhang et al. synthesized transition metal coordination complexes  $Zn(C_{18}H_{16}N_3O_2)_2 \cdot 2CH_3CH_2OH$ ,  $Cu(C_{18}H_{16}N_3O_2)_2 \cdot 2CH_3OH$ , and  $Cd(C_{18}H_{16}N_3O_2)_2 \cdot 2CH_3OH$  derived from the same ligand of L-tryptophan and 2-acetylpyridine are prepared and investigated the anticancer performances on MDA-MB-231 breast cancer cells. All three complexes can inhibit the cellular proliferation, but Cd-complex showed highest anti-proliferative activity. In addition to this, the same complex can inhibit proteasomal chymotrypsin like activity. [34]

In 2013, A. Kiruthika, et al. synthesized Schiff base ligands from acetylacetone/2-hydroxynaphthaldehyde/isatin with salicylaldehyde and o-phenylene diamine and Fe(III) complexes were synthesized [35]. These were characterized by different spectral studies and analytical techniques. From the spectral data, octahedral geometry is assigned to Fe(III) complexes and these complexes were converted to its nano metal oxides. Using 3D modelling molecular picture, the possible geometries of complexes were evaluated. The results of antibacterial investigations show that they are excellent antibacterial and antifungal agents with their MIC values 62.5 and 125 $\mu$ g / litre.

In 2013, Shakuntala. M synthesized new Schiff base ligand from 2-hydroxy-1-naphthaldehyde with 8-amino 2-naphthol, 1, 8-diaminonaphthalene, and 4-Bromo-1-naphthylamine, 5-amino-1-naphthol [36]. The ligand and its complexes with Zn(II), Cu(II), Ni(II), Mn(II) and ions characterized by using electronic and IR spectra, elementary analysis, cyclic voltammetry,  $^1H$  NMR, molar conductance, thermal and magnetic analysis. The ligands and complexes tested for their antimicrobial activity against one positive bacterium (*Klebsiella pneumonia*) and two negative bacterias (*Staphylococcus aureus* and *Escherichia coli*). Comparison between zones of inhibition



of complexes and ligands shows that complexes have higher activity than ligands. From the studies, concluded that the antibacterial activity is dependent on the molecular structure of the compound, solvent used and bacterial strains under consideration.

In 2014, K.R. Joshi, et al. synthesized nickel(II) and copper(II) complexes with Schiff bases 2-((3,4-difluorophenylimino)methyl)-6-methoxy-4-nitrophenol and 2-((2,4-dimethylphenylimino)methyl)-6-methoxy-4-nitrophenol [37]. The above Schiff bases are derived from the condensation reaction of 2,4-dimethylaniline/ 3,4-difluoroaniline with 2-hydroxy-3-methoxy-5-nitrobenzaldehyde. Characterization of these ligands and their metal complexes was done by IR,  $^1\text{H}$  NMR, electronic, mass spectra and TG analysis. Using Broth dilution method, these Schiff bases and their metal complexes were checked for antimicrobial activity against *Streptococcus pyogenes*, *Staphylococcus aureus*, *Pseudomonas aeruginosa*, *Escherichia coli*, *Aspergillus clavatus*, *Candida Albicans* and *Aspergillus niger*. Results shows that metalation increases with chelation.

In 2015, A. Pradhan et al. carried out a review based on the Schiff bases derived from 2-aminobenzthiazole, 4-aminobenzene, sulphonamide, 4-aminophenol, 4-amino salicylic acid, semicarbazide, aniline, 4-aminoantipyrine, thiosemicarbazide, o-phenyl enediamine, 2-aminopyrazine, 2-aminothiophenol, s-benzylthiocarbamate and p-anisidine and its complexes Co(II), Ni(II), Cu(II), Mn(II), Zn(II), Cd(II), Hg(II), VO(II), Pt(II), Pd(II), U(IV), Sb(II) and ZrO(II) [38]. Antimicrobial activity of the Schiff bases and the complexes were also discussed

In 2016, Geetha Kannappan and S. Syed Tajudeen synthesized Schiff Base–copper(II) complex. Their work includes synthesis, spectral characterization of Schiff base complexes of pyrazinamide (an anti-tubercular drug), isoniazid, nicotinohydrazide and benzhydrazide with benzaldehyde and dimethoxybenzaldehyde [39]. The copper complexes synthesized and isolated in powdered form and their 1:1 electrolytic nature

obtained from molar conductance values. Analytical data agreed that they have the composition of type  $[L_2CuClO_4]ClO_4$ . The stoichiometry and analytical data were further supported by magnetic susceptibility, mass spectrometry-liquid chromatography, Fourier transform infrared spectra, electronic spectra, electron paramagnetic resonance studies and cyclic voltammetry. They also made a preliminary attempt to compare the potencies of complexes with parent drug and significant results are obtained from copper(II) complexes.

In 2017, Hmeed, et al. carried out a review covers patented Schiff bases and their metal complexes having different therapeutic applications such as antialzheimer, antimicrobial, anticancer, urease inhibition, antituberculosis, detoxification, pesticidal activity, antiglycation and they used as antimicrobial wound dressing agents, imaging reagents and for quantitative determination of homocysteine in biological fluids [40].

Zhu, et al. investigated that when fluorination done at aldehyde part of the Schiff base, that will enhance its activity against insects [41]. Schiff bases derived from thiazole, aminothiazole, furfural, salicylaldehyde, pyridine aldehydes, taurine, amino acids, glucosamine, pyrazolone, aminopyridine, benzaldehyde and indole their metal chelates are found to be efficient inhibitors towards the growth of different pathogen.

### **Sulphur Containing Schiff Bases and Their Transition Metal Complexes: A Review**

In many fields, the presence of sulphur in the ligand backbone imparts unique properties in terms of selectivity, activity and the catalyst precursor's stability. Metal complexes of 'S' containing Schiff bases and their relevant metal complexes have received extensive attention during recent years, mostly due to the outstanding antitumor, antibacterial and antiviral properties. Metal-sulphur centres play a vital role in activity of metalloproteins in enzymatic reactions. The systematic search for M-S model

compounds led to discovering an interesting and novel structural chemistry, which stems from the numerous possibilities of coordination of sulphur containing ligands.

Schiff base complexes derived from salicylaldehyde and thiophene-2-aldehyde and sulfanethiadiazole displayed toxicities against insects [4,42]. Many pyran, quinazole, thiazole and benzothiazole derived Schiff bases possess efficient antifungal activity and the activity is enhanced when groups such as naphthyl, methoxy and halogen are attached [43,44]. In 1985, Vasilev and Devarski derived and studied herbicidal growth regulating activity of Zn(II) complexes of 2-aminobenzothiazole, 2-aminothiazole, 5-methoxybenzothiazole and 5-methyl benzothiazole [45]. Rhodium complexes of 2-amino-6-bromothiazole and 2-aminobenzothiazole exhibited antitumor activity.

In 1977, Ali and Tarafdar synthesized and characterized a benzoin derivative of Schiff base, H<sub>2</sub>BBDT and its transition metal complexes [M= Ni(II), Mn(II), Co(II), Cd(II) and Zn(II)] which is derived from S-benzylidithiocarbamate, having the general formula M(HBBDT)<sub>2</sub> by means of elemental analyses, IR and electronic spectra, magnetic susceptibility and conductivity measurements [46]. The Schiff base functions as a uninegative, tridentate ligand formed by deprotonation and enethiolization of the thioamide group and bonds through the thiolate sulphur, hydroxyl oxygen and azomethine nitrogen. Based on magnetic and spectral studies, a distorted octahedral geometry or octahedral is proposed for the complexes.

In 2002 A. P. Mishra, et al. synthesized complexes of Co, Ni, Cu in +2 oxidation state with Schiff bases salicylidene-N-phenylthiourea (HSNPTU), furfurylidene-N-phenylthiourea (FNPTU) and salicylidene-2-aminophenol (H<sub>2</sub>SAPh). Using microanalytical data, IR, Conductance, UV-Vis, ESR spectroscopy, magnetic susceptibility measurements and TGA their physical-chemical properties have been investigated [47]. Ligand field parameters of complexes and also the non-isothermal

kinetic have been calculated. Salicylidene-2-aminophenol Ni(II) and Co(II) complexes have the general formula  $[ML(H_2O)_3] \cdot 2H_2O$ . Cu(II) complexes have the formula  $[CuL(H_2O)] \cdot H_2O$ . The general formulae  $[ML_2] \cdot 2H_2O$  and  $[ML_2Cl_2] \cdot 2H_2O$  are respectively for Salicylidene-N-phenylthiourea and Furfurylidene-N-phenylthiourea complexes. The antibacterial properties of these complexes were also screened and some of the complexes have been tested against tubercular bacteria.

In 2010, Shahriar Ghammany et al. synthesized and the antitumour properties of two Fe complexes,  $[Fe(pythsal Br)]Cl_2$  and  $[Fe(pythsalI)]Cl_2$  with the NSNO-donor tetradentate ligands of Schiff bases pythsal HX [(5-X-N-(2-Pyridylethylsufanyl ethyl)salicylidenemine] where 'X' is I or Br. These are obtained from the inserted condensation of (1,2-pyridyl)-3-thia-5-aminopentane with the respective derivative of salicyladehyde in molar ratio 1:1. molar ratio and their iron (III) complexes were studied for their antitumor properties. These new complexes showed anti-tumour activity against two kinds of cancer cells Jurkat (human T lymphocyte carcinoma) and K562 (human chronic myeloid leukaemia).

In 2012, Anjali Jha, synthesized 2,5-disubstituted thiadiazole by both microwave irradiation methods and conventional and then this thiadiazole derivative is coupled with ethyl cyanoacetate (ECA), 2,4-pentanedione (AcAc) and malanodinitrile (MN) and these nucleated ligands were condensed with Ru(III), Cu(II) and Ni(II) [48]. These complexes were screened with U-937 lymphoma and HL-60 leukaemia cell lines. Ru complexes showed promising activity whereas Cu and Ni complexes exhibited moderate activity. On comparing their MIC values of ligand and complexes indicates that complexes display higher performance than ligands. Ru(III) complexes are better anticancer compounds

In 2014, Mohammad Nasir Uddin and coworkers prepared Schiff base by

condensing Thiophene-2-carbaldehyde with propane-1,2-diamine and 2-aminothiophenol [49] and synthesized its copper(II), cadmium(II), zinc(II) and nickel(II) complexes. Characterization conducted by elemental analysis, spectroscopic and magnetic measurements. Ligand is coordinated through nitrogen atom of the azomethine (-HC=N-) linkage and through sulfur atom of the thiophene moiety and it was recognized by NMR and IR spectra. Conductance measurements and magnetic susceptibility suggested non-electrolytic nature and octahedral geometry of the synthesized complexes. Antibacterial screening (*in vitro*) against different human pathogenic bacteria demonstrated that Cu(II) chelates shows high antibacterial activity and ligands exhibit only moderate activity.

In 2016, Abdel-Hady, et.al, synthesized new series of complexes of Schiff base (E)-N-(4-(2-hydroxybenzylideneamino) phenylsulfonyl) (S.S) with metal ions Cr(III), Pb(II), Ag(I), Cd(II), Fe(III), Co(II), Ni(II) and Ce(III) [50]. Characterization of these novel complexes were carried out by physico-chemical techniques like magnetic susceptibility, melting point, FT-IR, elemental analysis, <sup>1</sup>H NMR spectroscopy, conductance measurements, UV spectroscopy and mass spectral analysis. By using ICP-MS (Inductively Coupled Plasma-Mass Spectrometry), the metal ions concentrations have been determined. Complexes have been tested for antimicrobial performance against gram positive bacteria like *Streptococcus pneumonia*, *Bacillus subtilis* and gram negative bacteria like *Pseudomonas aeruginosa* and *Escherichia coli* and fungus like *Aspergillus fumigates* and *Candida albicans*. Spectroscopic studies revealed that coordination of most of complexes of (E)-N-(4-(2-hydroxybenzylideneamino) phenylsulfonyl) by two OH phenolic and 'N' azomethine in a regular octahedral arrangement in 2L:1M molar ratio in the form of [ML<sub>2</sub>(H<sub>2</sub>O)<sub>2</sub>].

In 2017, Shambuling Karabasannavar, et al. synthesized five metal complexes of Cd(II), Cu(II), Zn(II), Ni(II), and Co(II) with Schiff-base ligand, 3-((4-phenylthiazol-2-

ylimino)methyl)-2-hydroxybenzoic acid with metal ions [51]. Reaction proceeded through condensation reaction between 2-amino-4-phenyl thiazole and 3-aldehydo salicylic acid. Molar conductance,  $^1\text{H}$  NMR, TGA/TDA, FT-IR and ESI mass studies are used for structural elucidation. The square planar geometry of the complex and bidentate O-O donor atom is determined by spectral studies and the antimicrobial and antifungal activity is detected. In order to investigate the *in vitro* cytotoxicity properties, the brine shrimp biological assay was carried out against *Artemiasalina*. Experimental results of DNA cleavage show that Co(II), Zn(II) and Cu(II) complexes exhibited outstanding DNA cleavage performances by the generation of radical of hydroxyl group.

In 2017, Emad Yousif, et.al; synthesized five novel complexes of Pd(II), Vo(II), Au(III), Co(II), and Rh(III) with Schiff base derivatives of 2N-salicylidene-5-(p-nitrophenyl)-1,3,4-thiadiazole, HL in alcohol medium [52]. These complexes characterized both by qualitatively and quantitatively by mass spectroscopy, FTIR,  $^1\text{H}$ ,  $^{13}\text{C}$  NMR and UV-Vis spectroscopies and magnetic susceptibility, micro elemental analysis and conductivity measurements etc., These different metal ions coordinated to the ligand, HL through oxygen and nitrogen atoms. Most of these complexes exhibit square planar geometry except two complexes which are square pyramidal and tetrahedral in structure. In vitro antibacterial studies of these complexes gives that all these show moderate activity towards bacterial strains and slightly higher activity compared to HL ligand.

### **Schiff Bases Derived From Polynuclear Carbonyl Compounds and its Transition Metal Complexes: A Review**

In 2002, Joby Thomas, et al. synthesized and characterized Mn(II), Co(II) and Ni(II) chelates of anthracene-9-carboxaldehyde thiosemicarbazone and carried out thermoanalytical and antitumour studies on the obtained complexes [53].

In 2009, Anant Prakash et al. synthesised novel Schiff bases derived from anthracene-9-carboxaldehyde with different amino acids like L-glycine, L-tryptophan, L-histidine, L-methionine and L-valine. These newly developed ligands and their transition metal complexes Cr(III), Ni(II) and Ti(III) are characterised by physicochemical techniques like elemental analysis, magnetic susceptibility measurement, Molar conductance, thermogravimetric analysis and spectrochemical studies like electronic spectral investigations [54]. The stoichiometry of metal ligand ratio found to possess 1:2. These novel Schiff bases and these Cr(III), Ni(II) and Ti(III) complexes were screened for antimicrobial studies.

In 2013, Devi, et al. synthesized and characterized Ni(II), Co(II) and Cu(II) complexes of the Schiff base derivatives from anthracene-9-carboxaldehyde with tyrosine on the basis of different physicochemical techniques [55]. To determine the decomposition pattern and thermal stability, Ni(II), Co(II) and Cu(II) complexes were subjected to thermal analysis. From TG curves, kinetic parameters like frequency factor (A), activation energy ( $\Delta E$ ) and entropy of activation ( $\Delta S$ ) were determined. The thermal stability of studied complexes are in the order Co(II) > Cu(II) > Ni(II). In TG curve, Co(II) and Ni(II) complexes showed a one stage decomposition pattern and Cu(II) complex showed a pattern of two stage decomposition.

In 2018, Shaju, et.al., synthesized, characterised novel Schiff base derivative and its Cu(II) complex from anthracene-9-(10H)-one and 3-phenyl propanoic acid. Also investigated the redox nature of these complexes with the help of cyclic voltammetry [56]. The effect of scan rate on the behaviour of redox reactions was evaluated.

### **Schiff Bases Derived From Pyridine Derivatives and its Transition Metal Complexes: A Review**

In 2004, N. Raman, et.al. prepared Schiff bases derived from salicylidene-4-aminoantipyrine with substituted anilines/  $\text{PhNH}_2$  and their neutral Cu(II) complexes.

Structural features of these complexes were studied by microanalytical, IR, UV-Visible,  $^1\text{H}$  NMR, ESR and mass spectral data [57]. The antimicrobial performance of the ligands and the copper complexes against the bacteria *Klebsiella pneumonia*, *Staphylococcus aureus*, *Salmonella typhi*, *Pseudomonas aeruginosa* and *Bacillus subtilis* are also reported. These complexes show higher activity than those of the free Schiff bases. They have higher activity than the control except for *Klebsiella pneumonia* and *Pseudomonas aeruginosa*.

In 2012, Y.K. Gupta, et al. synthesized complexes of transition metals like Ni(II), Co(II), Zn(II), Cu(II), Hg(II) and Cd(II) with bis(2-pyridylcarboxyl aldehyde)ethylene diamine (a bidentate ligand) formed by the condensation of ethylenediamine and 2-pyridylcarboxyl aldehyde [58]. On the basis of different analytical techniques like elemental analysis, magnetic moment data, conductance measurements, infrared and  $^1\text{H}$  NMR spectroscopic data, metal complexes have been characterized. From that, it has been found that complexes are in the ratio 1:2 (metal: ligand). Based on this data, they proposed a geometry which is octahedral for the metal(II) complexes. Physiological activities against *Staphylococcus aureus*, *E. coli*, *Salmonella typhi* and *Bacillus subtilis* for the ligand and metal complexes were also screened.

In 2012, Krishnan Pothiraj, et al. synthesized four mononuclear Zn(II) and Cu(II) complexes of Schiff-base ligand and 2,2'-bipyridine/1,10-phenanthroline [59]. Characterization was also done on these complexes. Octahedral geometry has been proposed to complexes based on the data obtained from magnetic susceptibility and electronic spectral data. By absorption filtration, viscosity and electrochemical methods DNA binding behaviour of these complexes were evaluated and found that complexes bind to calf thymus DNA in an interactive mode. The antimicrobial studies reveal that complexes are superior antimicrobial agents than ligands.



In 2012, A. Angel, et al. synthesized and characterized [Cu(2AcpClPh)Cl]2H<sub>2</sub>O, [Cu(2AcPh)Cl]2H<sub>2</sub>O, [Cu(2BzpNO<sub>2</sub>Ph)Cl], [Cu(2AcpNO<sub>2</sub>Ph)Cl], [Cu(2BzpClPh)Cl] and [Cu(2BzPh)Cl] with 2-acetylpyridine-para-chloro-phenylhydrazone (H<sub>2</sub>AcpClPh), 2-acetylpyridine-para-nitro-phenylhydrazone (H<sub>2</sub>AcpNO<sub>2</sub>Ph), 2-acetylpyridine-phenylhydrazone (H<sub>2</sub>AcPh), 2-benzoylpyridine-phenylhydrazone (H<sub>2</sub>BzPh), 2-benzoylpyridine-para-nitro-phenylhydrazone (H<sub>2</sub>BzpNO<sub>2</sub>Ph) and 2-benzoylpyridine-para-chloro-phenylhydrazone (H<sub>2</sub>BzpClPh) [60]. Hydrazone derivatives exhibit poor antibacterial effect against *Enterococcus faecalis*, *Staphylococcus aureus* and *Pseudomonas aeruginosa*. But they demonstrated significant antifungal performance against the bacterial strain *Candida albicans*. The antifungal and antibacterial activities are appreciably increased by complexation with copper.

In 2012, N. S. Gwaram, et al. synthesized transition metal complexes of Schiff base derivatives 4-(2-aminoethyl)morpholine and 4-(2-aminoethyl)piperazine with 2-acetylpyridine and characterized using elemental analysis, UV-Vis spectral studies, NMR and FT-IR [61]. Cd(II) complexes displayed polymeric structure Zn(II) complex exhibited square pyramidal geometry while Ni(II) complexes showed an octahedral geometry.

In 2014, Raphael P. Vinod, et al. synthesized and investigated copper chelate of heterocyclic Schiff base 3-acetylpyridine phenylhydrazone (APPH) and are characterized by elemental, spectral, magnetic and conductance measurements [56]. Results showed that during chelation, APPH performed as bidentate ligand. The electrochemical response of this Schiff base and its chelate were reported. The square planar geometry of the chelate was confirmed by optical spectral studies and magnetic studies.

### **Schiff bases Derived From Indole and its Transition Metal Complexes: A Review**

In 2012, Ibrahim, et al. evaluated the gastroprotective activity of nickel(II)

complex of Schiff base ligand derived from the condensation reaction of 5-nitrosalicylaldehyde (TNS) and an indole derivative of tryptamine against ethanol-induced gastric ulcer in rats [62]. The results showed that these Schiff base ligand and nickel(II) complex showed effective gastric protection and leucocyte infiltration of the submucosal layer and reduced edema.

In 2014, Rhaman, et al. synthesized and characterised transition metal complexes of Zn(II), Co(II), Ni(II), Cu(II), Hg(II) and Cd(II) with a tridentate (Oxygen-Nitrogen-Nitrogen) ligand 3,5-dimethyl-*N'*-[(1*E*)-1'-pyridin-2'-ylethylidene]-1*H*-indole-2-carbohydrazide on the basis of analytical, infrared, nuclear magnetic resonance, magnetic susceptibility, electron paramagnetic resonance spectral studies, fast atom bombardment-mass, UV-and visible spectral data and X-ray powder diffraction [63]. Based on molar conductance and analytical data, the complexes may be formulated as  $[M(L)Cl_2] \cdot (H_2O)_n$ , where  $M=Zn, Hg$  and  $Cd$  and  $[M(L)_2] \cdot (H_2O)_n$ , where 'M' can be Cu, Ni and Co and. The spectral studies revealed that, a square pyramidal geometry for Zn(II), Cd(II) and Hg(II) complexes whereas octahedral geometry for Co(II), Ni(II) and Cu(II) complexes, Their antifungal activity against *Candida albicans* and *Aspergillus niger* and antibacterial activity against *Staphylococcus aureus* and *Escherichia coli* were screened.

In 2019, Tadele and Tsega studied the anticancer activity of the novel Schiff bases and their metal complexes was studied using different assays such as PI staining, 3-[4,5-dimethylthiazol-2-yl]-2,5-diphenyl-tetrazolium bromide (MTT), *Allium cepa*, Sulforhodamine, Sulfo- Rhodamine-B-stain (SRB), viability and potato disc against various animal and human cancer cell lines [64]. They exhibited very high activity against MCF-7 and HepG2 cell lines.

In 2019, E.L. Gammal, et al. synthesized novel mononuclear Cu(II), Cd(II),

Sn(IV), Fe(III) and binuclear Hg(II), Ni(II) and complexes with the Schiff base ligand: (E)-N'-((4-methyl-1H-indol-3-yl)methylene)nicotinothiazide [65]. The structures of the prepared compounds were elucidated by elemental analyses, magnetic measurements, 3D molecular modeling, Thermogravimetry and molar conductance techniques were by conducted by diverse spectroscopic ( $^1\text{H}$  NMR, IR, UV-Visible and EPR) techniques. Antioxidant activities of ligand and metal complexes were studied by DPPH scanning (*in vitro*) technique. Highest antioxidant activity shown by  $[\text{Sn}(\text{HL})\text{Cl}_2(\text{OH})_2]\cdot 2\text{H}_2\text{O}$  complex. Ligand and its metal complexes were screened for antibacterial activities against two strains of fungi *Aspergillus flavus* and *Candida albicans* and two bacterial strains *Staphylococcus aureus* and *Escherichia coli*. The binuclear complex,  $[\text{Hg}_2(\text{HL})\text{Cl}_4]\cdot \text{EtOH}$  showed excellent antifungal performance against *Aspergillus flavus* and excellent antibacterial activity higher than the standard drug Ampicillin.

### **Scope and Objectives of Present Investigation**

Many Schiff bases have been checked for their chelating ability with different transition and inner transition metals. The quest for novel Schiff bases and their metal chelates are continuing in the present decades. Literature survey revealed that there is a wide scope still remains for the investigation of novel Schiff bases and its metal chelates. In the present investigation, it is proposed to synthesize novel Schiff bases containing sulphur and its transition metal chelates. Since the polarizability of lone pairs on the sulphur atom is high one can expect an escalated chance for the chelation and other related properties. Exploring the structure and geometries of newly synthesized Schiff bases and metal chelates with the help of various analytical techniques will be helpful in explaining the significant properties and applications by correlating to their molecular structure.

Checking the chelating ability of the newly synthesized sulphur compounds may lead to open a new series of novel metal complexes which may have some pharmacological activity. To ensure the drug ability of the newly synthesized organic molecules and their metal chelates, it is decided to conduct the antimicrobial studies and molecular docking studies.

A thorough literature survey revealed that many Schiff base molecules bearing sulphur atoms is infrequently subjected to the corrosion inhibition studies on various metals in acidic medium. So in the present investigation it is proposed to screen corrosion inhibition properties of the newly synthesized Schiff bases on various metals in acidic media.

## CHAPTER 2

### MATERIALS AND METHODS

In this chapter, a brief sketch of the common reagents and general methods adopted for the preparation, purification and characterization of heterocyclic Schiff bases containing 'S' and their transition metal complexes are explained.

#### **Reagents Used**

For the preparation of amine, analar grade samples of para nitro benzoic acid, potassium hydroxide, thiosemicarbazide and phosphorous oxychloride were used. Analar grade samples of anthracene-9-carbaldehyde (synthetic material), anthrone, pyridine-2-carbaldehyde, 3-acetyl pyridine, 2-acetyl pyridine, indole-3-carbaldehyde, 2-aminothiazole, thiophene-2-carbaldehyde, 1,2-diaminocyclohexane were purchased from Fluka for the synthesis of heterocyclic ligands.

Solvents, rectified spirit and ethanol were purchased from E. Merck in pure form was used as the medium used for the synthesis of the 'S' containing heterocyclic ligands. Solvent DMSO purchased from E. Merck was used for the analysis of UV-Visible spectral studies and electrolytic conductance measurements. Metal salts like acetates, chlorides and nitrates from Qualigens (AR samples) were used for the synthesis of the heterocyclic Schiff base complexes. Almost all transition metal chelates were synthesized in pure ethanol medium.

Metal salts used for the analysis were the acetates or chlorides of copper, chromium, manganese, cobalt, nickel and zinc and nitrates of zirconium. For the preparation of Fe(III) complexes, ferric chloride (analar grade from Ranbaxy) was used, while nitrates of zirconium were used for the synthesis of Zirconium chelates/complexes. The entire metal salts were purchased from Qualigens and E. Merck

The general preparation procedure for the synthesis of the heterocyclic ligands and their transition metal complexes with various metal salts and other details are given in the subsequent chapters.

## **Analytical Techniques**

### ***CHNS analysis***

Elementar make Vario EL III model CHNS analyzer is used for the microanalysis of the heterocyclic Schiff bases and their transition metal chelates by assessing carbon, hydrogen, nitrogen and Sulphur.

### ***Metal content analysis***

Pyrolytic method was used as the preliminary estimation of metal percentage in the heterocyclic Schiff base complexes [66]. An electric Bunsen was used for heating the metal complexes. About 0.2g of the transition metal complex was weighed, transferred in a previously weighed silica crucible and heated for 2h. Metal oxides were produced by the decomposition of their consequent metal complexes. The metal oxide left behind was weighed after cooling and the metal percentage of for each complex was estimated.

For conducting further estimations, a known amount of the metal chelates were digested for 1h with a mixture of concentrated perchloric-nitric acid. After the digestion or decomposition of the metal complexes, the mixture was further extracted with concentrated HCl and the resultant solution was then quantitatively transferred into a volumetric flask. Different analyses were carried out for finding out the percentage of the metal by taking a definite volume of the solutions.

Estimation of chromium was done by photometric method using 1,5-diphenyl carbazide; a violet colour of chromium complex was formed with this reagent.

Thiocyanate method was used for the estimation of iron complexes. The cobalt metal ion can be estimated by both volumetrically and complexometrically. (Standard EDTA, hexamine buffer solution and xylenol orange indicator were mainly used for the complexometric estimation)

Complexometric titration was also employed for the estimations of nickel and zinc by using complexing agent as EDTA; Murexide and Eriochrome black-T were used as indicators for nickel and zinc metal ions respectively [67]. Iodometric titration was used for copper estimation by means of sodium thiosulphate as titrant and starch as indicator. Nickel content was estimated by the precipitation of the complex of nickel dimethyl glyoxime  $[\text{Ni}(\text{C}_4\text{H}_7\text{O}_2\text{N}_2)_2]$ , using dimethylglyoxime as the precipitating agent.

### ***Spectral studies***

To confirm the structures and geometry of the heterocyclic Schiff base ligands and their complexes, spectral tools like UV-Visible, GCMS, Infrared,  $^1\text{H}$  NMR and  $^{13}\text{C}$  NMR were used.

- ***UV-Visible spectra:*** Electronic spectra of these molecules and its transition metal complexes were traced in the range of 200-800nm in DMSO on a Shimadzu UV-Visible-1800 spectrophotometer. These spectra play an important role as a confirmation to magnetic moment studies to formulate the geometry of the complexes. Structural identification was also the main perspective of UV-Visible spectra.
- ***Infrared spectra:*** Infrared spectra of all synthesized heterocyclic compounds and metal complexes were traced in the range  $4000\text{-}400\text{cm}^{-1}$  by KBr disc technique. FT-IR spectrometer made by Shimadzu, Japan, specially indicated model IR affinity-1, was utilized for the analysis of the infrared spectra of all synthesized heterocyclic ligands and metal complexes. The IR spectroscopy is important since

it exhibits a characteristic absorption band for a particular group irrespective of the ligands and complexes in which the group is present. Thus it becomes a fingerprint for identification and a powerful tool for studying molecular structure. Moreover, the coordination of the metal ion with the ligands can be reputable with the corresponding spectra. Prediction of the coordination sites of these heterocyclic ligands to the metal ion can be done by the comparison between the infrared spectrum of these ligands with the metal chelates.

- **NMR spectra:** The performance of  $^1\text{H}$  NMR and  $^{13}\text{C}$  NMR spectral studies of ligands and complexes were carried out in DMSO as the solvent and studies were done using the instrument Bruker Avancelll, 400MHz model.
- **Mass spectra:** GCMS Qp-2010 plus model Shimadzu at a source temperature of  $300^\circ\text{C}$  were used for recording the mass spectra of the synthesized heterocyclic ligands. Before the mass spectral studies, gas chromatography was conducted on these synthesized Schiff bases for the confirmation of purities of the ligands.

Physicochemical studies such as molar conductance studies and magnetic susceptibility measurements were conducted to clarify the structure and geometry of the synthesized complexes

#### ***Molar conductance measurements***

ELICO conductivity meter was used to measure the molar conductivities of the metal complex solutions at room temperature which helps to ascertain the charge of the complex. In all measurements, the solution concentration was maintained as  $10^{-3}\text{M}$  at  $30\pm 2^\circ\text{C}$  and cell constant as '1'. By measuring this parameter, the electrolytic behavior of the compounds could understand [68].

#### ***Magnetic susceptibility measurements***

By adapting Gouy method, the magnetic susceptibilities of the complexes could



be measured. The apparatus UK (Mark 1) from Sherwood and Hg[Co(NCS)<sub>4</sub>] as the calibrant (do not decompose or absorb moisture, easy to prepare and pack well in the sample tube) were used for this purpose. “The molar susceptibility, a measure of magnetic field of a substance, is the algebraic summation of the susceptibilities of the constituent ions, atoms or molecules”. By using Pascal’s constants, diamagnetic corrections were applied [69]. It is done by taking in to the deliberation of the magnetic contribution of different atoms and structural units. From the corrected susceptibilities, the effective magnetic moments were calculating using the equation.

$$\mu_{\text{eff}} = 2.84 \sqrt{\chi_m \times T} \quad (1)$$

where  $\chi_m$  = Molar susceptibility (corrected for diamagnetism); T = Absolute temperature

$$\chi_m = \chi_g \times \text{Molecular mass} \quad (2)$$

where,  $\chi_g$  = Gram susceptibility

$$\chi_g = C \times L \times (R - R_0) / W \times 10^9 \quad (3)$$

Where, C = Tube calibration constant; L = Length of the complex (sample); R<sub>0</sub> = Value of empty glass tube; R = Value of sample + glass tube; W = Weight of sample.

The theoretical magnetic moment values were calculated using the formula,

$$\mu_{\text{eff}} = g \sqrt{S(S + 1)} \quad (4)$$

where ‘g’ is the Lande splitting factor or gyromagnetic ratio and ‘S’ is the total spin quantum number.

## CHAPTER 3

### TRANSITION METAL COMPLEXES OF SCHIFF BASES DERIVED FROM 5-(4-NITROPHENYL)-1,3,4-THIADIAZOL-2-AMINE (NPTDA) AND POLYNUCLEAR CARBONYL COMPOUNDS

Nowadays, the transition metal complexes with thiadiazole moieties have great commercial value and this has aroused considerable interest in the field coordination chemistry. However, there is no information available in the literature on metal complexes of Schiff base ligands synthesized from 5-(4-nitrophenyl)-1,3,4-thiadiazole-2-amine and its polynuclear carbonyl compounds. Therefore it was considered to be very useful and interesting to study the donor properties of novel 'S' containing Schiff bases (E)-N-(anthracen-9-ylmethylene)-5-(4-nitrophenyl)-1,3,4-thiadiazol-2-amine (A9CNPTDA) and N-(anthracen-10(9H)-ylidene)-5-(4-nitrophenyl)-1,3,4-thiadiazol-2-amine (ANNPTDA) and their transition metal complexes. An attempt for the characterization of the ligands and complexes were done with the aid of analytical tools such as elemental (CHNS) analysis, estimation of metal percentage, magnetic moment, molar conductance and various spectroscopic techniques.

The detailed synthesis and characterization of these two novel 'S' containing polynuclear derivatives of Schiff bases and their metallic complexes are discussed as two separate sections. Section I deals with synthesis and characterization of polynuclear Schiff base ligand, A9CNPTDA derived from the parent amine 5-(4-nitrophenyl)-1,3,4-thiadiazol-2-amine (NPTDA) and anthracene-9-carbaldehyde and its transition metal complexes. Section II consists of synthesis and characterization of another polynuclear 'S' containing Schiff base, ANNPTDA derived from the parent amine, NPTDA and anthrone and its transition metal complexes

### Synthesis of 5-(4-nitrophenyl)-1,3,4-thiadiazol-2-amine (NPTDA)

Parent amine, 5-(4-nitrophenyl)-1,3,4-thiadiazol-2-amine (NPTDA) was synthesized using the standard procedure by Yousif et al. [70] and the schematic representation of the synthesis is shown in Fig. 1.1. It was synthesized by refluxing equimolar mixture of 4-nitrobenzoic acid and thiosemicarbazide in phosphorus oxychloride solution for 3h. To the cooled mixture, distilled water was added and further refluxed for 5h. The solution obtained was neutralized with potassium hydroxide and the formed yellow precipitate was filtered, washed with cold distilled water, dried and melting point was found to be 247°C (Yield: 56%)

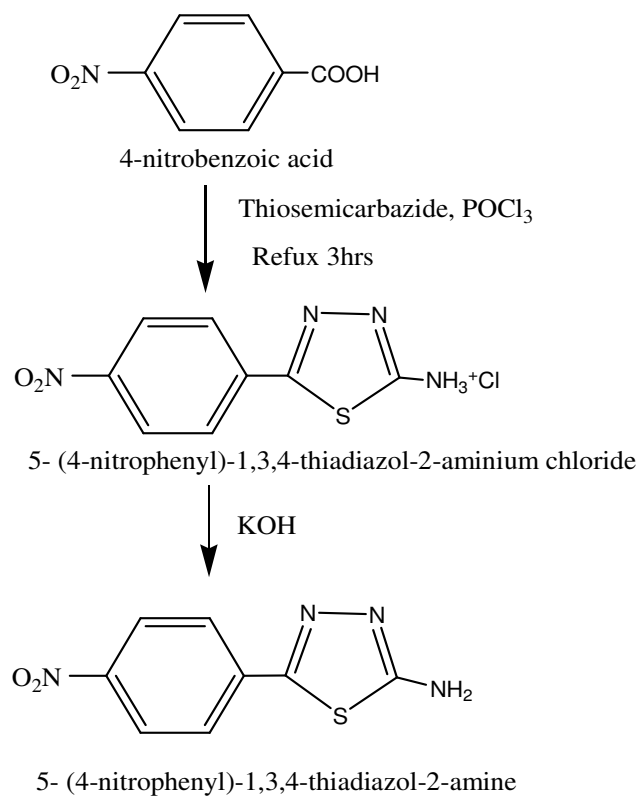


**Fig. 1.1:** Schematic representation of the synthesis of parent amine 5-(4-nitrophenyl)-1,3,4-thiadiazole-2-amine (NPTDA)

### Characterization of Parent Amine (NPTDA)

Characterization of amine was done by spectral studies. Electronic spectrum of 5-(4-nitrophenyl)-1,3,4-thiadiazol-2-amine exhibited a band at 39215cm<sup>-1</sup> which can be

consigned to  $\pi \rightarrow \pi^*$  transition and the  $n \rightarrow \pi^*$  transition band was appeared at lower frequency of  $27173\text{cm}^{-1}$ . The K-band is found to have more intensity compared to R-band, which is spectroscopically forbidden.

### ***FTIR spectral analysis***

Infrared spectrum of amine showed broad bands of medium intensity at about  $3422\text{cm}^{-1}$  and  $3309\text{cm}^{-1}$  which may be attributed to the asymmetric and symmetric N-H stretching frequency of amino part. Another peak appeared at  $1615\text{cm}^{-1}$  can be assigned to the C=N stretching in the ring. Strong peaks displayed at  $1603\text{cm}^{-1}$  and  $1526\text{cm}^{-1}$  are due to C=C stretching frequencies. There were also characteristic peaks at  $3121\text{cm}^{-1}$  and  $1105\text{cm}^{-1}$  because of the aromatic C-H and C-S stretching vibrations respectively. Also the C-N vibrational frequency was emerged at  $1280\text{cm}^{-1}$ . The presence of nitro group was confirmed by the presence of peaks at  $1463\text{cm}^{-1}$  and  $1349\text{cm}^{-1}$  and the in plane bending vibrations appeared at  $1012\text{cm}^{-1}$ . Also the peaks obtained at  $871\text{cm}^{-1}$  and  $714\text{cm}^{-1}$  can be assigned as out of plane bending vibrations.

### ***NMR spectral analysis***

A broad singlet peak that appeared at  $4.14\delta$  was consigned to the protons of the free terminal  $\text{NH}_2$  group present in the parent amine NPTDA and the spread in the peak may be attributed to quadrupole broadening (Fig. 1.2). The aromatic protons of both anthracene and benzenoid rings resonated as multiplets at  $8.1\delta$  and  $8.24\delta$ .

### ***Mass spectral analysis***

Molecular ion peak of NPTDA was observed at  $m/z$  222  $[\text{C}_8\text{H}_6\text{N}_4\text{O}_2\text{S}^{32}]^+$  as a strong peak, which establishes the stability of molecule. The emergence of the M+2 peak (isotopic peak) in the spectrum of parent amine at  $m/z$  224  $[\text{C}_8\text{H}_6\text{N}_2\text{S}]^+$ , is due to the presence of the  $\text{S}^{34}$  atom present in it. [M]:[M+2] ratio indicates one 'S' atom in the molecule. The base peak was displayed at  $m/z$  74 due to the fragment  $[\text{CH}_2\text{N}_2\text{O}_2\text{S}]^+$ . The

fragments  $[C_8H_6N_2S]^+$ ,  $[C_7H_4NS]^+$ ,  $[C_7H_4S]^+$  and  $[C_7H_7]^+$ ,  $[CH_2NS]^+$  displayed corresponding signals at  $m/z$  162, 134, 120, 91 and 60 respectively (Fig. 1.3).

The characterization records obtained were in excellent correlation with the reported data in literature. From the spectral data and synthetic route adopted, the amine was assumed the structure represented in Fig. 1.1.

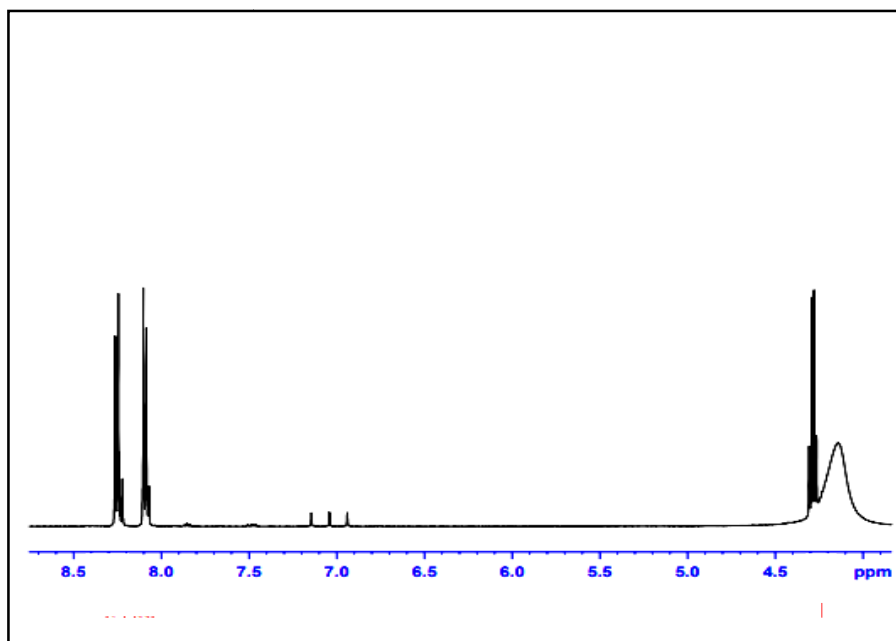


**Fig. 1.2:**  $^1H$  NMR spectrum of NPTDA

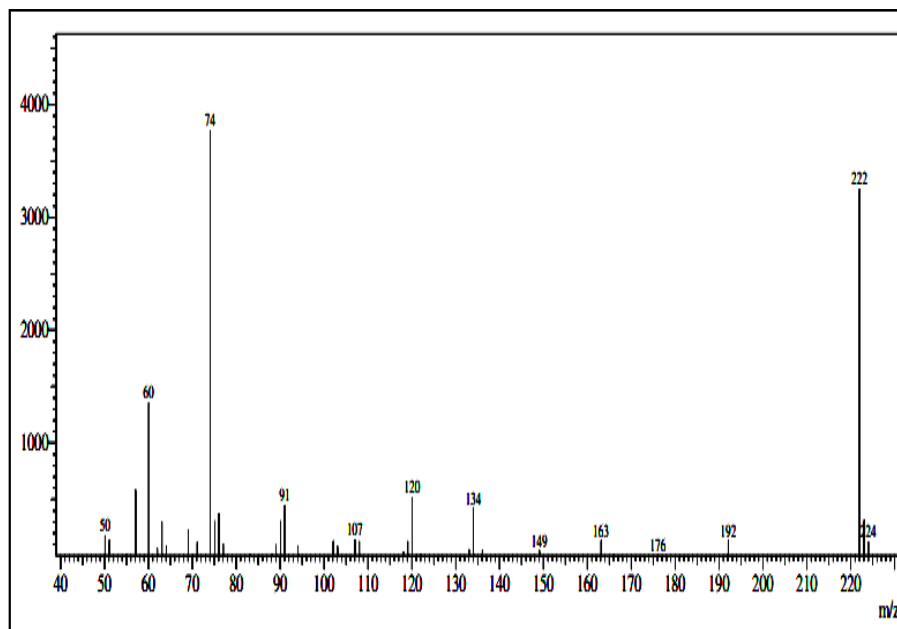


**Fig. 1.3:** Mass spectrum of NPTDA

## SECTION I

### STUDIES ON SCHIFF BASE, (E)-N-(ANTHRACEN-9-YLMETHYLENE)-5-(4-NITROPHENYL)-1,3,4 THIADIAZOL-2-AMINE (A9CNPTDA) AND ITS TRANSITION METAL COMPLEXES

A novel 'S' containing polynuclear Schiff base (E)-N-(anthracen-9-ylmethylene)-5-(4-nitrophenyl)-1,3,4-thiadiazol-2-amine (A9CNPTDA) was synthesized and characterized by elemental analysis and various spectroscopic techniques. The structure of A9CNPTDA and its transition metal complexes with chromium, manganese, iron, cobalt, nickel, copper, zinc and zirconium ions were established based on spectroscopic, magnetic and electrical studies. In this section, the detailed synthesis and characterization of both the ligand and complexes are discussed.

#### Synthesis of A9CNPTDA

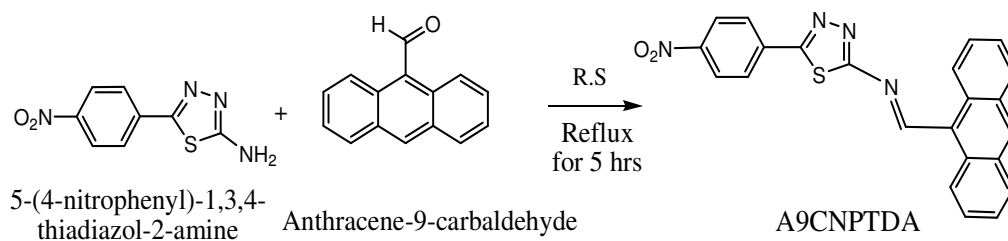


**Fig. 1.4:** Synthesis of A9CNPTDA

Polynuclear 'S' containing Schiff base, (E)-N-(anthracen-9-ylmethylene)-5-(4-nitrophenyl)-1,3,4-thiadiazol-2-amine (A9CNPTDA) was synthesized by adding a hot ethanolic solution of anthracene-9-carbaldehyde (2mM) in dropwise to stirred solution containing equimolar concentration of 5-(4-nitrophenyl)-1,3,4-thiadiazol-2-amine in ethanol medium. The mixture was refluxed for 5h, cooled and concentrated to derive reddish orange coloured needle-shaped crystals of A9CNPTDA. MP is 279<sup>0</sup>C (Yield: 73%).

## Characterization of A9CNPTDA

### *Elemental analysis*

The elemental analysis data of 'S' containing polynuclear Schiff base A9CNPTDA is given in Table 1.3. The experimentally obtained percentages of elements like carbon, hydrogen, nitrogen and sulphur were in good agreement with the calculated values.

### *Electronic spectral analysis*

Characterization of ligand, (E)-N-(anthracen-9-ylmethylene)-5-(4-nitrophenyl)-1,3,4-thiadiazol-2-amine (A9CNPTDA) was done using UV, IR, NMR and Mass spectral data. Electronic spectrum of the ligand showed important two peaks at 39062 (strong) and 27100 $\text{cm}^{-1}$  (weak), due to  $\pi \rightarrow \pi^*$  and  $n \rightarrow \pi^*$  transitions respectively. The decrease in the values compared to the parent amine is an indication of extension of conjugation during the formation of ligands.

### *FTIR spectral analysis*

The absorption bands in the IR spectrum of parent amine NPTDA, due to N-H stretching frequency of amino group at 3600-3300 $\text{cm}^{-1}$  were disappeared in the spectrum of Schiff base, which confirms the formation of A9CNPTDA. Another important band emerged at 1691 $\text{cm}^{-1}$  was due to the stretching mode of azomethine linkage. There was an aromatic C-H stretching frequency at 3102 $\text{cm}^{-1}$  and C-N stretching at 1274 $\text{cm}^{-1}$  and band at 1104 $\text{cm}^{-1}$  corresponds to  $\nu_{\text{C-S}}$ . Two important peaks appeared at 1527 $\text{cm}^{-1}$  and 1347 $\text{cm}^{-1}$  indicated the presence of nitro group in this polynuclear Schiff base A9CNPTDA. C=C present in the aromatic rings displayed peaks at 1556 $\text{cm}^{-1}$  and 1445 $\text{cm}^{-1}$  and in plane bending vibrations appeared at 1008 $\text{cm}^{-1}$ . Also the peaks obtained at 854 $\text{cm}^{-1}$  and 607 $\text{cm}^{-1}$  can be assigned as out of plane bending vibrations. Characteristic

infrared absorption frequencies ( $\text{cm}^{-1}$ ) of this polynuclear sulphur containing Schiff base A9CNPTDA is represented in Table 1.4.

### *NMR spectral analysis*

The  $^1\text{H}$  NMR spectrum of the 'S' containing Schiff base, A9CNPTDA are shown in Fig. 1.5. Six non equivalent protons which are in different electronic environments gave their characteristic peaks in the PMR spectrum. The detailed assignments of peaks are shown in Table 1.1. A peak at  $11.5\delta$  (s) can be assigned to the azomethine proton. The aromatic protons of the anthracene ring resonated as multiplets between  $7.75$ - $9.03\delta$ . Doublet protons appeared at  $8.02\delta$  and  $8.30\delta$  was due to the proton in the benzene ring.

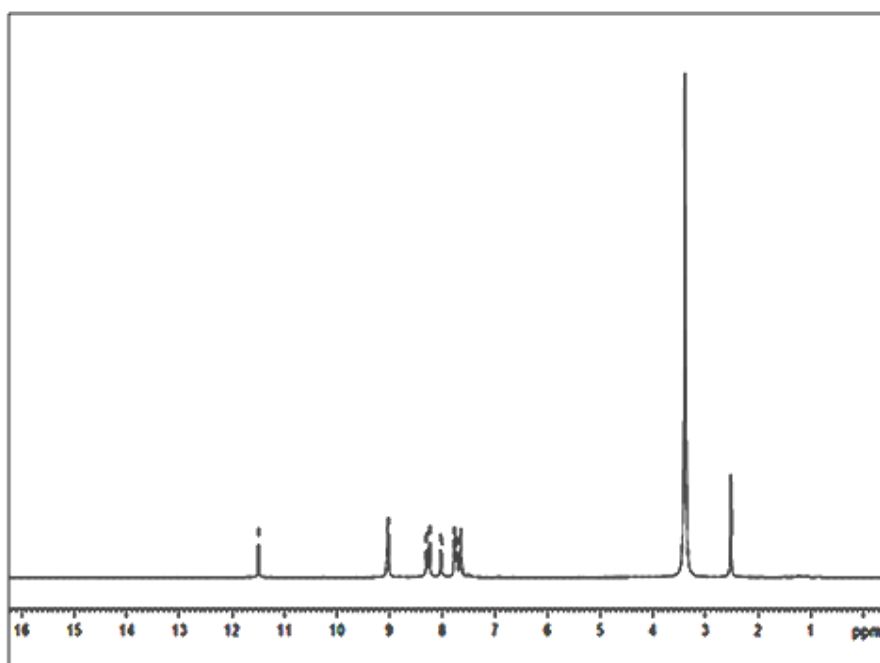


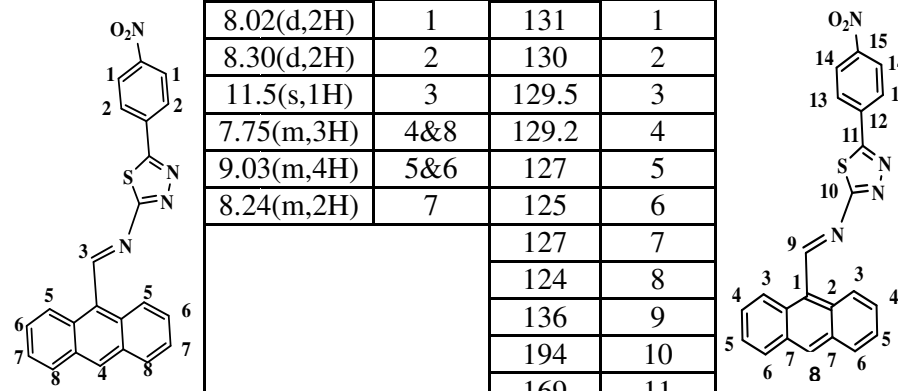
**Fig. 1.5:**  $^1\text{H}$  NMR spectrum of A9CNPTDA

Fifteen chemically different carbon atoms present in A9CNPTDA showed 15 distinct signals in the  $^{13}\text{C}$  NMR spectrum (Fig. 1.6). Peak at 136ppm corresponds to the carbon atom of azomethine linkage and labelled carbon atoms present in the anthracene



and benzene rings observed between 123-154ppm. The details of the peaks corresponding to different carbon atoms are expressed in Table 1.1.

**Table 1.1:**  $^1\text{H}$  NMR and  $^{13}\text{C}$  NMR spectral data of A9CNPTDA

$^1\text{H}$ NMR			$^{13}\text{C}$ NMR	
	$\delta$ value	Labelled proton	$\delta$ value	Labelled carbon
	8.02(d,2H)	1	131	1
	8.30(d,2H)	2	130	2
	11.5(s,1H)	3	129.5	3
	7.75(m,3H)	4&8	129.2	4
	9.03(m,4H)	5&6	127	5
	8.24(m,2H)	7	125	6
			127	7
			124	8
			136	9
			194	10
			169	11
			147	12
			123	13
			135	14
			154	15

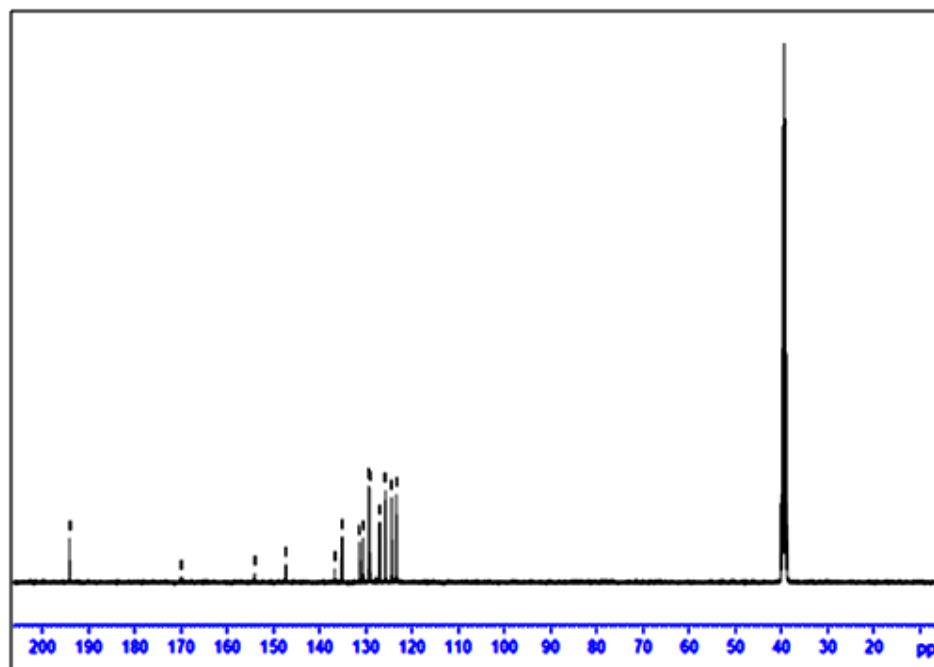


**Fig. 1.6:**  $^{13}\text{C}$  NMR spectrum of A9CNPTDA

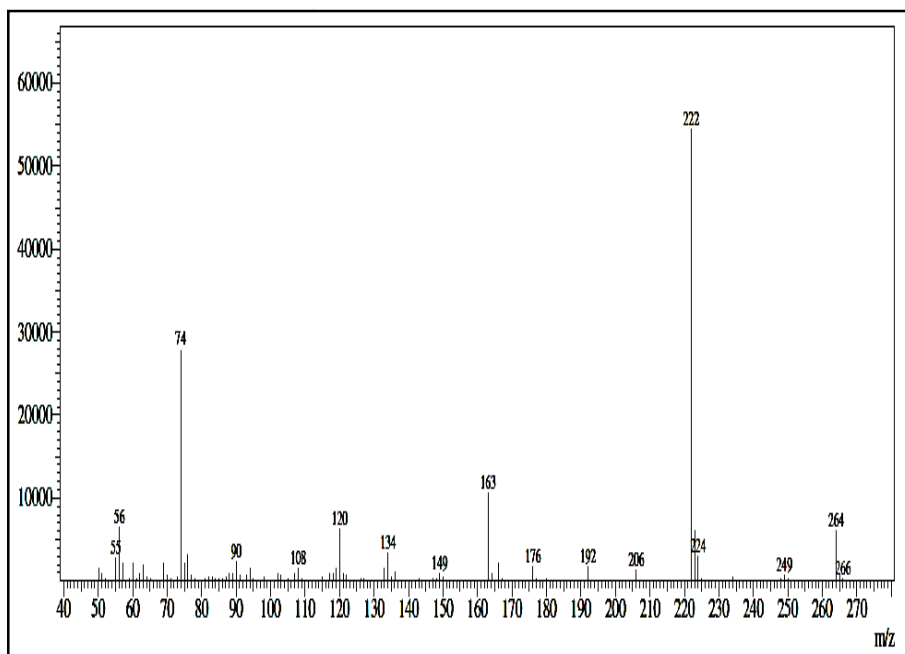


**Fig. 1.7:** Mass spectrum of A9CNPTDA

### *Mass spectral analysis*

The separation of Schiff base was ascertained by the single sharp signal in GCMS showing the purity of the ligand A9CNPTDA. The mass spectrum of A9CNPTDA is represented in Fig. 1.7. In the spectrum, molecular ion peak was absent and the base peak was shown at  $m/z$  222 due to the fragment  $[C_8H_6N_4O_2S]^+$ , originated by the loss of A9C part from the molecule. The fragments  $[C_8H_7N_2S]^+$ ,  $[C_7H_4S]^+$ ,  $[C_7H_7]^+$  and  $[CH_2N_2S]^+$  displayed signals at  $m/z$  163, 120, 91 and 74 respectively.

From the above discussions the structure of polynuclear Schiff base A9CNPTDA can be assigned and given in Fig 1.8

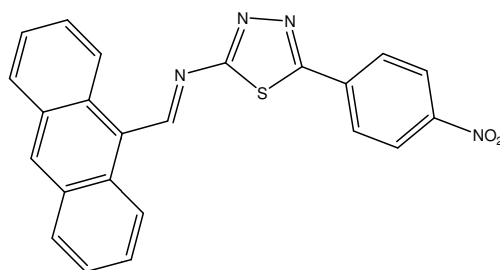


**Fig. 1.8:** Structure of A9CNPTDA

## Synthesis of Complexes

Cr(III), Mn(II), Fe(III), Co(II), Ni(II), Cu(II), Zn(II) and ZrO(II) complexes of polynuclear 'S' containing Schiff base, (E)-N-(anthracen-9-ylmethylene)-5-(4-nitrophenyl)-1,3,4-thiadiazol-2-amine (A9CNPTDA) were synthesized as follows.

Acetate salts of chromium, manganese, nickel and copper were used for the synthesis of corresponding metal complexes. Chloride salts of iron and zinc were used for the preparation of Fe(III) and Zn(II) complexes. For the synthesis of Co(II) and ZrO(II) complexes, metal nitrates were employed.

2mM solution of the polynuclear 'S' containing Schiff base, A9CNPTDA in 10ml ethanol was refluxed on a water bath. To the boiling solution, 2mM hot ethanolic solution of the corresponding metal salt (acetates/chlorides/nitrates) was added and again refluxed for 6h. The pH of the mixture was adjusted to 7-8 by adding a few drops of sodium acetate solution ( $\text{CH}_3\text{COONa}$ ). Then reduced its volume by evaporation, cooled and the crystallized metal complexes were collected, washed and dried over  $\text{CaCl}_2$ .

Zirconyl nitrate solution in ethanol medium was added dropwise to the hot ethanolic solution of Schiff base ligand (molar ratio 1:1) and refluxed for five hours at  $80^\circ\text{C}$  [71]. The resulting orange coloured precipitate was collected by filtration, washed with ethanol and hot water and finally dried. Melting points of the complexes were noted, and these were higher than that of ligand A9CNPTDA.

## Characterization of Complexes

All the complexes of this ligand were amorphous solids and stable to light and air. They are insoluble in water and soluble in organic solvents like DMSO and DMF. They are characterized by elemental analysis, spectral studies, molar conductance studies, magnetic moment measurements etc;

### *Elemental analysis*

This analysis provides an important key to structural elucidation of complexes. Percentage of C, H, N and S as well as the metal content were estimated by microanalytical methods. There is a good correlation between observed and calculated values of elemental analysis. 1:1 stoichiometry exists between metal and this polynuclear Schiff base derivative A9CNPTDA in all complexes.

The elemental and metal percentage data of A9CNPTDA-complexes obtained theoretically and experimentally are listed in Table 1.3.

### *Electronic spectral analysis*

In the case of complexes, bathochromic shift was occurred for both  $\pi \rightarrow \pi^*$  and  $n \rightarrow \pi^*$  bands which is a clear evidence for the complex formation. The electronic spectra of all complexes of A9CNPTDA showed two peaks with red shift with respect to that of ligand, which confirms the complexation. The electronic spectral bands of polynuclear sulphur containing Schiff base A9CNPTDA and its metal complexes are summarized in Table 1.2.

**Table 1.2:** Electronic spectral data of parent amine (NPTDA), Schiff base (A9CNPTDA) and its transition metal complexes

Compound	Electronic bands in $\text{cm}^{-1}$	
	$\pi \rightarrow \pi^*$	$n \rightarrow \pi^*$
NPTDA	39215	27173
A9CNPTDA	39062	27100
[CrL(Ac) <sub>3</sub> (H <sub>2</sub> O)]	37878	26666
[MnL(Ac) <sub>2</sub> (H <sub>2</sub> O) <sub>2</sub> ]	38759	26954
[FeLCl <sub>3</sub> (H <sub>2</sub> O)]	37878	27027
[CoL(NO <sub>3</sub> ) <sub>2</sub> (H <sub>2</sub> O) <sub>2</sub> ]	38910	27027
[NiL(Ac) <sub>2</sub> (H <sub>2</sub> O) <sub>2</sub> ]	38910	26881
[CuL(Ac) <sub>2</sub> (H <sub>2</sub> O) <sub>2</sub> ]	38759	26954
[ZnLCl <sub>2</sub> ]	38610	26954
[ZrOL(NO <sub>3</sub> ) <sub>2</sub> ]	37735	25252, 26954

### ***Magnetic moment analysis***

The geometry of the complexes can be predicted from the magnetic moment measurements. Magnetic moment values of Cr(III) complex was found to be 3.83BM (Calculated  $\mu_{\text{eff}}$  value of  $d^3$  system by spin only formula is 3.87BM), which clearly indicate octahedral geometry of A9CNPTDA-Cr<sup>3+</sup> complex. The observed magnetic moment value for the Mn(II) complex was 6.56BM which clearly establishes its octahedral geometry. The increase in the value compared to expected spin only value of Mn(II) chelate (5.9BM) is an indication of orbital contribution towards the effective magnetic moment [72]. Fe(III), Co(II) and Ni(II) complexes were found to be in distorted octahedral geometry since they exhibited magnetic moment values 5.15BM, 3.23BM and 2.14BM respectively [73,74].  $\mu_{\text{eff}}$  value of Cu(II) chelate was 2.19BM, which is reliable with data accessible from the literature review, for distorted octahedral geometry Cu(II) chelates [75]. Diamagnetic character was observed for Zn(II) and ZrO(II) complexes, which is quite justifiable with their  $d^{10}$  or  $d^0$  configuration respectively and hence tetrahedral and square pyramidal geometry respectively were ascertained for them [32,76]. Magnetic moments of all synthesized metal complexes of A9CNPTDA are listed in Table 1.3.

### ***Molar conductance analysis***

Molar conductance measurement was done for all complexes and the data is given in Table 1.3. The molar conductance value of the complexes was very low, in the range of  $2.5\text{-}7\Omega^{-1}\text{cm}^2\text{mol}^{-1}$ . These values suggest non-electrolytic behaviour and absence of counter ions outside the coordination sphere of metal chelates.

### ***FTIR spectral analysis***

In complexes, the involvement of azomethine group in coordination with metal ion was confirmed by shifting its stretching frequency to lower value [60,77]. The

presence of new broad band signal around  $3400\text{cm}^{-1}$  in Cr(II), Mn(II), Fe(III), Co(II), Ni(II) and Cu(II) complexes of A9CNPTDA confirmed the presence of coordinated water molecule. In Co(II) and ZrO(II) complexes, three bands appeared for N-O bond with a difference of  $130\text{cm}^{-1}$  correspond to monodentate nitrate group. Also, the emergence of stretching frequencies in the range  $614\text{-}694\text{cm}^{-1}$  and  $489\text{-}543\text{cm}^{-1}$  confirmed the formation of M-N bonds and M-S bond. Cr(II), Mn(II), Ni(II) and Cu(II) complexes were showed two characteristic infrared absorption bands in the range  $1670\text{-}1540\text{cm}^{-1}$  with a difference of  $<150\text{cm}^{-1}$  corresponds to asymmetric and symmetric stretching frequency of monodentate  $-\text{COO}$  (acetate) group. An additional new band emerged at  $989\text{cm}^{-1}$  in the IR spectrum of Zirconium - A9CNPTDA complex assigned to the stretching frequency of the  $\text{Zr}=\text{O}$  bond. Important and characteristic IR spectral data of A9CNPTDA and its transition metal complexes are reported and compared in Table 1.4.

Based on the physicochemical analysis, structures were derived for the metal complexes of A9CNPTDA and given in Fig. 1.9.

**Table 1.3:** Microanalytical, magnetic and conductance data of the ligand A9CNPTDA and its transition metal complexes

Complex	Colour	Yield (%)	Mol. Wt.	M.P (°C)	Metal % Found (Cald.)	C % Found (Cald.)	H % Found (Cald.)	N % Found (Cald.)	S % Found (Cald.)	$\mu_{\text{eff}}$ (BM)	Molar Conductance ( $\Omega^{-1}\text{cm}^2\text{mol}^{-1}$ )	Geometry
A9CNPTDA (L)	Dark brown	83	410	279	-	67.02 (67.3)	3.31 (3.44)	13.25 (13.65)	7.34 (7.81)	-	-	-
[CrL(Ac) <sub>3</sub> H <sub>2</sub> O]	Green	50	657	>300	7.64 (7.91)	48.56 (49.73)	3.82 (3.89)	7.15 (7.73)	4.18 (4.43)	3.83	3.9	Octahedral
[MnL(Ac) <sub>2</sub> (H <sub>2</sub> O) <sub>2</sub> ]	Brown	55	619	>310	8.24 (8.88)	51.16 (52.35)	3.88 (3.9)	8.97 (9.04)	4.98 (5.18)	6.56	4.58	Octahedral
[FeLCl <sub>3</sub> (H <sub>2</sub> O)]	Black	50	590	280	10.28 (9.49)	46.3 (47.59)	3.03 (3.16)	9.11 (9.25)	5.12 (5.29)	5.15	2.91	Distorted Octahedral
[CoL(NO <sub>3</sub> ) <sub>2</sub> (H <sub>2</sub> O) <sub>2</sub> ]	Yellow	55	629	>300	9.99 (9.38)	42.29 (43.89)	2.56 (2.88)	11.96 (13.35)	4.84 (5.09)	3.23	5.2	Distorted Octahedral
[NiL(Ac) <sub>2</sub> (H <sub>2</sub> O) <sub>2</sub> ]	Yellow	50	623	270	9.69 (9.47)	51.16 (52.03)	3.43 (3.88)	8.15 (8.99)	5.01 (5.14)	2.14	2.6	Distorted Octahedral
[CuL(Ac) <sub>2</sub> (H <sub>2</sub> O) <sub>2</sub> ]	Black	55	628	>310	9.89 (10.19)	48.49 (50.77)	3.26 (3.77)	8.02 (9.11)	4.78 (5.21)	2.19	6.52	Distorted Octahedral
[ZnLCl <sub>2</sub> ]	Creamish orange	60	545	>300	11.39 (11.93)	50.28 (50.53)	2.46 (2.58)	9.96 (10.25)	5.59 (5.86)	D	4.12	Tetrahedral
[ZrOL(NO <sub>3</sub> ) <sub>2</sub> ]	Orange	60	641	>300	13.82 (14.2)	40.64 (43.05)	2.06 (2.2)	12.29 (13.1)	4.77 (5)	D	5.7	Square Pyramidal

**Table 1.4:** Characteristic infrared absorption frequencies ( $\text{cm}^{-1}$ ) of A9CNPTDA and its transition metal complexes

Complex	$\nu_{\text{H}_2\text{O}}$	$\nu_{\text{C-H}}$	$\nu_{\text{COOasy}}$	$\nu_{\text{C=N}}$	$\nu_{\text{COOsy}}$	$\nu_{\text{C=C}}$	$\nu_{\text{NO}_2/\text{NO}_3}$	$\nu_{\text{M-N}}$	$\nu_{\text{M-S}}$
A9CNPTDA (L)	-	3102	-	1691	-	1508	1436 1347	-	-
[CrL(Ac) <sub>3</sub> H <sub>2</sub> O]	3390(br)	3118	1662	1627	1512	1595 1502	1428 1336	648	534
[MnL(Ac) <sub>2</sub> (H <sub>2</sub> O) <sub>2</sub> ]	3340(br)	3110	1680	1649	1555	1595 1510	1454 1342	623	516
[FeLCl <sub>3</sub> (H <sub>2</sub> O)]	3387(br)	3118	-	1614	-	1593 1494	1454 1327	682	523
[CoL(NO <sub>3</sub> ) <sub>2</sub> (H <sub>2</sub> O) <sub>2</sub> ]	3394(br)	3112	-	1629	-	1588 1502	1470 1437 1340	692	543
[NiL(Ac) <sub>2</sub> (H <sub>2</sub> O) <sub>2</sub> ]	3388(br)	3118	1664	1627	1529	1589 1500	1492 1330	694	538
[CuL(Ac) <sub>2</sub> (H <sub>2</sub> O) <sub>2</sub> ]	3400(br)	3109	1689	1591	1538	1599 1521	1469 1342	624	489
[ZnLCl <sub>2</sub> ]	-	3115	-	1658	-	1600 1514	1444 1432	614	525
[ZrOL(NO <sub>3</sub> ) <sub>2</sub> ]	-	3110	-	1629	-	1588 1506	1468 1400 1340	665	534



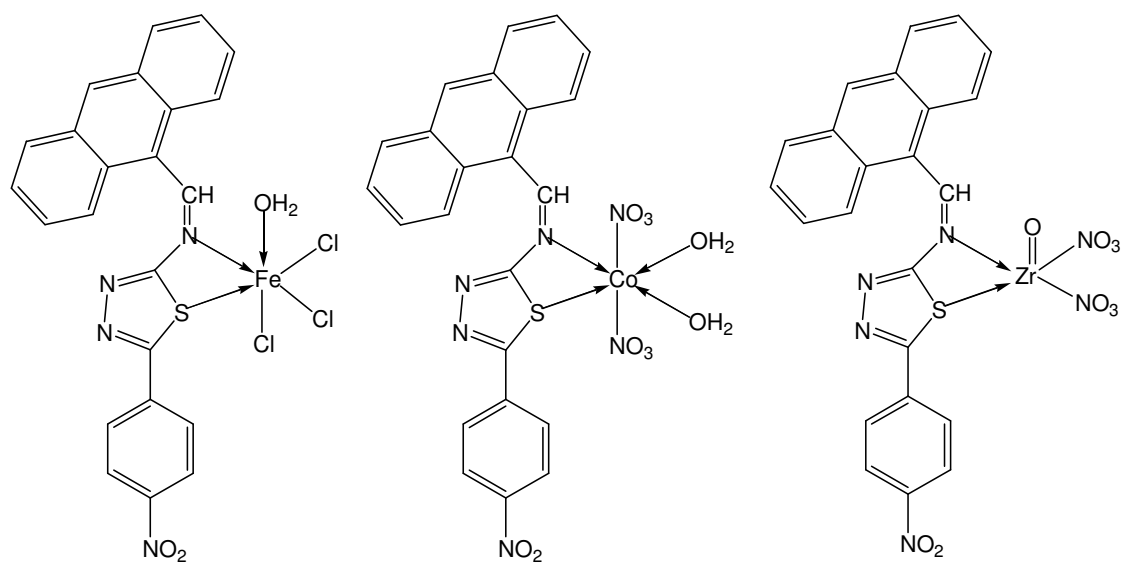
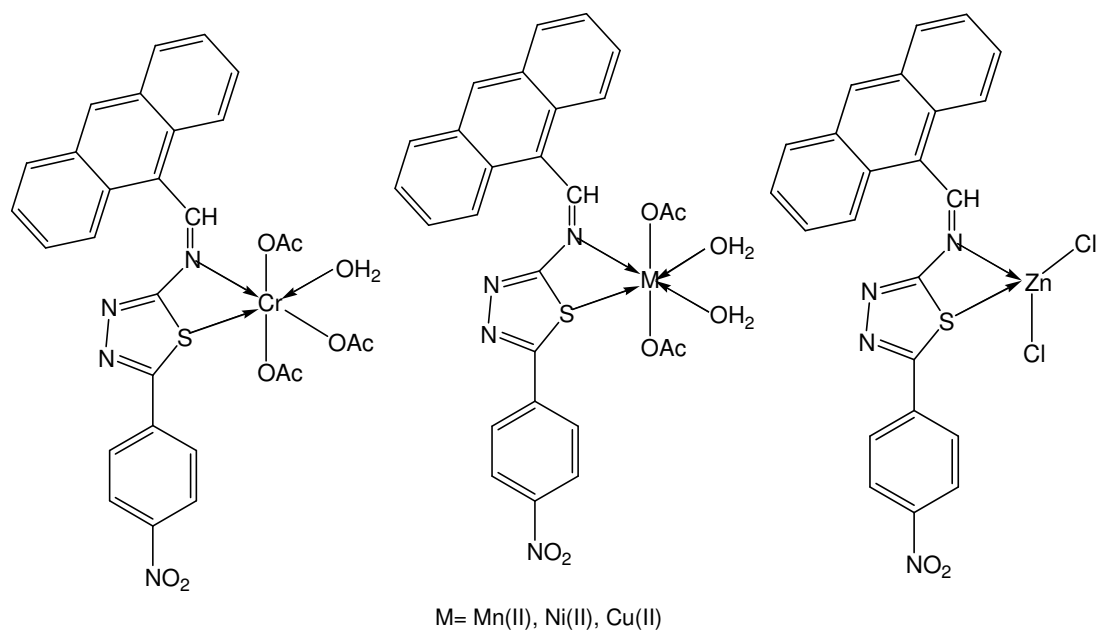


**Fig. 1.9:** Structures of transition metal complexes of A9CNPTDA

## SECTION II

### STUDIES ON SCHIFF BASE, N-(ANTHRACEN-10(9H)-YLIDENE)-5-(4-NITROPHENYL)-1,3,4-THIADIAZOL-2-AMINE (ANNPTDA) AND ITS TRANSITION METAL COMPLEXES

Another polynuclear Schiff base, N-(anthracen-9(10H)-ylidene)-5-(4-nitrophenyl)-1,3,4-thiadiazol-2-amine (ANNPTDA) derived from NPTDA and anthrone was synthesized and characterized using physico chemical techniques such as elemental and spectral analysis. The chelation ability of this ligand was explored by preparing transition metal complexes of Cr(II), Ni(II), Cu(II), Zn(II) and ZrO(II). Based on elemental, spectroscopic, magnetic and electrical studies, the geometry of the complexes derived, which are discussed in detail in this section.

#### Synthesis of ANNPTDA

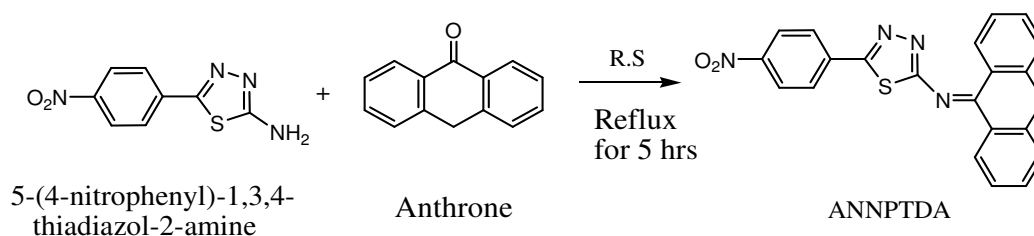


**Fig. 1.10:** Synthesis of ANNPTDA

Polynuclear Schiff base N-(anthracen-9(10H)-ylidene)-5-(4-nitrophenyl)-1,3,4-thiadiazol-2-amine (ANNPTDA) was synthesized by the condensation of equimolar mixture of 5-(4-nitrophenyl)-1,3,4-thiadiazol-2-amine and anthrone in ethanol medium. The reaction mixture was refluxed for 5h, concentrated, and cooled. Off-white coloured crystals of ANNPTDA was filtered, washed and dried and MP was 212<sup>0</sup>C (Yield: 75%)

#### Characterization of ANNPTDA

##### *Elemental analysis*

The elemental analysis data of polynuclear thiadiazole Schiff base ANNPTDA is

given in Table 1.6. The experimentally obtained percentages of elements like carbon, hydrogen, nitrogen and sulphur were in good agreement with the calculated values.

#### ***Electronic spectral analysis***

The electronic spectra of ANNPTDA contain two peaks; one at  $39062\text{cm}^{-1}$  corresponds to  $\pi \rightarrow \pi^*$  transition and the other at  $27174\text{cm}^{-1}$  corresponds to  $n \rightarrow \pi^*$  transition.

#### ***FTIR spectral analysis***

Stretching frequencies corresponding to different bonds in ANNPTDA were observed in its IR spectrum. Formation of C=N linkage was proved by the stretching vibration shown at  $1662\text{cm}^{-1}$ .  $\nu_{\text{C-H}}$  stretching frequencies of methylene group of anthrone ring were observed at 2924 and  $2875\text{cm}^{-1}$ . Two important peaks appeared at 1480 and  $1400\text{cm}^{-1}$  indicated the presence of nitro group in the molecule.  $\nu_{\text{C-H}}$  of aromatic ring was observed at  $3066\text{cm}^{-1}$ . C=C present in the aromatic rings displayed distinct peaks at 1597 and  $1510\text{cm}^{-1}$ . A clear broad signal obtained at  $3425\text{cm}^{-1}$  was due to the presence of N-H stretching frequency (tautomer). Emergence of new peaks appeared at  $1317\text{cm}^{-1}$  and  $1101\text{cm}^{-1}$  is a clear indication of C-N and C-S bond in the molecule. In plane and out of plane deformations were shown at  $933\text{cm}^{-1}$  and  $842,705\text{cm}^{-1}$  respectively.

#### ***NMR spectral analysis***

The  $^1\text{H}$  NMR spectrum of the Schiff base, ANNPTDA is shown in Fig. 1.11. All the ten different aromatic protons gave multiplets between 7.34-8.3 $\delta$  in the NMR spectrum. Sharp singlet at 4.3 $\delta$  can be assigned to the  $\text{CH}_2$  (methylene) proton in the anthrone ring. In DEPT-135 spectrum (Fig. 1.12), only one  $\text{CH}_2$  group in the anthrone ring gave an inverse peak at 62.13ppm. All other CH groups gave upward peaks

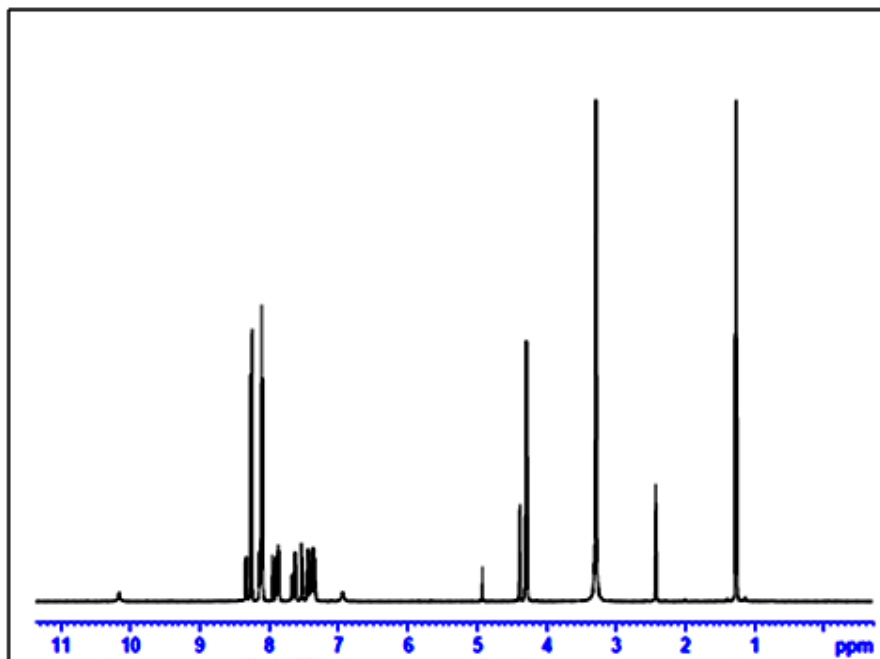


**Fig. 1.11:**  $^1\text{H}$  NMR spectrum of ANNPTDA

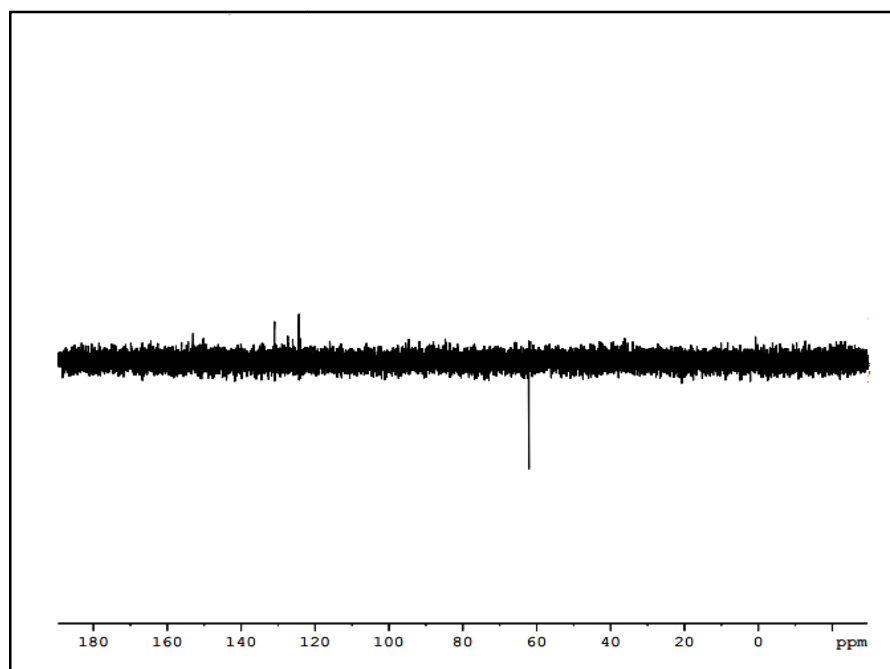


**Fig. 1.12:** DEPT-135 spectrum of ANNPTDA

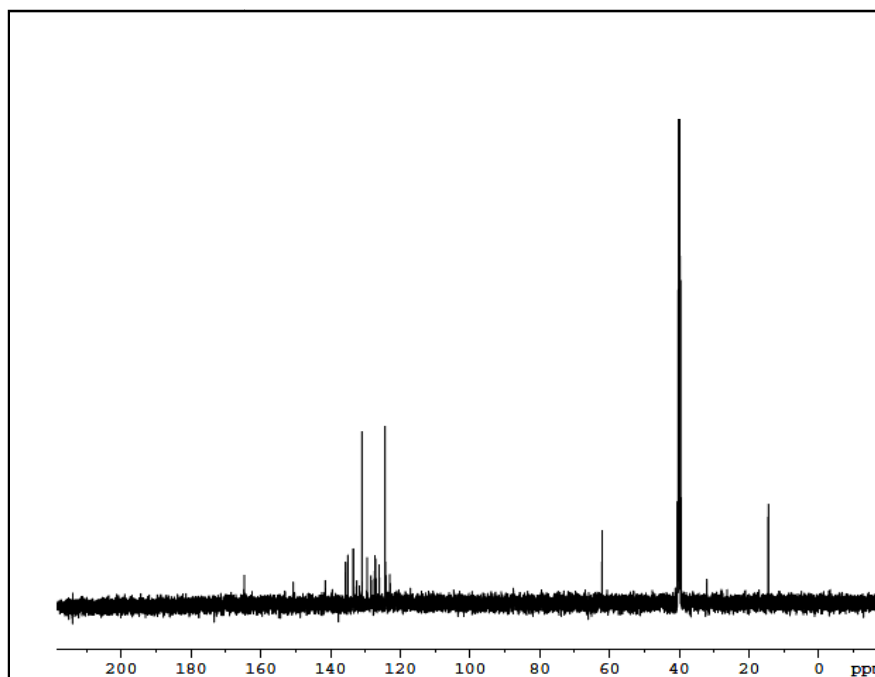


**Fig. 1.13:** <sup>13</sup>C NMR spectrum of ANNPTDA

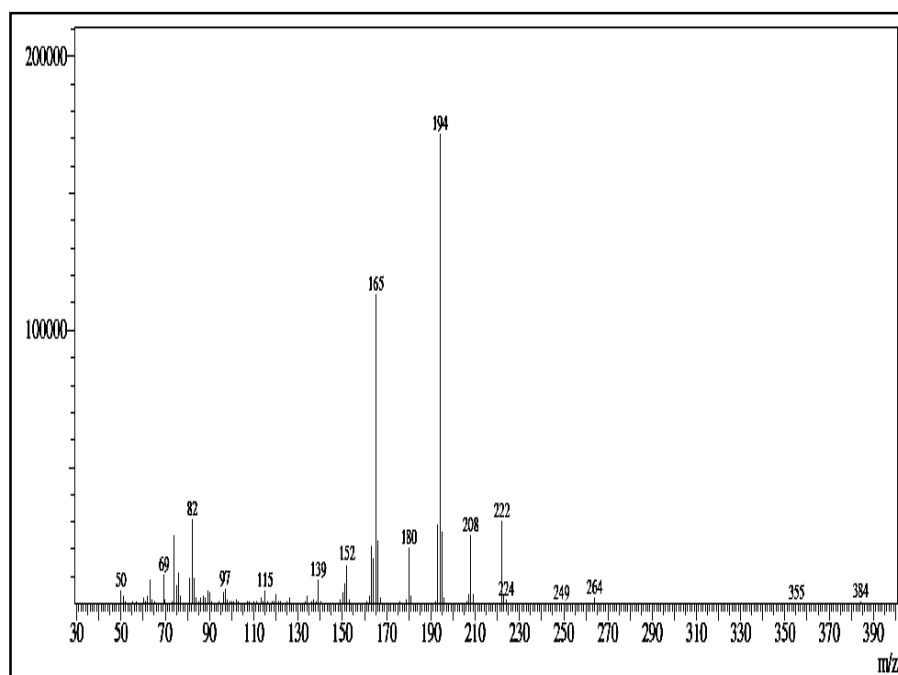


**Fig. 1.14:** Mass spectrum of ANNPTDA

The <sup>13</sup>C NMR spectrum of the Schiff base ANNPTDA is provided in Fig. 1.13. All seventeen different carbon atoms, which are sp<sup>2</sup> hybridized, gave 17 different peaks between 123-164ppm (17 different aromatic sp<sup>2</sup> C' atoms). Peak at 128ppm corresponds

to the carbon atom of azomethine group. Sharp peak at 39ppm corresponds to the carbon atom of CH<sub>2</sub> group in the anthrone ring.

### ***Mass spectral analysis***

In the mass spectrum of Schiff base ANNPTDA, signal of molecular ion was absent. A sharp base peak appeared at m/z 194 was due to the fragment [C<sub>14</sub>H<sub>13</sub> N]<sup>+</sup>. The fragment [C<sub>8</sub>H<sub>9</sub>N<sub>2</sub>S]<sup>+</sup> displayed signal at m/z 165. Mass spectrum of ligand is presented in Fig. 1.14.

From the above discussions, the structure of 'S' containing polynuclear Schiff base ANNPTDA was assigned and given in Fig. 1.15.

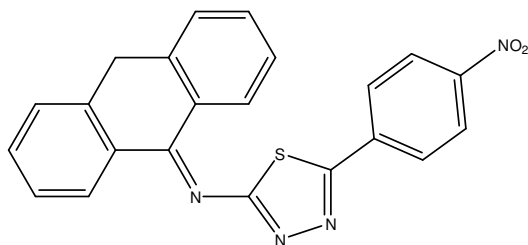


**Fig. 1.15:** Structure of ANNPTDA

### **Synthesis of Complexes**

The complexing capability of polynuclear thiadiazole Schiff base, ANNPTDA were checked with Cr(III), Ni(II), Cu(II), Zn(II) and ZrO(II) ions. Zirconyl nitrate is used for the synthesis of Zirconium complex. Acetate salts of other metal ions were used for the synthesis of respective complexes. The Schiff base ligand ANNPTDA (3mmol) was dissolved in minimum quantity of ethanol (15ml) and refluxed on a water bath (30min). Hot ethanolic solution of appropriate amount corresponding metal salt (acetate/nitrate) was added to the boiling medium and again refluxed for 6h. Then reduced its volume by evaporation, cooled and kept overnight and the crystallized metal complexes were collected, washed with water ethanol mixture and dried over CaCl<sub>2</sub>.

## Characterization of Complexes

Almost all the metal complexes of ANNPTDA were seen to be stable in air and light. They were soluble in aprotic polar solvents like DMF and DMSO. But their solubility was very less in organic solvents like diethyl ether, ethanol, chloroform, benzene, etc.

### *Elemental analysis*

Percentage of C, H, N and S as well as the metal content were estimated by microanalytical methods. 1:2 stoichiometry exist between Cr(III), Ni(II) and Cu(II) metal ions with the ligand ANNPTDA while 1:1 stoichiometry was displayed by Zn(II) and ZrO(II) ions with this ligand. The elemental and metal percentage data of the complexes obtained theoretically and experimentally are listed in Table 1.6. These values obtained are in good agreement with theoretical explanations.

### *Electronic spectral analysis*

In the case of complexes bathochromic shift occurred for these bands which are a clear evidence for the complex formation. The electronic bands are summarized in Table 1.5.

**Table 1.5:** Electronic spectral data of Schiff base, ANNPTDA and its transition metal complexes

Compound	Electronic bands in $\text{cm}^{-1}$	
	$\pi \rightarrow \pi^*$	$n \rightarrow \pi^*$
ANNPTDA	39062	27174
$[\text{CrL}_2(\text{Ac})_3\text{H}_2\text{O}]$	38461	26881
$[\text{NiL}_2(\text{Ac})_2(\text{H}_2\text{O})_2]$	38610	26595
$[\text{CuL}_2(\text{Ac})_2(\text{H}_2\text{O})_2]$	38610	26809
$[\text{ZnL}(\text{Ac})_2(\text{H}_2\text{O})]$	38461	27027
$[\text{ZrOL}(\text{NO}_3)_2(\text{H}_2\text{O})]$	38610	27027

The electronic spectra of all complexes of ANNPTDA mainly showed two peaks,  $n \rightarrow \pi^*$  and  $\pi \rightarrow \pi^*$ , which showed increase in  $\lambda_{\max}$  as compared to that of the ligand. This red shift confirms the extension of conjugation and hence the complexation. Other peaks due to charge transfer,  $\pi$  bonding etc. were less significant in the spectra.

### ***Magnetic moment analysis***

Information regarding the geometry of transition metal complexes were obtained by magnetic moment measurements. Effective magnetic moments of ANNPTDA-Complexes are displayed in Table 1.6. Cr(III), Ni(II) and Cu(II) complexes showed a slight increase in their  $\mu_{\text{eff}}$  values (4.02BM, 2.92BM and 2.25 BM respectively) compared to the theoretical values which lead to octahedral geometries of these complexes. This slight change in magnetic moment observed may be due to the contribution from the magnetic moment due to orbital motion of electrons. Diamagnetic magnetic moment are expected and confirmed for Zn(II) and ZrO(II) complexes due to  $d^{10}$  or  $d^0$  configuration respectively and assumed tetrahedral and square pyramidal geometry respectively.

### ***Molar conductance analysis***

Molar conductance measurement was done for all complexes and is given in Table 1.6. The molar conductance values of all the complexes were in the range of  $2\text{-}13\Omega^{-1}\text{cm}^2\text{mol}^{-1}$ . These values suggest non-electrolytic behaviour and absence of counter ions outside the coordination sphere of metal complexes.

### ***FTIR spectral analysis***

Significant infrared absorption frequencies ( $\text{cm}^{-1}$ ) of ANNPTDA and its transition metal complexes are summarized and distinguished in Table 1.7. In ANNPTDA-complexes the involvement of 'N' atom of azomethine linkage in coordination with metal was confirmed by the downward frequency shift from  $1662\text{cm}^{-1}$ . The presence of broad bands observed at  $3360$  and  $3319\text{cm}^{-1}$  in the infrared spectra of



Cr(III) and Ni(II) complexes respectively and new signals around  $3485\text{cm}^{-1}$ ,  $3391\text{cm}^{-1}$  and  $3347\text{cm}^{-1}$  in the spectra of Cu(II), Zn(II) and ZrO(II) complexes respectively confirmed the presence of coordinated water molecule in these complexes. Also, the appearance of stretching frequencies in the range  $690\text{-}694\text{cm}^{-1}$  and  $458\text{-}572\text{cm}^{-1}$  respectively corresponding to M-O and M-N bonds, confirmed the formation of ANNPTDA complexes. Cr(III), Ni(II), Cu(II) and Zn(II) complexes of ANNPTDA showed peaks around  $1595\text{cm}^{-1}$  and  $1700\text{cm}^{-1}$  due to symmetric and asymmetric stretching of monodentate acetate moieties. New additional bands displayed at  $1317\text{-}133\text{cm}^{-1}$  and  $1058\text{-}1101\text{cm}^{-1}$  indicated the stretching frequencies of C-N and C-S bonds in complexes.

Structures of transition metal complexes of ANNPTDA are depicted in Fig. 1.16. Ligand ANNPTDA was found to act as zerovalent unidentate moiety in all the complexes, coordinating only through azomethine nitrogen.

**Table 1.6:** Microanalytical, magnetic and conductance data of the ligand ANNPTDA and its transition metal complexes

Complex	Colour	Yield (%)	Mol. Wt.	M.P ( <sup>o</sup> C)	Metal% Found (Cald.)	C % Found (Cald.)	H % Found (Cald.)	N % Found (Cald.)	S % Found (Cald.)	$\mu_{\text{eff}}$ (BM)	Molar Conductance ( $\Omega^{-1}\text{cm}^2\text{mol}^{-1}$ )	Geometry
ANNPTDA (L)	Flesh coloured	75	398	212	-	65.18 (66.32)	3.12 (3.54)	14.83 (14.06)	7.98 (8.05)	-	-	-
[CrL <sub>2</sub> (Ac) <sub>3</sub> H <sub>2</sub> O]	Black	70	1043	280	5.4 (4.99)	55.19 (57.52)	3.01 (3.77)	10.18 (10.73)	5.66 (6.14)	4.02	9.7	Octahedral
[NiL <sub>2</sub> (Ac) <sub>2</sub> (H <sub>2</sub> O) <sub>2</sub> ]	Orange	50	1009	280	5.8 (5.84)	56.15 (57.1)	3.34 (3.79)	10.12 (11.1)	5.68 (6.35)	2.92	12.1	Octahedral
[CuL <sub>2</sub> (Ac) <sub>2</sub> (H <sub>2</sub> O) <sub>2</sub> ]	Brownish green	80	1014	>300	6.82 (6.31)	55.78 (56.83)	2.95 (3.78)	10.83 (11.04)	6.25 (6.32)	2.25	5.8	Octahedral
[ZnL(Ac) <sub>2</sub> (H <sub>2</sub> O)]	Black	70	599	240	9.99 (10.85)	51.52 (52.05)	2.81 (3.70)	8.37 (9.34)	4.44 (5.34)	D	10.9	Tetrahedral
[ZrOL(NO <sub>3</sub> ) <sub>2</sub> (H <sub>2</sub> O)]	Yellow	70	647	220	14.01 (14.07)	39.9 (40.8)	2.21 (2.49)	11.56 (12.98)	4.16 (4.95)	D	2.8	Square Pyramidal

**Table 1.7:** Characteristic infrared absorption frequencies ( $\text{cm}^{-1}$ ) of ANNPTDA and its transition metal complexes

Complex	$\nu_{\text{H}_2\text{O}}$	$\nu_{\text{COOasy}}$	$\nu_{\text{C=N}}$	$\nu_{\text{COOsy}}$	$\nu_{\text{C=C}}$	$\nu_{\text{NO}_2/\text{NO}_3}$	$\nu_{\text{C-N}}$	$\nu_{\text{C-S}}$	$\nu_{\text{M-O}}$	$\nu_{\text{M-N}}$
ANNPTDA (L)	-	-	1662	-	1510	1480 1400	1317	1101	-	-
[CrL <sub>2</sub> (Ac) <sub>3</sub> H <sub>2</sub> O]	3360(br)	1714	1660	1597	1522	1450 1411	1319	1101	694	506
[NiL <sub>2</sub> (Ac) <sub>2</sub> (H <sub>2</sub> O) <sub>2</sub> ]	3319(br)	1677	1661	1591	1512	1463 1401	1319	1095	692	458
[CuL <sub>2</sub> (Ac) <sub>2</sub> (H <sub>2</sub> O) <sub>2</sub> ]	3485	1686	1659	1595	1513	1462 1402	1318	1107	690	572
[ZnL(Ac) <sub>2</sub> (H <sub>2</sub> O)]	3391	1702	1627	1592	1497	1450 1393	1335	1058	690	491
[ZrOL(NO <sub>3</sub> ) <sub>2</sub> (H <sub>2</sub> O)]	3347	-	1658	-	1505	1462 1401 1349	1317	1093	688	571

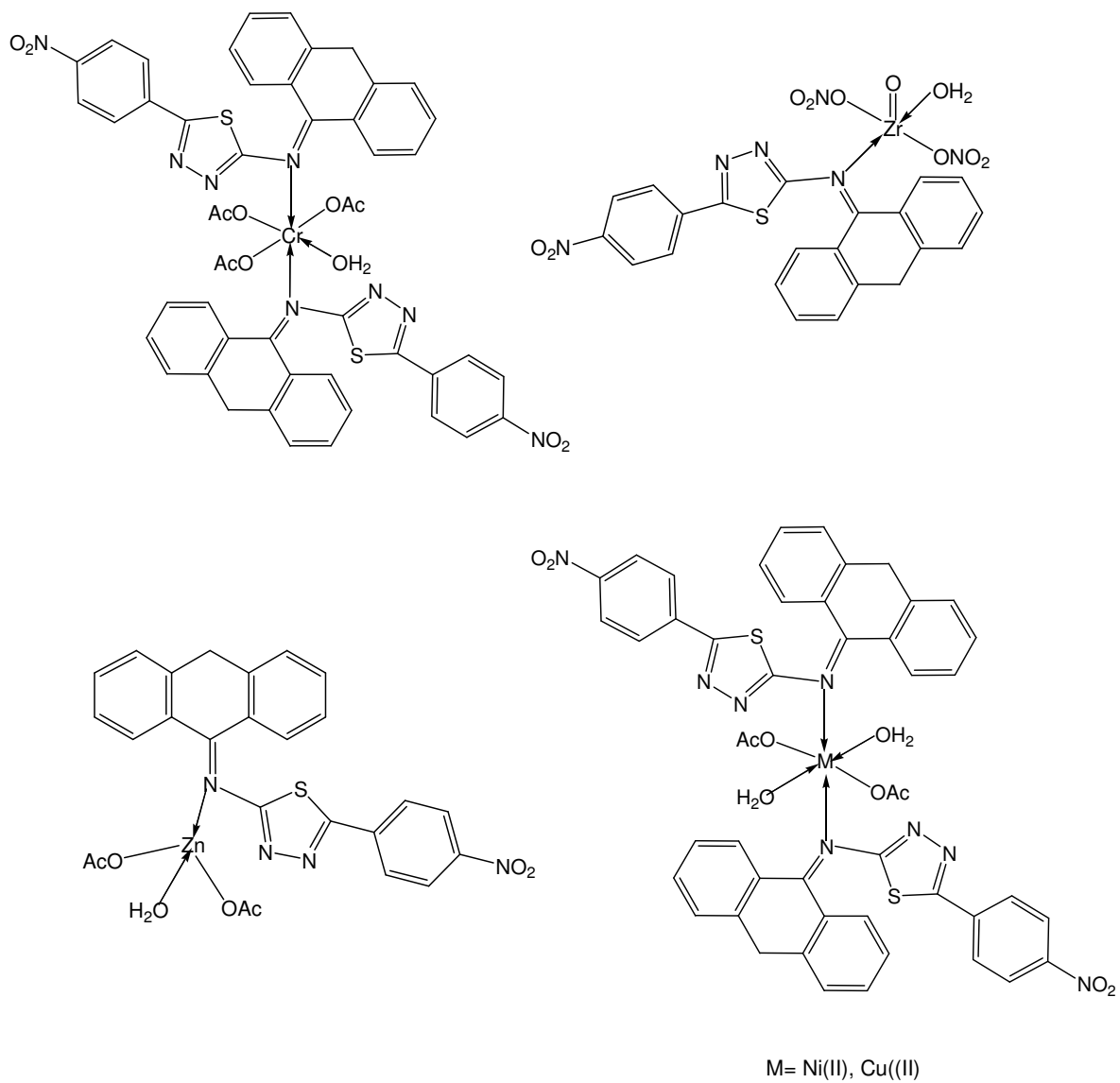


**Fig. 1.16:** Structures of transition metal complexes of ANNPTDA

## CHAPTER 4

### **TRANSITION METAL COMPLEXES OF SCHIFF BASES DERIVED FROM 5-(4-NITROPHENYL)-1,3,4-THIADIAZOL-2-AMINE (NPTDA) AND CARBONYL COMPOUNDS WITH PYRIDINE RING**

This chapter deals with the synthesis and characterization of novel 'S' containing pyridine derivative of thiadiazole Schiff bases (E)-5-(4-nitrophenyl)-N-((pyridine-2-yl)methylene)-1,3,4-thiadiazol-2-amine (P2CNPTDA), (E)-5-(4-nitrophenyl)-N-(1-(pyridine-3-yl)ethylidene)-1,3,4-thiadiazol-2-amine (3APNPTDA), (E)-5-(4-nitrophenyl)-N-(1(pyridin-2-yl)ethylidene)-1,3,4-thiadiazol-2-amine (2APNPTDA) and their transition metal complexes. Attempts to characterize the ligands and complexes were done with the aid of analytical tools such as elemental analysis, spectral studies such as Fourier transform infrared, UV-visible, NMR ( $^1\text{H}$  and  $^{13}\text{C}$ ), and mass spectroscopy. The detailed synthesis and characterization of these three novel 'S' containing pyridine derivatives of Schiff bases and their metallic complexes are discussed in detail as three separate sections in this chapter.

## SECTION I

### STUDIES ON SCHIFF BASE, (E)-5-(4-NITROPHENYL)-N-((PYRIDINE-2-YL)METHYLENE)-1,3,4-THIADIAZOL-2AMINE (P2CNPTDA) AND ITS TRANSITION METAL COMPLEXES

A novel thiadiazole based pyridine derivative of Schiff base (E)-5-(4-nitrophenyl)-N-((pyridine-2-yl)methylene)-1,3,4-thiadiazol-2amine (P2CNPTDA) was synthesized and characterized by elemental analysis and various spectroscopic techniques. The structure of the Schiff base, P2CNPTDA derived from NPTDA (parent amine) and pyridine 2-carbaldehyde and its transition metal complexes were established based on spectroscopic, magnetic and electrical studies. The detailed synthesis and characterization of the ligand P2CNPTDA and their transition metal complexes are discussed in this section..

#### Synthesis of P2CNPTDA

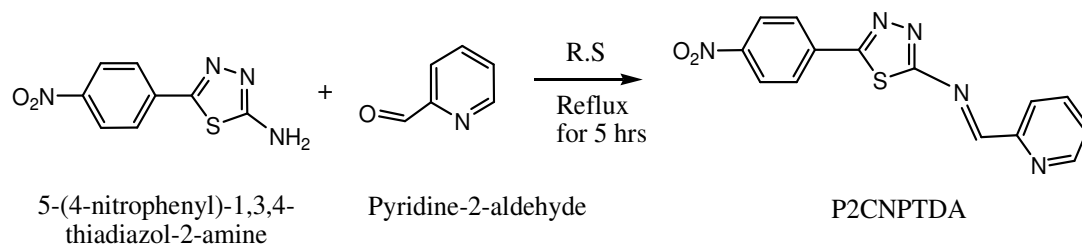


**Fig. 1.17:** Synthesis of P2CNPTDA

A hot ethanolic solution of pyridine 2-carbaldehyde was added to a refluxing solution of 5-(4-nitrophenyl)-1,3,4-thiadiazol-2-amine in ethanol and refluxed 5h on a water bath. The resulting solution was concentrated to obtain dark brown crystals of P2CNPTDA, which was filtered, washed and dried. Recrystallization from methanol gave 80 % yield of the desired product MP: 210<sup>0</sup>C

## Characterisation of P2CNPTDA

### *Elemental analysis*

Percentage of C, H, N and S were estimated by microanalytical methods. Calculated values of P2CNPTDA were in close agreement with experimental results.

### *Electronic spectral analysis*

In electronic spectrum recorded at a concentration of  $10^{-4}$ M in Shimadzu UV-Visible spectra, the ligand P2CNPTDA showed peaks at  $39062\text{cm}^{-1}$  and  $27560\text{cm}^{-1}$  due to  $\pi \rightarrow \pi^*$  and  $n \rightarrow \pi^*$  transitions. The decrease in the values compared to the parent amine, NPTDA indicates the extension of conjugation during the formation of the Schiff base P2CNPTDA.

### *FTIR spectral analysis*

Characterization of ligand, (E)-5-(4-nitrophenyl)-N-((pyridine-2-yl)methylene)-1,3,4-thiadiazol-2-amine was done using IR spectral data. The IR spectrum of this thiadiazole Schiff base, P2CNPTDA recognized the unique stretching and bending vibrational frequencies, as depicted in Table 1.9. The absorption bands due to N-H stretching frequency of amino group at  $3500\text{-}3200\text{cm}^{-1}$  was absent in the IR spectra of the P2CNPTDA, which proved the formation of Schiff base. An intense band observed at  $1629\text{cm}^{-1}$  was assigned to the stretching mode of azomethine linkage (C=N). The peaks at  $1595\text{cm}^{-1}$  and  $1510\text{cm}^{-1}$  can be consigned to C=C vibrations in aromatic rings. The aromatic C-H stretching frequency at  $3097\text{cm}^{-1}$ , C-S stretching frequencies at  $1103\text{cm}^{-1}$  and C-N stretching at  $1271\text{cm}^{-1}$  were clearly appeared in the spectra. There is a small change in the presence of nitro group by Schiff base formation; two peaks were present at  $1493\text{cm}^{-1}$  and  $1338\text{cm}^{-1}$  corresponds to N-O stretching frequency. In plane bending vibrations of the Schiff base P2CNPTDA were sighted at  $1082\text{cm}^{-1}$ . Also the peaks gained at  $850\text{cm}^{-1}$  and  $970\text{cm}^{-1}$  can be consigned as out of plane bending vibrations.

### *NMR spectral analysis*

Characteristics peak at 7.126 $\delta$  can be assigned to the azomethine proton. The aromatic protons both in the pyridine and benzene rings gave characteristic peaks between 8.02-8.32 $\delta$ . The  $^1\text{H}$  NMR spectrum of P2CNPTDA recorded in  $\text{dms}\text{-d}_6$  solvent on 400MHz-NMR instrument is displayed as Fig. 1.18.

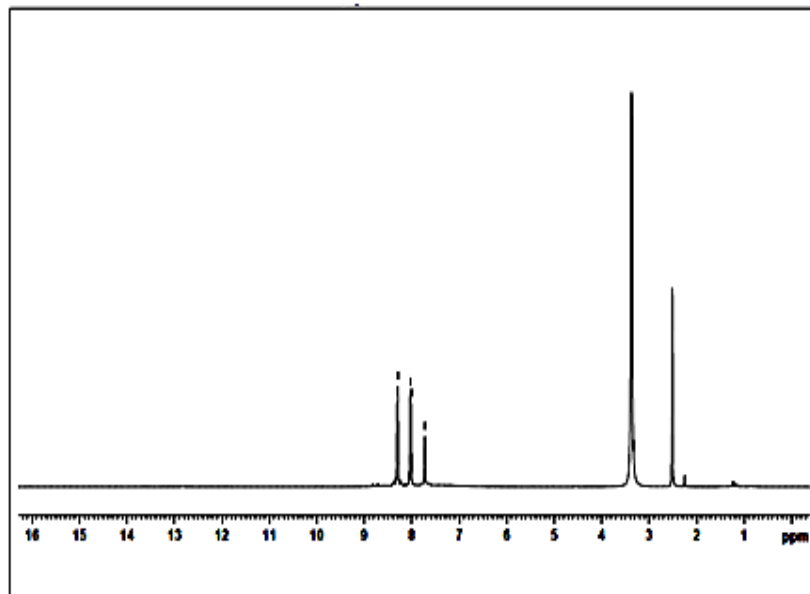


**Fig. 1.18:**  $^1\text{H}$  NMR spectrum of P2CNPTDA

The proton decoupled  $^{13}\text{C}$  NMR spectrum of P2CNPTDA is shown in Fig. 1.19. The carbon atom of the azomethine linkage was recognized at 147ppm. The aromatic carbons of the thiadiazole, benzene and pyridine rings exhibited four signals in the range 124-169ppm. The assignment of peaks to diverse carbon atoms of P2CNPTDA were shown in the  $^{13}\text{C}$  NMR spectrum.

### *Mass spectral analysis*

In gas chromatogram, there was only one distinct peak which authenticates the purity of the sample P2CNPTDA. Molecular ion peak ( $\text{M}^+$  peak) was absent but a clear base peak at  $m/z$  222 with high intensity observed corresponding to the fragment



$[\text{C}_8\text{H}_6\text{N}_4\text{O}_2\text{S}]^+$ , which is formed due to the loss of  $[\text{C}_6\text{H}_5\text{N}]^+$  from the ligand. The clear signal with high intensity appeared at  $m/z$  74 corresponding to the fragment,  $[\text{CH}_2\text{N}_2\text{S}]^+$ . The fragments  $[\text{C}_7\text{H}_4\text{NS}]^+$  and  $[\text{CH}_2\text{N}_2\text{S}]^+$  appeared at  $m/z$  134 and 120 respectively. Mass spectrum of P2CNPTDA is given as Fig. 1.20.

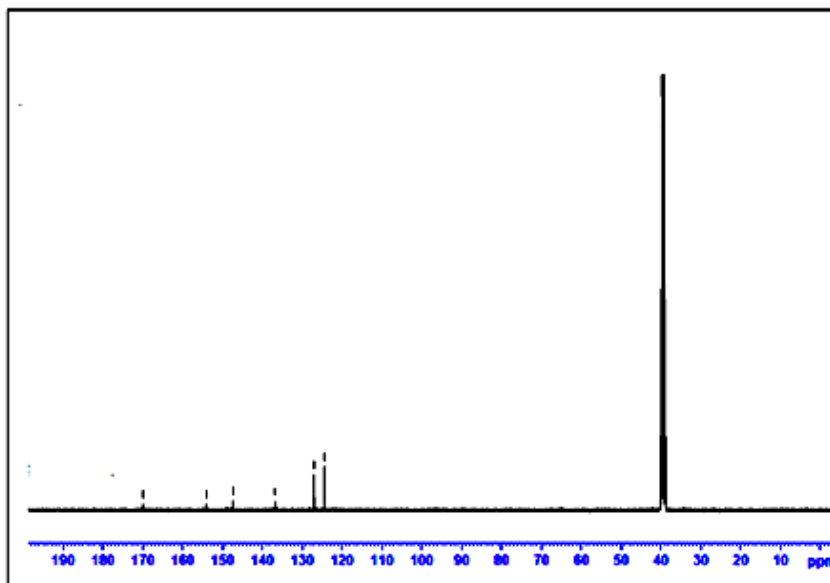


**Fig. 1.19:**  $^{13}\text{C}$  NMR spectrum of P2CNPTDA

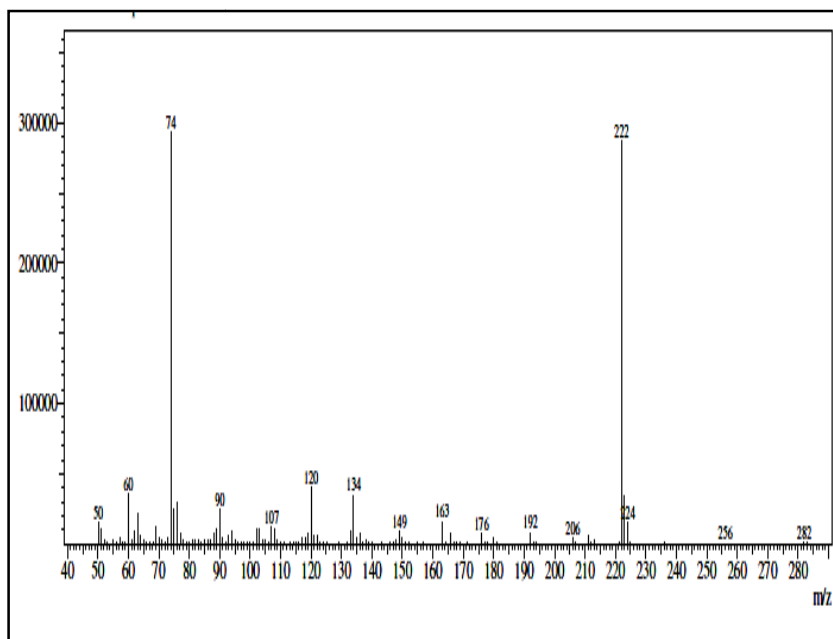


**Fig. 1.20:** Mass spectrum of P2CNPTDA

From the above discussions, the structure of 'S' containing Schiff base P2CNPTDA, derived from pyridine 2-carbaldehyde and NPTDA can be assigned and it is given in Fig. 1.21

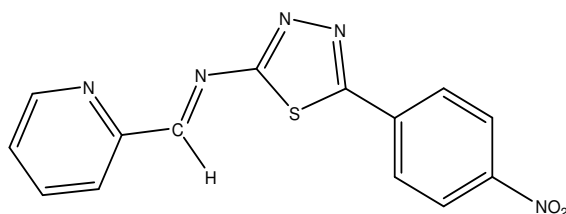


**Fig. 1.21:** Structure of P2CNPTDA

### Synthesis of Complexes

Copper complex was prepared by using cupric acetate. 2mmol ethanolic solution of NPTDA (5-(4-nitrophenyl)-1,3,4-thiadiazol-2-amine) and P2C (Pyridine2-carbaldehyde) (2mmol) were mixed together and adjusted the pH to 7-8 by the addition of sodium acetate to this mixture and the solution was then refluxed for 5h. The reaction mixture was kept overnight and the complex was precipitated as brown coloured crystals. Filtered, washed with ethanol and warm water, dried and melting point was determined.

Nickel acetate, zinc acetate, ferric chloride, zirconyl nitrate and cadmium nitrate were used for the preparation of Ni(II), Zn(II), Fe (III), ZrO(II) and Cd(II) complexes. The procedure taken up for the preparation of the complexes was the same as that employed for Cu(II) complex synthesis. (Yield: 40-80%).

### Characterisation of Complexes

All complexes of P2CNPTDA are stable amorphous powder having high melting points and they are highly soluble in organic solvents (DMSO, DMF, CHCl<sub>3</sub>) and insoluble in water. There is a good correlation between observed and calculated values of elemental analysis and 1:1 stoichiometry exists between metal and ligand

### *Electronic spectral analysis*

In the case of complexes the electronic bands due to K band and R band are found to shift to higher wavelength. This is a clear proof for the formation of complexes. The electronic spectral bands of the Schiff base, P2CNPTDA and its complexes are summarized in Table 1.8.

**Table 1.8:** Electronic spectral data of Schiff base, P2CNPTDA and its transition metal complexes

Compound	Electronic bands in $\text{cm}^{-1}$	
	$\pi \rightarrow \pi^*$	$n \rightarrow \pi^*$
P2CNPTDA	39062	31949
[FeLCl <sub>3</sub> (H <sub>2</sub> O)]	38167	27472
[NiL(Ac) <sub>2</sub> (H <sub>2</sub> O) <sub>2</sub> ]	37878	27777
[CuL(Ac) <sub>2</sub> (H <sub>2</sub> O) <sub>2</sub> ]	38167	30487
[ZnL(Ac) <sub>2</sub> ]	38610	26954
[CdL(NO <sub>3</sub> ) <sub>2</sub> ]	38610	27548
[ZrOL(NO <sub>3</sub> ) <sub>2</sub> ]	38610	27027

### *Magnetic moment analysis*

Measurements of the values of magnetic susceptibility of the complexes offered strong support for determining the exact geometry. The effective magnetic moment data of P2CNPTDA-complexes are shown in Table 1.9. Ni(II) and Cu(II) complexes of P2CNPTDA were assigned octahedral structure because they showed magnetic moment values 2.43BM and 1.92BM respectively. Fe-P2CNPTDA chelate displayed magnetic moment value of 4.84BM, which may be due to antiferromagnetic exchange in this complex. Diamagnetic character was found for Zn(II), Cd(II) and ZrO(II) complexes, which is quite justifiable with the absence of unpaired electron ( $d^{10}$  or  $d^0$ ) in their electronic configuration

### ***Molar conductance analysis***

Molar conductance measurement was done for all complexes and is given in Table 1.9. Molar conductance values of the complexes are in the range of  $3.3\text{-}17.4\Omega^{-1}\text{cm}^2\text{mol}^{-1}$ . These values suggest the non-electrolytic behavior of the complexes.

### ***FTIR spectral analysis***

In complexes a considerable lowering of stretching frequencies of the azomethine group (from  $1629\text{cm}^{-1}$ ) was observed due to the involvement of azomethine nitrogen of this heterocyclic ligand P2CNPTDA in complexation. Additional broad bands appeared in Fe(III), Ni(II) and Cu(II) complexes in the range  $3280\text{-}3421\text{cm}^{-1}$  implies the coordination of water molecules in the complexes. In ZrO(II) and Cd(II) complexes of P2CNPTDA, three additional bands were observed for N-O stretching frequency, which corresponds to monodentate nitrate group. Appearance of additional M-N and M-O bands in the spectrum of complexes proves the coordination of N and O atom to the metal. Ni(II), Cu(II) and Zn(II) complexes of P2CNPTDA showed peaks in the range  $1683\text{-}1698\text{cm}^{-1}$  and  $1593\text{-}1599\text{cm}^{-1}$  due to asymmetric and symmetric stretching of monodentate acetate moieties respectively. In Cd(II) and ZrO(II) complexes, three bands appeared for N-O bond with a difference of  $145\text{cm}^{-1}$  correspond to monodentate nitrate group. A peak at  $494\text{cm}^{-1}$  in the spectrum of iron complex can be assigned to M-Cl stretching. In all complexes, peaks due to C-N and C-S stretching frequencies were appeared in the range  $1271\text{-}1272\text{cm}^{-1}$  and  $1095\text{-}1108\text{cm}^{-1}$  respectively. Characteristic infrared absorption frequencies of P2CNPTDA and its transition metal complexes are given in Table 1.10.

Structures of the transition metal complexes of P2CNPTDA derived based on elemental, spectral, magnetic and electronic studies are represented in Fig. 1.22.

**Table 1.9:** Microanalytical, magnetic and conductance data of the ligand P2CNPTDA and its transition metal complexes

Complex	Colour	Yield (%)	Mol. Wt.	M.P (°C)	Metal% Found (Cald.)	C % Found (Cald.)	H % Found (Cald.)	N % Found (Cald.)	S% Found (Cald.)	$\mu_{\text{eff}}$ (BM)	Molar Conductance ( $\Omega^{-1}\text{cm}^2\text{mol}^{-1}$ )	Geometry
P2CNPTDA (L)	Dark brown	70	311	208	-	52.23 (54.01)	2.07 (2.91)	21.18 (22.5)	9.66 (10.3)	-	-	-
[FeLCl <sub>3</sub> (H <sub>2</sub> O)]	Dark Brown	40	492	280	10.96 (11.38)	33.88 (34.21)	2.19 (2.26)	13.26 (14.25)	6.52 (6.52)	4.84	9.2	Distorted Octahedral
[NiL(Ac) <sub>2</sub> (H <sub>2</sub> O) <sub>2</sub> ]	Dark Yellow	50	524	280	11.07 (11.26)	41.54 (43.59)	3.35 (3.49)	10.94 (11.55)	4.68 (5.29)	2.43	8.8	Octahedral
[CuL(Ac) <sub>2</sub> (H <sub>2</sub> O) <sub>2</sub> ]	Coffee brown	80	529	>300	12.48 (12.1)	42.07 (43.24)	3.38 (3.46)	11.12 (11.46)	5.32 (5.25)	1.92	5.7	Octahedral
[ZnL(Ac) <sub>2</sub> ]	Yellow	85	494	250	15.12 (13.68)	26.15 (28.31)	1.71 (1.78)	10.24 (10.32)	4.64 (4.72)	D	3.3	Tetrahedral
[CdL(NO <sub>3</sub> ) <sub>2</sub> ]	Yellow	60	547	235	21.14 (20.48)	30.82 (32.01)	2.12 (2.15)	17.45 (17.42)	5.56 (5.7)	D	17.4	Tetrahedral
[ZrOL(NO <sub>3</sub> ) <sub>2</sub> ]	Slight yellow	80	542	>310	17.15 (16.79)	30.18 (33.56)	2.18 (2.64)	15.95 (17.12)	15.68 (15.93)	D	4.4	Square Pyramidal

**Table 1.10:** Characteristic infrared absorption frequencies ( $\text{cm}^{-1}$ ) of P2CNPTDA and its transition metal complexes

Complex	$\nu_{\text{H}_2\text{O}}$	$\nu_{\text{COOasy}}$	$\nu_{\text{C=N}}$	$\nu_{\text{COOsy}}$	$\nu_{\text{C=C}}$	$\nu_{\text{NO}_2/\text{NO}_3}$	$\nu_{\text{M-O}}$	$\nu_{\text{C-N}}$	$\nu_{\text{C-S}}$	$\nu_{\text{M-N}}$
P2CNPTDA (L)	-	-	1629	-	1510	1493 1338	-	1271	1103	-
[FeLCl <sub>3</sub> (H <sub>2</sub> O)]	3280	-	1626	-	1504	1340	638	1264	1108	494
[NiL(Ac) <sub>2</sub> (H <sub>2</sub> O) <sub>2</sub> ]	3421	1683	1625	1595	1505	1498 1339	610	1271	1104	493
[CuL(Ac) <sub>2</sub> (H <sub>2</sub> O) <sub>2</sub> ]	3410	1698	1624	1593	1516	1437 1333	634	1247	1095	490
[ZnL(Ac) <sub>2</sub> ]	-	1689	1625	1599	1523	1490 1348	646	1271	1103	495
[CdL(NO <sub>3</sub> ) <sub>2</sub> ]	-	-	1621	-	1539	1503 1487 1363	657	1271	1108	476
[ZrOL(NO <sub>3</sub> ) <sub>2</sub> ]	-	-	1595	-	1504	1496 1428 1339	687	1272	1103	464

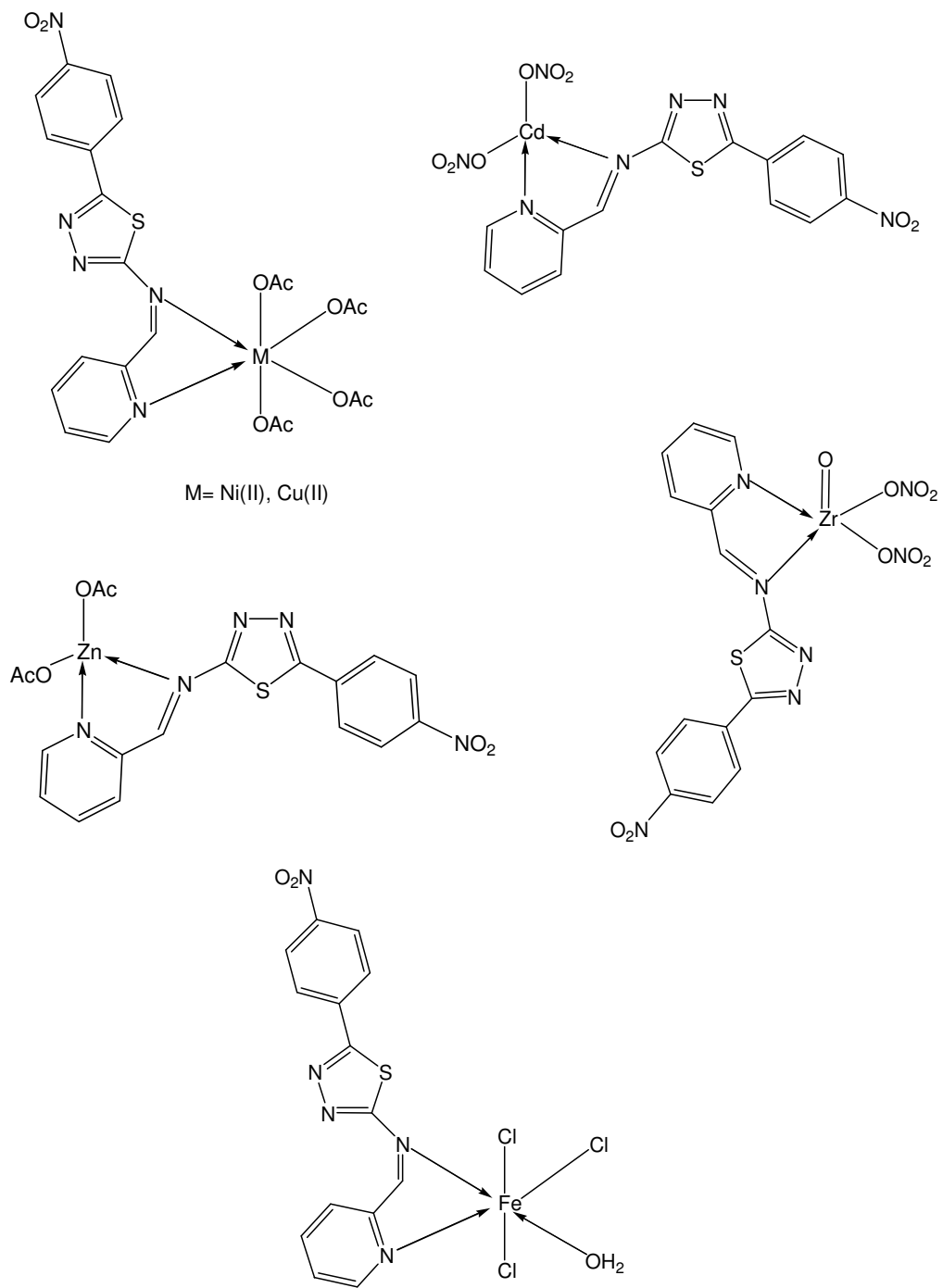


**Fig. 1.22:** Structures of transition metal complexes of P2CNPTDA

## SECTION II

### STUDIES ON SCHIFF BASE (E)-5-(4-NITROPHENYL)-N-(1(PYRIDINE-3-YL)ETHYLIDENE)-1,3,4THIADIAZOL-2-AMINE (3APNPTDA) AND ITS TRANSITION METAL COMPLEXES

Heterocyclic sulphur containing Schiff base, (E)-5-(4-nitrophenyl)-N-(1-(pyridine-3-yl)ethylidene)-1,3,4-thiadiazol-2-amine (3APNPTDA), derived from 3-acetyl pyridine and the parent amine NPTDA was prepared and its ability to form metal chelates was established by synthesizing transition metal complexes. Formulation of the structures and geometries of the synthesized ligand and complexes were made based on spectral, magnetic, electronic and elemental data.

#### Synthesis of 3APNPTDA

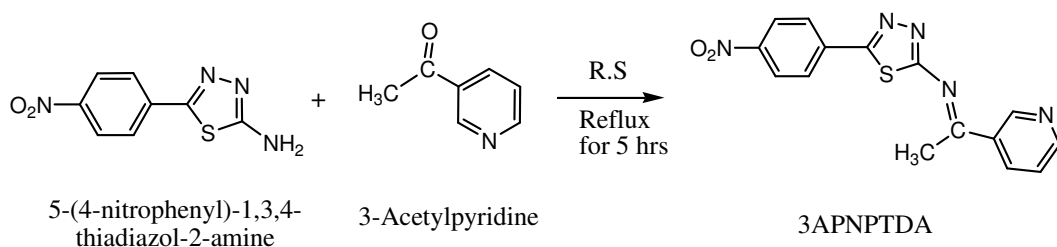


**Fig. 1.23:** Synthesis of 3APNPTDA

A hot ethanolic solution of 3-acetylpyridine was added to a refluxing solution of 5-(4-nitrophenyl)-1,3,4-thiadiazol-2-amine in ethanol and refluxed 5h on a water bath. The resulting solution was concentrated in order to obtain yellow crystals, which was collected and washed with ethanol. Recrystallization from ethanol gave 70% yield of the desired product. MP: 235°C.



## Characterisation of 3APNPTDA

### *Elemental analysis*

The elemental analysis data of thiadiazole pyridine derivative, 3APNPTDA is given in Table 1.12. The experimentally obtained percentages of elements like carbon, hydrogen, nitrogen and sulphur were in good agreement with the calculated

### *Electronic spectral analysis*

Two characteristic absorption bands were observed in the UV-visible spectrum of the Schiff base, 3APNPTDA. In the  $\pi \rightarrow \pi^*$  region one characteristic band exhibited at  $38910\text{cm}^{-1}$ . The  $n \rightarrow \pi^*$  electronic transition was observed at  $26954\text{cm}^{-1}$  with relatively low intensity, as it is spectroscopically forbidden.

### *FTIR spectral analysis*

The characteristic group especially the functional groups of the Schiff base 3APNPTDA were established by using IR spectral data. A strong band appeared in the IR spectrum at  $1593\text{cm}^{-1}$  can be assigned to stretching frequency of azomethine (C=N) group. The peak at  $1506\text{cm}^{-1}$  can be consigned to C=C vibrations in aromatic rings. Aromatic C-H stretching frequency was found at  $3107\text{cm}^{-1}$  and C-N stretching appeared as a strong band at  $1232\text{cm}^{-1}$ . Another peak at  $2924\text{cm}^{-1}$  was an indication of the C-H stretching frequency of  $\text{CH}_3$  group. The presence of nitro group was confirmed by the appearance of the peaks at  $1342\text{cm}^{-1}$  and  $1301\text{cm}^{-1}$ . The peak found at  $1105\text{cm}^{-1}$  was due to the C-S linkage. In plane bending vibrations come into sighted at  $1068\text{cm}^{-1}$ . Also the peaks gained at  $970\text{cm}^{-1}$  and  $854\text{cm}^{-1}$  can be consigned as out of plane bending vibrations.

### *NMR spectral analysis*

The  $^1\text{H}$  NMR spectrum of the pyridine derivative 3APNPTDA, derived from 3-acetyl pyridine and the parent amine, NPTDA is shown in Fig. 1.24. The methyl group

at acetyl moiety appeared as a singlet signal at 2.6 $\delta$ . The aromatic protons of anthracene and pyridine rings resonated between 7.75-8.30 $\delta$ .

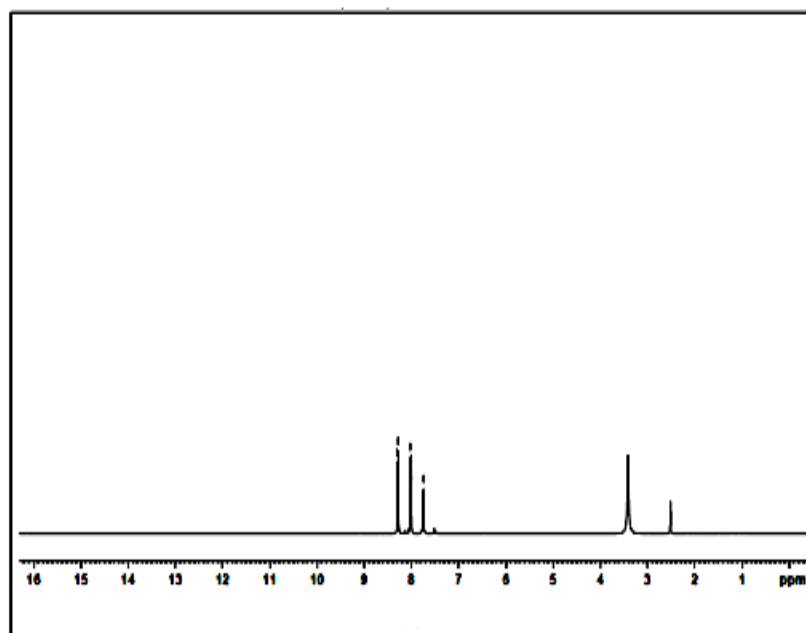


**Fig. 1.24:**  $^1\text{H}$  NMR spectrum of 3APNPTDA

Characteristics  $^{13}\text{C}$  NMR spectrum of Schiff base 3APNPTDA is shown in Fig. 1.25. Methyl C atom observed as a sharp signal at 39ppm. All other carbon atoms in the aromatic rings observed in the range 124-169ppm

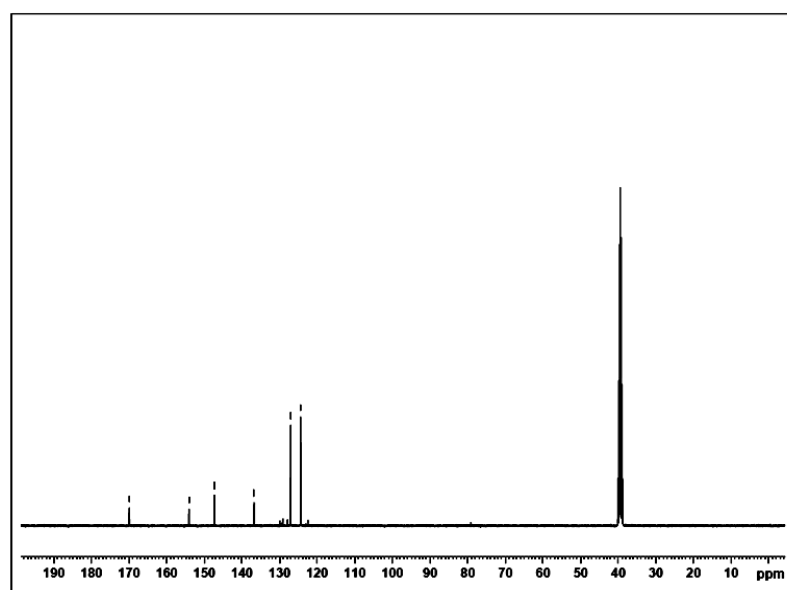


**Fig. 1.25:**  $^{13}\text{C}$  NMR spectrum of 3APNPTDA

### Mass spectral analysis

Only one distinct peak was appeared in the gas chromatogram of the sample which establish the purity of the compound 3APNPTDA. Molecular ion peak ( $M^+$  peak) was absent but a clear base peak with high intensity observed at  $m/z$  74 corresponding to the fragment  $[CH_2N_2S]^+$ . Another peak at  $m/z$  222 monitored  $[C_8H_6N_4O_2S]^+$  with high intensity, which is formed due to the loss of 3-acetyl pyridine part from the ligand 3APNPTDA. Other signals appeared at  $m/z$  134, 120 and 60 were assigned due to the fragments  $[C_7H_4N_2S]^+$ ,  $[C_7H_4S]^+$  and  $[CH_2NS]^+$  respectively. Mass spectrum of 3APNPTDA is shown in Fig. 1.26.

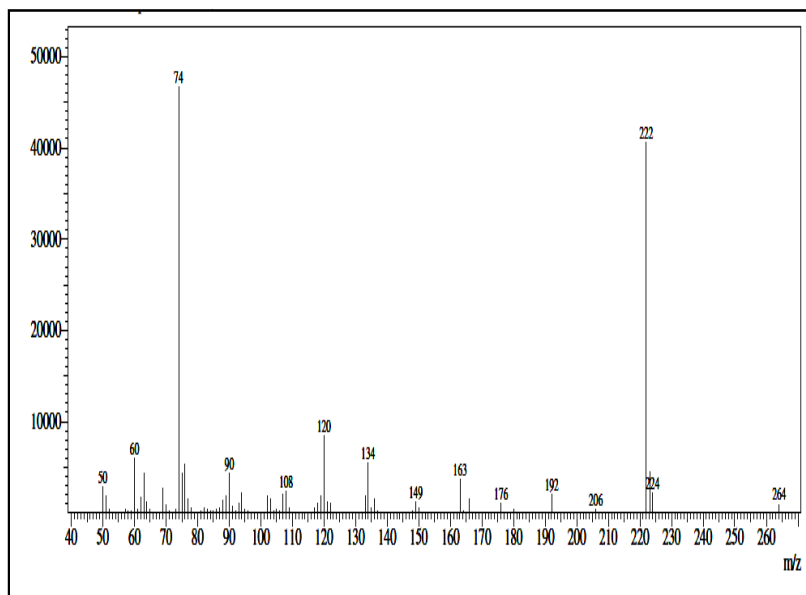


**Fig. 1.26:** Mass spectrum of 3APNPTDA

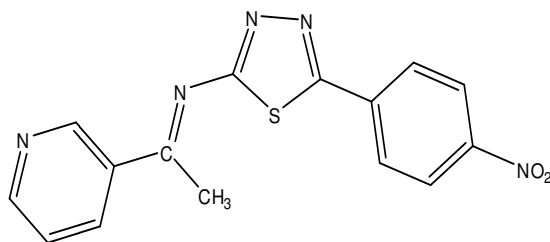


**Fig. 1.27:** Structure of 3APNPTDA

## Synthesis of Complexes

The ethanolic solution of chromium(III) acetate, manganese(II) acetate, ferric(III) chloride, nickel(II) acetate, copper(II) acetate, zinc(II) chloride and zirconyl nitrate was added dropwise to the hot ethanolic solution of 3-acetyl pyridine derivative of 'S' containing Schiff base 3APNPTDA in 1:1 molar ratio and refluxed this mixture to about seven hours and concentrated. The resulting crystals were collected, washed with ethanol and hot water and dried (Yield = 50-75%).

## Characterisation of Complexes

There is a good correlation between observed and calculated values of elemental analysis and 1:1 stoichiometry was exist between metal and ligand in all complexes. All the complexes of 3APNPTDA are stable amorphous powder and it is soluble in organic solvents like DMSO,  $\text{CHCl}_3$  and DMF and insoluble in water. Physical properties of all complexes were studied and tabulated in Table 1.12.

### *Electronic spectral analysis*

Electronic spectra of complexes prepared showed two characteristic peaks corresponding to  $\pi \rightarrow \pi^*$  and  $n \rightarrow \pi^*$  transitions.

**Table 1.11:** Electronic spectral data of Schiff base, 3APNPTDA and its transition metal complexes

Compound	Electronic bands in $\text{cm}^{-1}$	
	$\pi \rightarrow \pi^*$	$n \rightarrow \pi^*$
3APNPTDA	38910	26954
$[\text{CrL}(\text{Ac})_3\text{H}_2\text{O}]$	38610	26809
$[\text{MnL}(\text{Ac})_2(\text{H}_2\text{O})_2]$	37313	26455
$[\text{FeLCl}_3(\text{H}_2\text{O})]$	38610	26385
$[\text{NiL}(\text{Ac})_2(\text{H}_2\text{O})_2]$	37235	26455
$[\text{CuL}(\text{Ac})_2(\text{H}_2\text{O})_2]$	38610	26809
$[\text{ZnLCl}_2]$	37174	26666
$[\text{ZrOL}(\text{NO}_3)_2]$	38660	26455

Both the peaks exhibited a downward shift in frequency during Schiff base formation and complexation due to increased conjugation. The electronic bands are summarized and characteristic IR absorption bands are given in Table 1.11. This is clear proof for the formation of complexes.

#### ***Magnetic moment analysis***

Measurements of the values of magnetic susceptibility of the complexes offered strong support for determining the exact geometry. The effective magnetic moment data of 3APNPTDA-complexes are shown in Table 1.12. Cr(III), Mn(II), Fe(III), Ni(II) and Cu(II) complexes of 3APNPTDA were assigned octahedral structure because they showed magnetic moment values 3.92BM, 5.85BM and 1.83BM respectively. Fe-3APNPTDA chelate displayed low magnetic moment value of 5.02BM, which may be due to antiferromagnetic exchange in this complex. A slight increase in the magnetic moment showed by Ni-3APNPTDA (3.15BM) from the theoretical value (2.87BM) is mainly due to spin-orbit coupling. Diamagnetic character was found for Zn(II) and ZrO(II) complexes, which is quite justifiable with the absence of unpaired electron ( $d^{10}$  or  $d^0$ ) in its configuration

#### ***Molar conductance analysis***

Molar conductance measurement was done for all complexes and is given in Table 1.12. Molar conductance values of the complexes are in the range of  $6-28\Omega^{-1}\text{cm}^2\text{mol}^{-1}$ . These values suggest non-electrolytic behavior and absence of counter ions outside the coordination sphere of metal chelates.

#### ***FTIR spectral analysis***

Infrared spectra can be utilized mainly for analyzing the coordination sites of the ligand. In 3APNPTDA complexes, the stretching frequencies of the azomethine linkage showed a downward shift during complexation due to the decreased electron density at

azomethine group. Additional bands in the range 3245-3423 $\text{cm}^{-1}$  implies the coordination of water molecules in the complexes and 1310-1472 $\text{cm}^{-1}$  implies the coordination of nitrate molecules respectively. C-N and C-S stretching frequency shown in the region of 1272-1279 $\text{cm}^{-1}$  and 1100-1126 $\text{cm}^{-1}$  respectively. Appearance of M-O and M-N bands in the spectrum clarify the coordination of O and N atom to the metal. Cr(III), Mn(II), Ni(II) and Cu(II) complexes of 3APNPTDA showed peaks in the range 1629-1693 $\text{cm}^{-1}$  and 1514-1557 $\text{cm}^{-1}$  due to asymmetric and symmetric stretching of monodentate acetate moieties. In ZrO(II) complex, three bands appeared for N-O bond with a difference of 160 $\text{cm}^{-1}$  correspond to monodentate nitrate group. A peak at 468 $\text{cm}^{-1}$  in the spectrum of 3APNPTDA-Zn complex can be assigned to Zn-Cl stretching. Characteristic infrared absorption frequencies ( $\text{cm}^{-1}$ ) of 3APNPTDA and its transition metal complexes are given in Table 1.13.

Electrical, magnetic and spectral studies revealed that all these complexes are neutral having 1:1 stoichiometry between ligand and metal. The structures of complexes derived are represented in Fig. 1.28.

**Table 1.12:** Microanalytical, magnetic and conductance data of the ligand 3APNPTDA and its transition metal complexes

Complex	Colour	Yield (%)	Mol. Wt.	M.P ( <sup>o</sup> C)	Metal % Found (Cald.)	C % Found (Cald.)	H % Found (Cald.)	N % Found (Cald.)	S % Found (Cald.)	$\mu_{\text{eff}}$ (BM)	Molar Conductance ( $\Omega^{-1}\text{cm}^2\text{mol}^{-1}$ )	Geometry
3APNPTDA (L)	Yellow	70	325	230	-	55.12 (55.38)	3.18 (3.41)	20.24 (21.53)	9.15 (9.86)	-	-	-
[CrL(Ac) <sub>3</sub> H <sub>2</sub> O]	Light Green	60	572	280	9.87 (9.09)	42.58 (44.97)	3.72 (4.29)	11.14 (11.92)	5.44 (5.46)	3.92	28.0	Octahedral
[MnL(Ac) <sub>2</sub> (H <sub>2</sub> O) <sub>2</sub> ]	Black	65	534	>320	9.98 (10.29)	41.12 (42.70)	3.41 (3.96)	12.60 (13.11)	5.38 (6.0)	5.85	19.2	Octahedral
[FeLCl <sub>3</sub> (H <sub>2</sub> O)]	Dark Yellow	70	506	>310	10.55 (11.07)	34.71 (35.64)	2.03 (2.59)	12.18 (13.85)	6.02 (6.34)	5.02	12.7	Octahedral
[NiL(Ac) <sub>2</sub> (H <sub>2</sub> O) <sub>2</sub> ]	Yellowish Orange	75	538	>320	11.66 (10.97)	41.17 (42.40)	3.65 (3.93)	12.22 (13.01)	5.77 (5.96)	3.15	19.0	Octahedral
[CuL(Ac) <sub>2</sub> (H <sub>2</sub> O) <sub>2</sub> ]	Black	70	543	>310	12.27 (11.79)	40.13 (42.03)	2.80 (3.9)	11.53 (12.9)	5.41 (5.91)	1.83	19.4	Octahedral
[ZnLCl <sub>2</sub> ]	Cream	60	461	260	14.73 (14.10)	36.69 (39.03)	2.16 (2.40)	13.79 (15.17)	5.64 (6.95)	D	9.7	Tetrahedral
[ZrOL(NO <sub>3</sub> ) <sub>2</sub> ]	Orange needle	60	556	242	17.02 (16.37)	30.00 ((32.37)	1.45 (1.99)	16.90 (17.62)	5.09 (5.76)	D	6.8	Square Pyramidal

**Table 1.13:** Characteristic infrared absorption frequencies ( $\text{cm}^{-1}$ ) of 3APNPTDA and its transition metal complexes

Complex	$\nu_{\text{H}_2\text{O}}$	$\nu_{\text{COOAsy}}$	$\nu_{\text{C=N}}$	$\nu_{\text{COOsy}}$	$\nu_{\text{C=C}}$	$\nu_{\text{NO}_2/\text{NO}_3}$	$\nu_{\text{C-N}}$	$\nu_{\text{C-S}}$	$\nu_{\text{M-O}}$	$\nu_{\text{M-N}}$
3APNPTDA (L)	-	-	1593	-	1506	1342 1301	1232	1105	-	-
[CrL(Ac) <sub>3</sub> (H <sub>2</sub> O)]	3363	1687	1587	1557	1505	1364 1335	1272	1126	620	526
[MnL(Ac) <sub>2</sub> (H <sub>2</sub> O) <sub>2</sub> ]	3245	1647	1586	1515	1503	1340 1317	1273	1102	617	506
[FeLCl <sub>3</sub> (H <sub>2</sub> O)]	3285	-	1586	-	1505	1430 1315	1276	1104	610	494
[NiL(Ac) <sub>2</sub> (H <sub>2</sub> O) <sub>2</sub> ]	3423	1629	1590	1514	1502	1338 1310	1279	1100	618	509
[CuL(Ac) <sub>2</sub> (H <sub>2</sub> O) <sub>2</sub> ]	3385	1693	1559	1528	1505	1403 1347	1273	1106	589	478
[ZnLCl <sub>2</sub> ]	-	-	1572	-	1512	1428 1348	1272	1103	603	468 M-Cl
[ZrOL(NO <sub>3</sub> ) <sub>2</sub> ]	-	-	1544	-	1514	1472 1344 1310	1273	1105	675	586



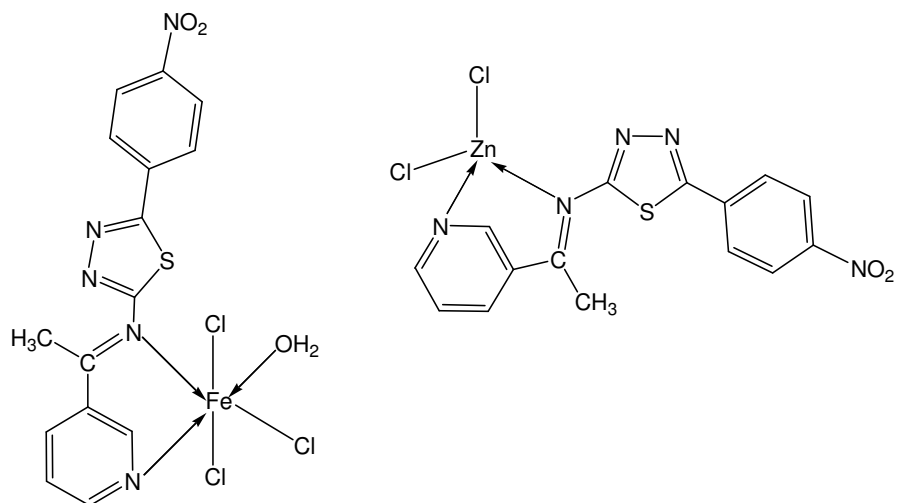
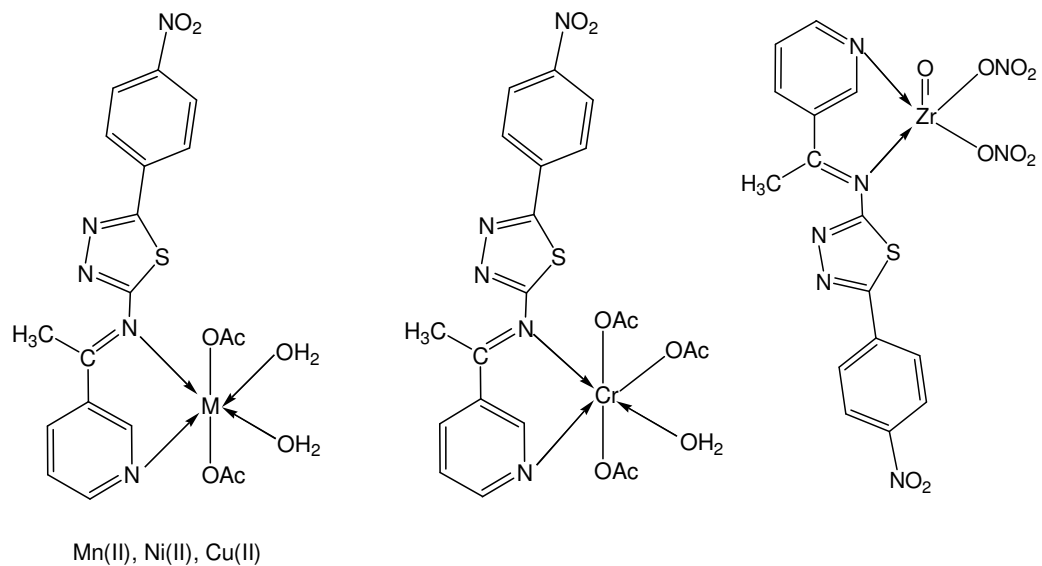


**Fig. 1.28:** Structures of transition metal complexes of 3APNPTDA

### SECTION III

#### STUDIES ON SCHIFF BASE (E)-5-(4-NITROPHENYL)-N-(1(PYRIDIN-2-YL)ETHYLIDENE)-1,3,4-THIADIAZOL-2-AMINE (2APNPTDA) AND ITS TRANSITION METAL COMPLEXES

Another novel thiadiazole and pyridine based Schiff base, (E)-5-(4-nitro phenyl)-N-(1(pyridin-2-yl)ethylidene)-1,3,4-thiadiazol-2-amine (2APNPTDA) was synthesized and characterized by elemental analysis and various spectroscopic techniques. The structure of the ligand 2APNPTDA and its transition metal complexes with chromium, cobalt, nickel, copper, zinc and zirconium ions were established based on spectroscopic, magnetic and electrical studies. The detailed synthesis and characterization of both the ligand and complexes are discussed in this section.

##### Synthesis of 2APNPTDA

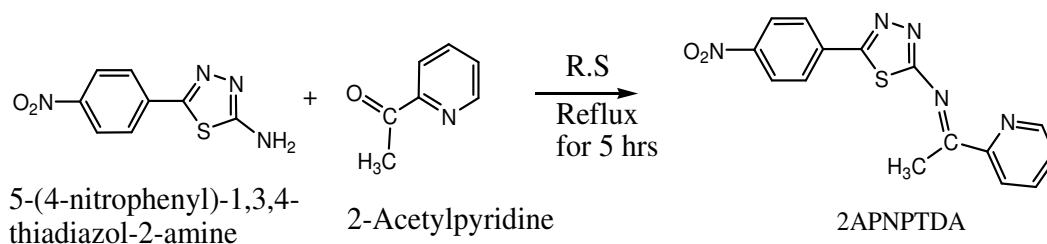


**Fig. 1.29:** Synthesis of 2APNPTDA

Hot ethanolic solution of 2-acetyl pyridine was added to a refluxing solution of 5-(4-nitrophenyl)-1,3,4-thiadiazol-2-amine in ethanol and refluxed 5 hrs on a water bath. The resulting solution was concentrated to obtain yellowish brown crystals of 2APNPTDA, which was filtered, washed and dried. Recrystallization from methanol gave 80 % yield of the desired product. MP: 220<sup>0</sup>C

##### Characterisation of 2APNPTDA

###### *Elemental analysis*

The elemental analysis data of thiadiazole and 2-acetyl pyridine derivative of

Schiff base 2APNPTDA is given in Table 1.15. The experimentally obtained percentages of elements like carbon, hydrogen, nitrogen and sulphur were in good agreement with the calculated values.

#### ***Electronic spectral analysis***

Characterization of ligand, (E)-5-(4-nitrophenyl)-N-(1(pyridin-2-yl)ethylidene)-1,3,4-thiadiazol-2-amine (2APNPTDA) was done using IR and UV spectral data. Electronic spectrum of the ligand showed peaks at  $39370\text{cm}^{-1}$  and  $27100\text{cm}^{-1}$  due to  $\pi \rightarrow \pi^*$  and  $n \rightarrow \pi^*$  transitions respectively. The decrease in the values compared to the parental amine is an indication of extension of conjugation during the formation of ligand 2APNPTDA.

#### ***FTIR spectral analysis***

Characteristic infrared absorption frequencies ( $\text{cm}^{-1}$ ) of thiadiazole pyridine derivative 2APNPTDA are represented in Table 1.15. Another important band was at  $1692\text{cm}^{-1}$  (C=N) due to the stretching mode of azomethine linkage. The peaks at  $1592\text{cm}^{-1}$  and  $1493\text{cm}^{-1}$  can be consigned to C=C vibrations in aromatic rings. Aromatic C-H stretching frequency was found at  $3111\text{cm}^{-1}$  and C-N stretching appeared at  $1269\text{cm}^{-1}$ . Another peak at  $2929\text{cm}^{-1}$  was an indication of the C-H stretching frequency of  $\text{CH}_3$  group. The presence of nitro group was confirmed by the appearance of the peaks at  $1385\text{cm}^{-1}$  and  $1312\text{cm}^{-1}$ . The peak found at  $1104\text{cm}^{-1}$  was due to the carbon sulphur linkage and C-N stretching frequency was appeared at  $1269\text{cm}^{-1}$ . In plane bending vibrations come into sighted at  $1059\text{cm}^{-1}$  and the peaks gained at  $983\text{cm}^{-1}$  and  $853\text{cm}^{-1}$  can be consigned as out of plane bending vibrations.

#### ***NMR spectral analysis***

The  $^1\text{H}$  NMR spectrum of the 'S' containing Schiff base, 2APNPTDA which is derived from 2-acetyl pyridine and NPTDA are shown in Fig. 1.30. Eight non equivalent

hydrogen atoms which were in different electronic environments gave characteristic peaks in the NMR spectrum. The methyl group attached to the pyridine ring appeared as a singlet signal at 2.6 $\delta$ , and the protons present in the aromatic (pyridine and benzene) rings exhibited signals in the range 7.12-8.32 $\delta$ .

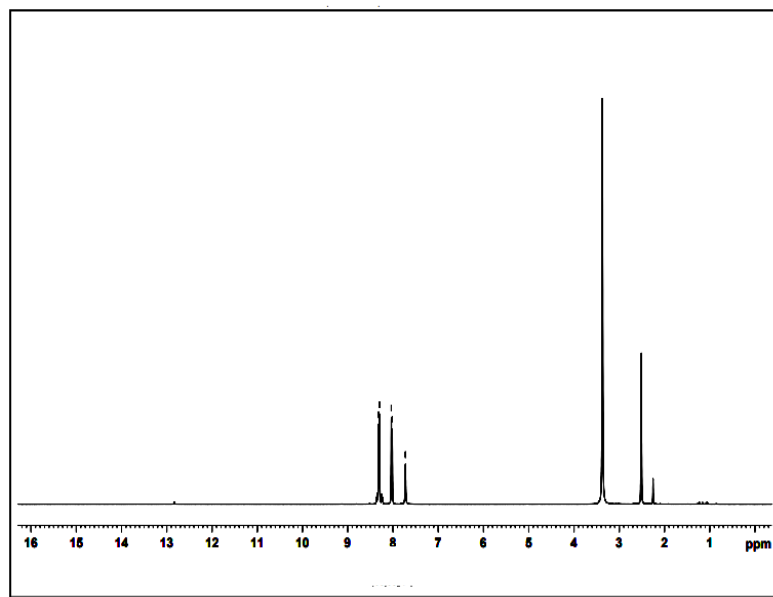


**Fig. 1.30:**  $^1\text{H}$  NMR spectrum of 2APNPTDA

Characteristics  $^{13}\text{C}$  NMR spectrum of Schiff base 2APNPTDA is shown in Fig. 1.31. Methyl C atom observed as a sharp signal at 38ppm. Peaks due to other carbon atoms in the aromatic rings were observed in the range 124-169ppm

#### ***Mass spectral analysis***

In GCMS, the ligand 2APNPTDA shows a highly intensified base peak at  $m/z$  222 due to the fragment  $[\text{C}_8\text{H}_6\text{N}_4\text{O}_2\text{S}]^+$ , which is formed due to the loss of 2-acetyl pyridine part from the ligand 2APNPTDA. Another clear signal with high intensity appeared at  $m/z$  74 corresponding to the fragment,  $[\text{CH}_2\text{N}_2\text{S}]^+$ . The fragments  $[\text{C}_8\text{H}_7\text{N}_2\text{S}]^+$ ,  $[\text{C}_7\text{H}_4\text{NS}]^+$ ,  $[\text{C}_7\text{H}_4\text{S}]^+$ ,  $[\text{CH}_2\text{N}_2\text{S}]^+$  and  $[\text{CH}_2\text{NS}]^+$  were appeared at  $m/z$  163, 134, 120, 74, 60 respectively. The mass spectrum of the Schiff base 2APNPTDA is provided in Fig. 1.32.

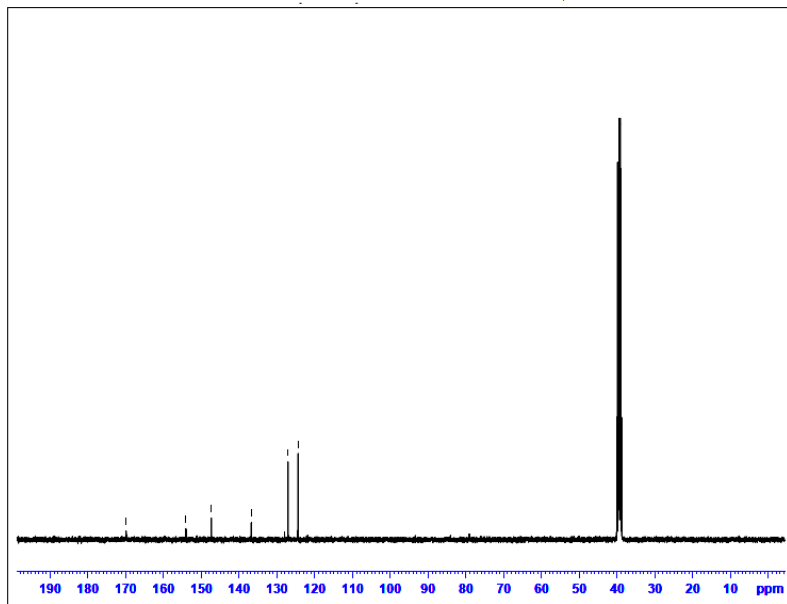


**Fig. 1.31:**  $^{13}\text{C}$  NMR spectrum of 2APNPTDA

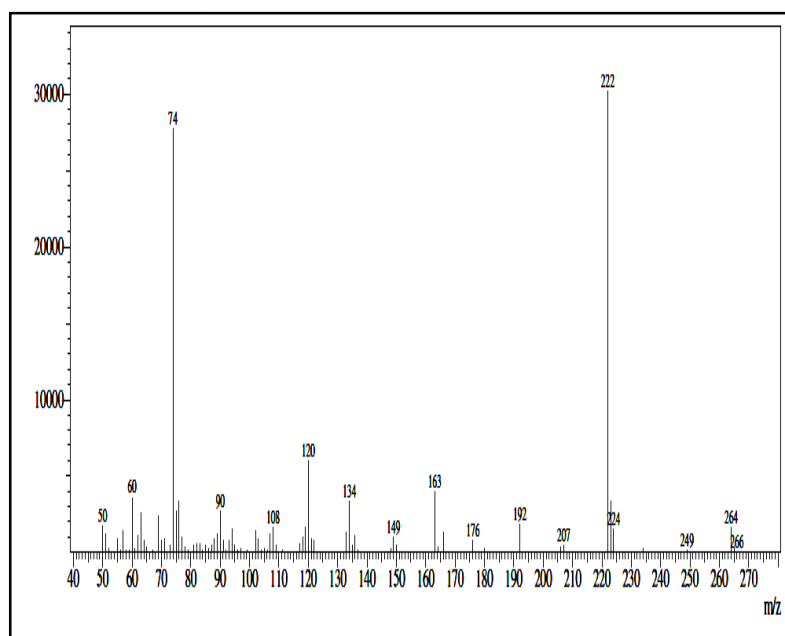


**Fig. 1.32:** Mass spectrum of 2APNPTDA

From the above discussions, the structure of ‘S’ containing pyridine derivative Schiff base, 2APNPTDA was derived and represented in Fig 1.33.

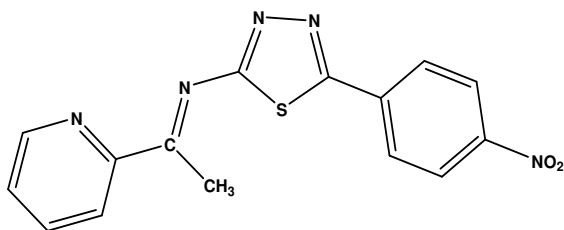


**Fig. 1.33:** Structure of 2APNPTDA

### Synthesis of Complexes

Cr(III), Co(II), Ni(II), Cu(II), Zn(II) and ZrO(II) complexes of 2APNPTDA were prepared in ethanolic medium by adopting conventional refluxing method. Equimolar mixtures of NPTDA and 2-acetylpyridine were refluxed in rectified spirit for 4h. To the boiling solution, ethanolic solution of chromium acetate (2mmol) was added and again refluxed for 5h. The reaction mixture was kept overnight, and the complex was precipitated as brown coloured crystals. Filtered, washed with alcohol and warm water, dried, and melting point was determined. Cobalt nitrate, nickel(II) acetate, copper(III) acetate, zinc(II) acetate and zirconyl(IV) nitrate were used for the preparation of respective complexes. (Yield = 60-90%).

### Characterisation of Complexes

The metal complexes of Cr(III), Co(II), Ni(II), Cu(II), Zn(II) and ZrO(II) are coloured and stable towards light, air and they have high m.p.s (above 280°C). Analytical records suggested that the M:L ratio in all transition metals complexes of 2APNPTDA to be 1:1 (Table 1.15). These complexes are insoluble in water, but they are soluble in DMSO, DMF and CDCl<sub>3</sub>. Molar conductivity values of 2APNPTDA-Complexes in DMSO are shown in Table 1.15. Elemental analysis provides an important key to structural elucidation of complexes. Percentage of C, H, N and S as well as the metal content were estimated by microanalytical methods. There is a good correlation between observed and calculated values.

### *Electronic spectral analysis*

In all metal complexes of 2APNPTDA, the intra ligand electronic transitions ( $n \rightarrow \pi^*$  and  $\pi \rightarrow \pi^*$ ) were shifted to longer wavelength region. This clearly proves the occurrence of complexation. Electronic spectral data of all transition metal complexes of 2APNPTDA are provided in Table 1.14

**Table 1.14:** Electronic spectral data of Schiff base, 2APNPTDA and its transition metal complexes

Compounds	Electronic bands in $\text{cm}^{-1}$	
	$\pi \rightarrow \pi^*$	$n \rightarrow \pi^*$
2APNPTDA	39370	27100
[CrL(Ac) <sub>3</sub> (H <sub>2</sub> O)]	38461	26666
[CoL(NO <sub>3</sub> ) <sub>2</sub> (H <sub>2</sub> O) <sub>2</sub> ]	38910	26178
[NiL(Ac) <sub>2</sub> (H <sub>2</sub> O) <sub>2</sub> ]	38610	26809
[CuL(Ac) <sub>2</sub> (H <sub>2</sub> O) <sub>2</sub> ]	39062	26954
[ZnL(Ac) <sub>2</sub> ]	39062	26385
[ZrOL(NO <sub>3</sub> ) <sub>2</sub> ]	38610	26455

### *Magnetic moment analysis*

Magnetic moment data measurements of the complexes helped to establish their geometry. Results are shown in Table 1.15. Cr(III), Co(II) and Ni(II) complexes of 2APNPTDA were considered octahedral configurations, as they exhibited magnetic moment values of 3.84BM, 3.2BM and 2.82BM respectively. Cu(II)-2APNPTDA chelate displayed a higher magnetic moment of 2.16BM due to the spin-orbit coupling occurs and octahedral geometry was found to fit it. For the zinc complex diamagnetic nature was expected for Zn(II) and ZrO(II) complexes and these results were harmonized with the fact that these metal ions have  $d^{10}$  or  $d^0$  configurations. Tetrahedral and square pyramidal geometries were therefore suggested for them.

### ***Molar conductance analysis***

Molar conductance values of the complexes are in the range of  $1.8-14\Omega^{-1}\text{cm}^2\text{mol}^{-1}$ . These values suggest non-electrolytic behaviour and absence of counter ions outside the coordination sphere of metal chelates.

### ***FTIR spectral analysis***

Selected IR spectral bands for the ligand and its complexes are given in Table 1.16. The IR spectral bands of free ligand 2APNPTDA is characterized mainly by the strong bands at  $1662\text{cm}^{-1}$ ,  $1592\text{cm}^{-1}$ ,  $1385\text{cm}^{-1}$ ,  $1269\text{cm}^{-1}$  and  $1104\text{cm}^{-1}$  attributed the stretching frequencies of  $-\text{C}=\text{N}$ ,  $\text{C}=\text{C}$ ,  $-\text{NO}_2$ ,  $\text{C}-\text{N}$  and  $\text{C}-\text{S}$  respectively. The FTIR spectrum of the free ligand (2APNPTDA) was compared with the spectra its transition metal complexes. Characteristic absorption bands in the range  $3304-3375\text{cm}^{-1}$  were accredited to the coordinated water. The absorption frequencies in the range  $1626-1686\text{cm}^{-1}$ ,  $1504-1585\text{cm}^{-1}$ ,  $1270-1275\text{cm}^{-1}$ ,  $1092-1106\text{cm}^{-1}$  were consigned to  $-\text{C}=\text{N}$ ,  $-\text{C}=\text{C}$ ,  $-\text{C}-\text{N}$  and  $-\text{C}-\text{S}$  bond stretching respectively in complexes. The imine peak (azomethine peak) in the metal complexes of 2APNPTDA showed change in shifts to lower region compared to the free ligand, which indicates the coordination of azomethine N atom to the metal ion. A peak at  $474\text{cm}^{-1}$  in 2APNPTDA-Zn(II) complex can be assigned to Zn-Cl stretching. Also, the emergence of stretching frequencies in the range  $615-717\text{cm}^{-1}$  and  $420-505\text{cm}^{-1}$  confirmed corresponding to the formation of M-O bonds and M-N bond respectively.

From the above studies proper geometries were found for all complexes of 2APNPTDA and are given in Fig. 1.34.



**Table 1.15:** Microanalytical, magnetic and conductance data of the ligand 2APNPTDA and its transition metal complexes

Complex	Colour	Yield (%)	Mol. Wt.	M.P ( <sup>o</sup> C)	Metal% Found ((Cald.)	C % Found (Cald.)	H% Found (Cald.)	N % Found (Cald.)	S % Found (Cald.)	$\mu_{\text{eff}}$ (BM)	Molar Conductance ( $\Omega^{-1}\text{cm}^2\text{mol}^{-1}$ )	Geometry
2APNPTDA (L)	Yellowish brown	70	325	220	-	52.57 (55.38)	3.31 (3.41)	22.35 (21.53)	10.03 (9.86)	-	-	-
[CrL(Ac) <sub>3</sub> (H <sub>2</sub> O)]	Brown	85	572	310	9.89 (9.09)	44.13 (44.97)	3.98 (4.29)	10.77 (11.92)	5.39 (5.46)	3.84	7.2	Octahedral
[CoL(NO <sub>3</sub> ) <sub>2</sub> (H <sub>2</sub> O) <sub>2</sub> ]	Black	60	544	>310	11.5 (10.85)	31.27 (33.1)	2.54 (2.78)	17.85 (18.01)	5.69 (5.89)	3.21	8.2	Octahedral
[NiL(Ac) <sub>2</sub> (H <sub>2</sub> O) <sub>2</sub> ]	Black	80	538	>300	11.43 (10.97)	40.03 (42.4)	3.56 (3.93)	13.04 (13.01)	5.99 (5.92)	2.87	1.8	Octahedral
[CuL(Ac) <sub>2</sub> (H <sub>2</sub> O) <sub>2</sub> ]	Black	70	543	>360	12.61 (11.97)	40.37 (42.03)	2.95 (3.9)	13.04 (12.9)	5.42 (5.91)	2.16	3.5	Octahedral
[ZnL(Ac) <sub>2</sub> ]	Dark green	90	508	>300	11.98 (12.79)	30.13 (29.47)	1.95 (2.04)	10.33 (10.11)	4.70 (4.63)	D	14.0	Tetrahedral
[ZrOL(NO <sub>3</sub> ) <sub>2</sub> ]	Reddish orange	60	556	280	17.06 (16.37)	31.76 (32.37)	1.92 (1.99)	17.30 (17.62)	5.68 (5.76)	D	4.58	Square Pyramidal

**Table 1.16:** Characteristic infrared absorption frequencies ( $\text{cm}^{-1}$ ) of 2APNPTDA and its transition metal complexes

Complex	$\nu_{\text{H}_2\text{O}}$	$\nu_{\text{COOAsy}}$	$\nu_{\text{C=N}}$	$\nu_{\text{COOSy}}$	$\nu_{\text{C=C}}$	$\nu_{\text{NO}_2/\text{NO}_3}$	$\nu_{\text{C-N}}$	$\nu_{\text{C-S}}$	$\nu_{\text{M-O}}$	$\nu_{\text{M-N}}$
2APNPTDA (L)	-	-	1692	-	1592	1385 1312	1269	1104	-	-
[CrL(Ac) <sub>3</sub> H <sub>2</sub> O]	3329	1714	1626	1522	1504	1449 1346	1273	1101	615	505
[CoL(NO <sub>3</sub> ) <sub>2</sub> (H <sub>2</sub> O) <sub>2</sub> ]	3310	-	1685	-	1584	1524 1470 1346	1274	1099	717	457
[NiL(Ac) <sub>2</sub> (H <sub>2</sub> O) <sub>2</sub> ]	3375	1690	1675	1586	1525	1485 1342	1275	1105	617	420
[CuL(Ac) <sub>2</sub> (H <sub>2</sub> O) <sub>2</sub> ]	3304	1700	1639	1596	1585	1476 1342	1270	1106	685	525
[ZnL(Ac) <sub>2</sub> ]	-	1699	1686	1586	1519	1382 1349	1275	1103	643	M-Cl 474
[ZrOL(NO <sub>3</sub> ) <sub>2</sub> ]	-	-	1633	-	1544	1508 1468 1337	1275	1092	614	462

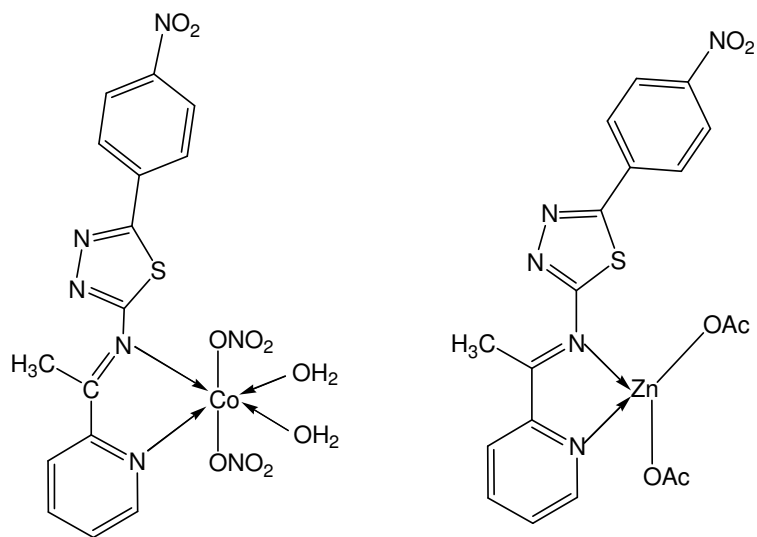
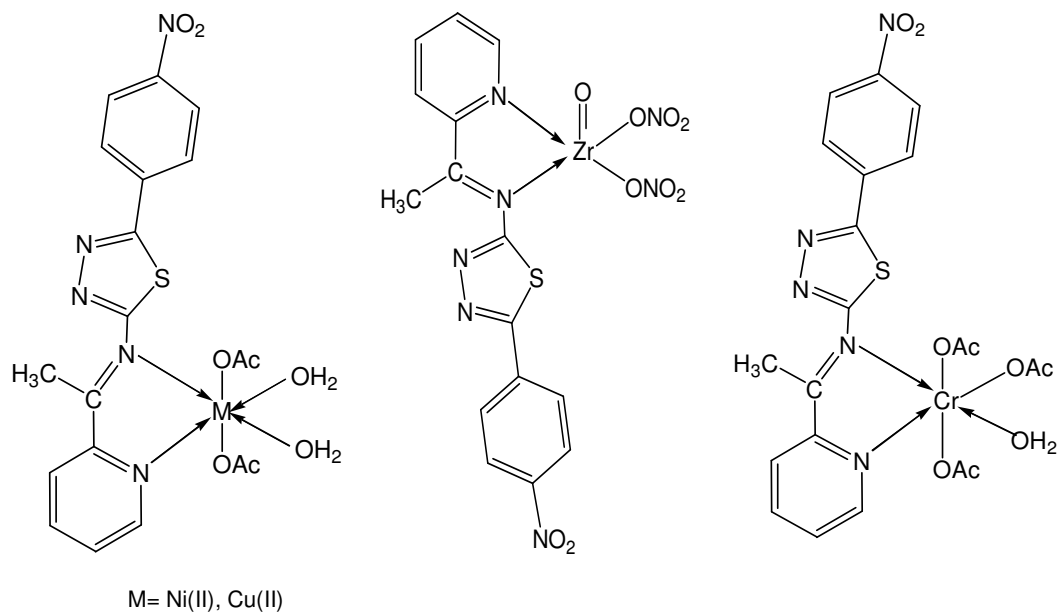


**Fig. 1.34:** Structures of transition metal complexes of 2APNPTDA

## CHAPTER 5

### TRANSITION METAL COMPLEXES OF SCHIFF BASES DERIVED FROM INDOLE-3-CARBALDEHYDE AND THIOPHENE 2- CARBALDEHYDE

Two novel sulphur containing Schiff bases such as N-((1H-indol-3-yl)methylene)thiazol-2-amine (I3A2AT), which is an indole and thiazole derivative and (13E)-N1,N2-bis((thiophene-2-yl)methylene)cyclohexane-1,2-diamine (T2CDACH), which is derived from thiophene-2-carbaldehyde and 1,2-diaminocyclohexane were synthesized and characterized by means of elemental analysis and spectral studies such as FTIR, UV-visible, NMR ( $^1\text{H}$  and  $^{13}\text{C}$ ) and Mass spectroscopy. Chelating ability of these heterocyclic Schiff base ligands were proved by synthesizing transition metal complexes. Elemental (CHNS) analysis, FTIR, UV-visible spectroscopy, magnetic moment measurements, estimation of metal content and molar conductance studies were used to characterize the metal complexes.

This chapter is divided into two sections. Section I deals with synthesis and characterization of the indole and thiazole derived Schiff base ligand N-((1H-indol-3-yl)methylene)thiazol-2-amine (I3A2AT) and its transition metal complexes. Synthesis and characterization of the Schiff base ligand (13E)-N1,N2-bis((thiophene-2-yl)methylene) cyclohexane-1,2-diamine (T2CDACH) and its transition metal complexes were discussed in section II

## SECTION I

### STUDIES ON SCHIFF BASE, N-((1H-INDOL-3-YL)METHYLENE)THIAZOL-2-AMINE (I3A2AT) AND ITS TRANSITION METAL COMPLEXES

Novel thiazole and indole derivative of Schiff base, N-((1H-indol-3-yl)methylene)thiazol-2-amine, (I3A2AT) was synthesized and characterized by various physicochemical techniques like UV-Visible, FTIR, NMR and Mass spectroscopy. The structure of transition metal complexes of the ligand with chromium, manganese, nickel, copper, zinc and zirconium ions were established based on elemental, spectroscopic, magnetic and electrical studies. The detailed synthesis and characterization of both the ligand I3A2AT and their complexes are discussed in this section.

#### Synthesis of I3A2AT

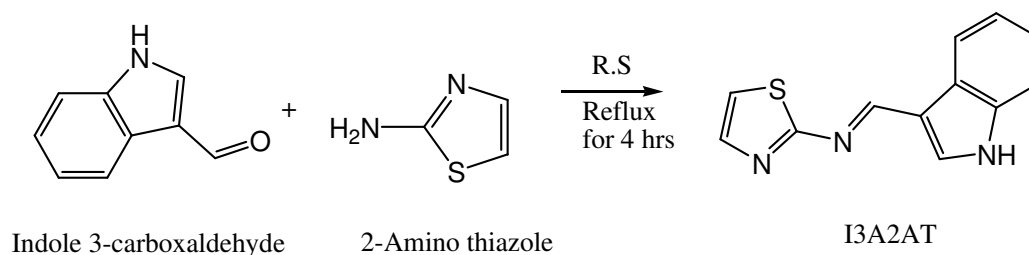


**Fig. 1.35:** Synthesis of I3A2AT

The N-((1H-indol-3-yl)methylene)thiazol-2-amine (I3A2AT) was synthesized by adding hot ethanolic solution of 2-aminothiazole in dropwise to stirred solution containing equimolar concentration of indole-3-aldehyde in ethanol medium. The mixture was refluxed for 4h, kept for 1h to cool down to room temperature and the brown glittering crystals separated were filtered, washed with ethanol-water (1:1) mixture, and dried [78]. Yield-70% (MP: 120<sup>0</sup>C)

## Characterization of I3A2AT

### *Elemental analysis*

The elemental analysis data of thiazole derivative of Schiff base I3A2AT is given in Table 1.18. Experimentally obtained percentages of elements like carbon, hydrogen, nitrogen and sulphur were in good agreement with the calculated values.

### *Electronic spectral analysis*

Schiff base I3A2AT exhibited two important peaks in the UV–Visible spectrum. High intense peak at  $29600\text{cm}^{-1}$  corresponds to allowed  $\pi \rightarrow \pi^*$  and the peak at  $25600\text{cm}^{-1}$  was assigned to the spectroscopically forbidden  $n \rightarrow \pi^*$  transition.

### *FTIR spectral analysis*

IR spectrum of I3A2AT consists of characteristic stretching frequencies corresponding to various bonds. Presence of azomethine group is proved by the peak observed at  $1627\text{cm}^{-1}$ . Aromatic C-H stretching frequency appeared at  $3114\text{cm}^{-1}$  and the stretching frequency due to NH vibration was identified at  $3347\text{cm}^{-1}$  as a medium band. C=C stretching frequencies of thiazole and indole rings were observed at 1575, 1495,  $1516\text{cm}^{-1}$  and C-S vibration and C-N stretching frequencies observed at  $1112\text{cm}^{-1}$  and  $1241\text{cm}^{-1}$  respectively. Bands corresponding to in plane bending were observed at  $1083\text{cm}^{-1}$  and  $1027\text{cm}^{-1}$  and out of plane bending bands observed at 757 and  $638\text{cm}^{-1}$ .

### *NMR spectral analysis*

Eight non-equivalent protons displayed their own distinct peak in the proton NMR spectrum of I3A2AT. Azomethine protons exhibited a singlet peak at  $7.19\delta$ . Weak and broad singlet appeared at  $12.0\delta$  corresponds to the proton present in the NH group in the indole moiety and the broadness can be explained by quadrupole interaction between  $^{14}\text{N}$  and  $^1\text{H}$  nuclei. Aromatic proton present in the indole ring exhibited signals in the range  $7.12\text{--}7.18\delta$ . The signals appeared at  $7.43$  and  $8.01\delta$  were due to the protons in the

thiazole ring and no inverse peak was observed in DEPT 135 which establish that there is no CH<sub>2</sub> moiety in the Schiff base.

Nine chemically different carbon atoms present in I3A2AT showed 9 distinct signals in the <sup>13</sup>C NMR spectrum. Peak at 185ppm corresponds to the carbon atom of azomethine group. Quaternary carbon atom present in the thiazole ring and indole ring displayed signals in the range 112-138ppm. <sup>1</sup>H NMR, DEPT-135 and <sup>13</sup>C NMR spectral datas of indole based 'S' containing Schiff base I3A2AT are provided in Fig. 1.36, 1.37 and 1.38 respectively.

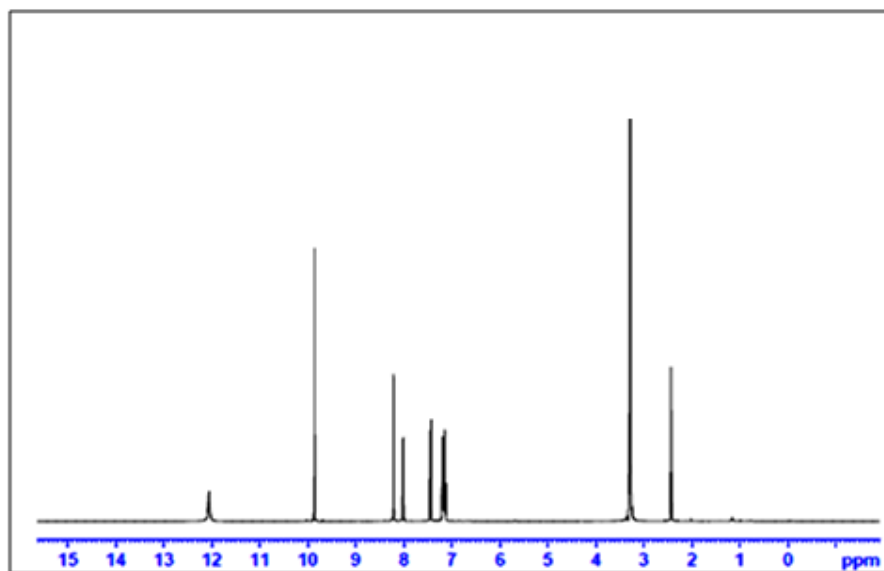


**Fig. 1.36:** <sup>1</sup>H NMR spectrum of I3A2AT

### *Mass spectral analysis*

In the mass spectrum of I3A2AT, the molecular ion peak at m/z 227 was very much weak. The base peak was appeared as weak signal at m/z 144 by the fragment [C<sub>9</sub>H<sub>8</sub>N<sub>2</sub>]<sup>+</sup> which is generated by the loss of thiazole part. The formation of fragments at m/z 89, m/z 100, m/z 116 and m/z 128 were due to the fragments [C<sub>3</sub>H<sub>7</sub>NS]<sup>+</sup>, [C<sub>3</sub>H<sub>4</sub>N<sub>2</sub>S]<sup>+</sup>, [C<sub>8</sub>H<sub>6</sub>N]<sup>+</sup> and [C<sub>9</sub>H<sub>6</sub>N]<sup>+</sup> respectively. The electron impact mass spectrum of ligand I3A2AT is represented in Fig. 1.39.

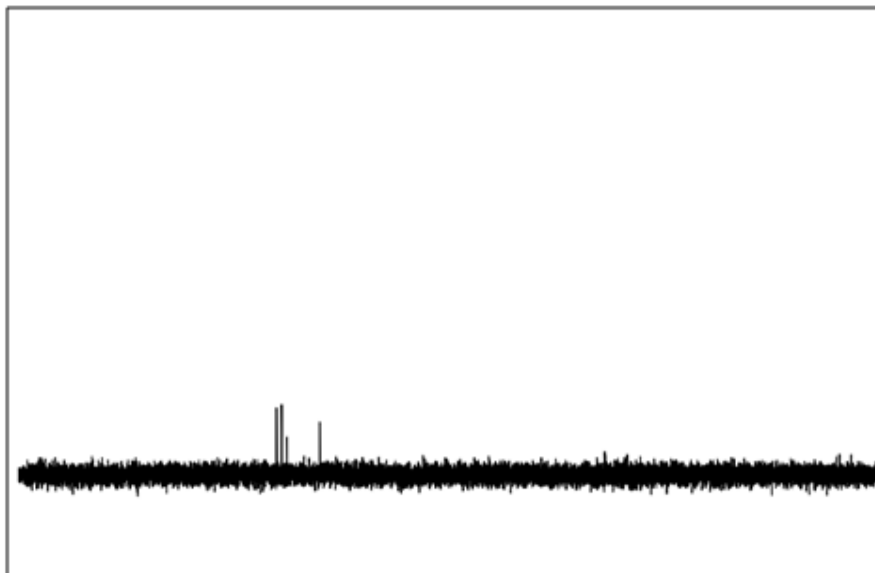


**Fig. 1.37:** DEPT 135 spectrum of I3A2AT

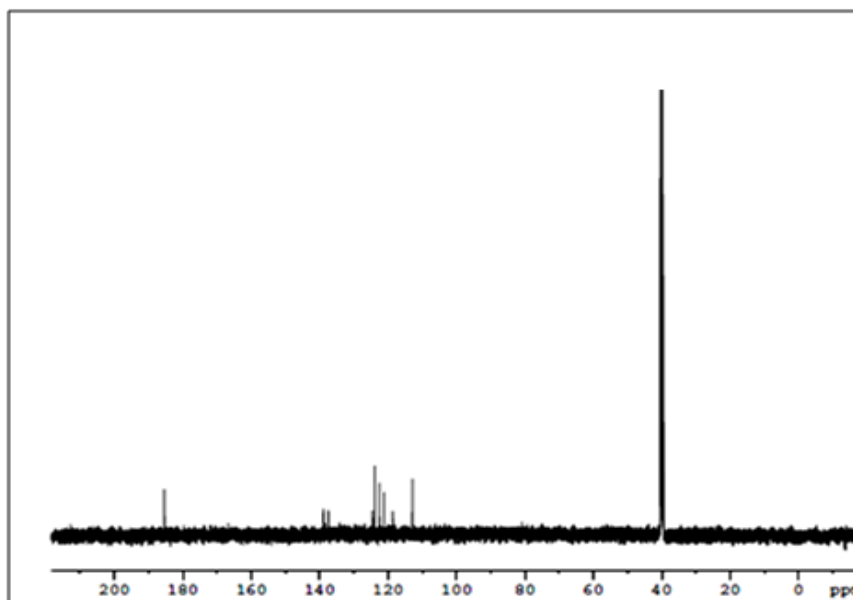


**Fig. 1.38:** <sup>13</sup>C NMR spectrum of I3A2AT

From the preceding discussions, the structure of 'S' containing indole derivative Schiff base I3A2AT is represented in Fig. 1.40.



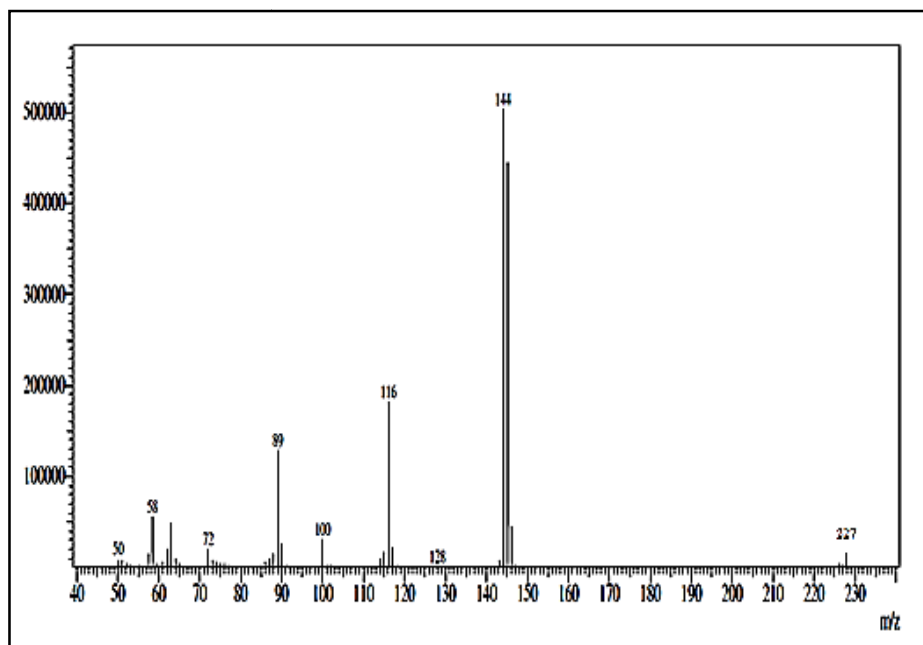


**Fig. 1.39:** Mass spectrum of I3A2AT

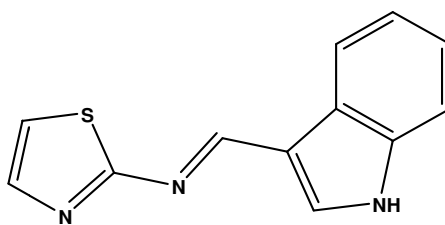


**Fig. 1.40:** Structure of I3A2AT

### Synthesis of Complexes

The complexing capability of indole and thiazole derivative of Schiff base, I3A2AT were checked with Cr(III), Mn(II), Ni(II), Cu(II), Zn(II) and Zirconyl ions. Zirconyl nitrate is used for the synthesis of Zirconium complex. Acetate salts of other metal ions were used for the synthesis of respective complexes. Schiff base ligand I3A2AT (2mmol) was dissolved in minimum quantity of ethanol (15ml) and refluxed on a water bath (30min). Hot ethanolic solution of appropriate amount corresponding metal salt (acetate/nitrate) was added to the boiling medium and again refluxed for 4h. Then reduced its volume by evaporation, cooled and kept overnight and the crystallized metal

complexes were collected, washed with water ethanol mixture and dried over CaCl<sub>2</sub>.

### Characterization of Complexes

Adopted analytical techniques and the details for the characterization of I3A2AT-complexes include elemental analysis, conductance measurements, magnetic moment measurements, and spectral studies like electronic and IR spectroscopy are given in following paragraphs. All complexes were amorphous solid, coloured, non-hygroscopic, stable to light and air and highly soluble in DMSO, acids and other solvents.

A distinct idea about the precise molecular formula of complexes can be derived by the estimation of elements. It is seen that the theoretical values were very close to the observed values. Cr(III), Mn(II), Ni(II), Cu(II), Zn(II) and ZrO(II) complexes of I3A2AT were found to possess 1:1 stoichiometry. The data of CHNS analysis is listed in Table 1.18.

#### *Electronic spectral analysis*

From electronic spectra of the complexes d-d transitions and intra ligand electronic transitions were obtained. Electronic spectral data of I3A2AT and complexes are provided in Table 1.17.

**Table 1.17:** Electronic spectral data of Schiff base, I3A2AT and its transition metal complexes

Compound	Electronic bands in cm <sup>-1</sup>	
	$\pi \rightarrow \pi^*$	$n \rightarrow \pi^*$
I3A2AT	39062	33783
[CrL(Ac) <sub>2</sub> (H <sub>2</sub> O)]	38610	33222
[MnLAc(H <sub>2</sub> O) <sub>3</sub> ]	38314	32358
[NiLCl(H <sub>2</sub> O) <sub>3</sub> ]	38610	26809
[CuLAc(H <sub>2</sub> O) <sub>3</sub> ]	38461	33557
[ZnLAc(H <sub>2</sub> O)]	38610	33557
[ZrOLNO <sub>3</sub> (H <sub>2</sub> O)]	38610	33333

A clear indication of complexation was obtained from the shift of these bands from lower to higher wavelength region.

#### ***Magnetic moment analysis***

Magnetic moment data measurements gave an insight leading to the geometry of the complexes. Complexes of chromium and manganese were found to have octahedral geometry since they displayed their magnetic moment values 3.74BM and 5.91BM, respectively. Copper and nickel complexes showed their magnetic moment as 3.04BM and 1.92BM respectively, which designated high spin octahedral geometries. For zinc and zirconium complexes, observed diamagnetic characters justify their tetrahedral and square pyramidal geometries. Results are tabulated in Table 1.18.

#### ***Molar conductance analysis***

For all the complexes of I3A2AT, the molar conductance measurements were done in the medium of DMSO. It was concluded from the conductance measurements that, counter ions were not present outside the coordination sphere of all complexes of I3A2AT ( $3.1-10.2\Omega^{-1}\text{cm}^2\text{mol}^{-1}$ ) and therefore non-electrolytic character was consigned to them (Table 1.18).

#### ***FTIR spectral analysis***

The downward shift in the vibrational frequencies of azomethine bond is seen in all complexes compared to the ligand I3A2AT ( $1627\text{cm}^{-1}$ ) establishes the strong coordination of metal with imine nitrogen through coordinate bond. Broad bands seen in the FTIR spectra of all the chelates at the range of  $3101-3325\text{cm}^{-1}$  can be ascribed to coordinated water molecules. In Cr(III), Mn(II), Cu(II), Zn(II) and ZrO(II) complexes, the asymmetric and symmetric stretching vibrational frequencies of the carboxylate group were observed in the range  $1679-1698\text{cm}^{-1}$  and  $1543-1590\text{cm}^{-1}$  respectively which indicates the monodentate nature of this group. N-H peak disappeared in all

complexes of I3A2AT indicated that the N atom was coordinated to metal atom, after protonation. Again, the new C-N and C-S stretching frequencies were observed in these complexes in the range  $1237\text{-}1242\text{cm}^{-1}$  and  $1101\text{-}1125\text{cm}^{-1}$  respectively. M-O and M-N bonds confirmed their presence as prominent peaks in low field area of IR spectrum. Spectral data of I3A2AT and their transition metal complexes are specified in Table 1.19.

The structures of the complexes of this heterocyclic Schiff base I3A2AT was established based on above justifications and it are represented in Fig. 1.41. In all the chelates, the Schiff base act as monovalent bidentate ligand.

**Table 1.18:** Microanalytical, magnetic and conductance data of the ligand I3A2AT and its transition metal complexes

Complex	Colour	Yield (%)	Mol. Wt.	M.P ( <sup>o</sup> C)	Metal% Found (Cald.)	C % Found (Cald.)	H % Found (Cald.)	N % Found (Cald.)	S % Found (Cald.)	$\mu_{\text{eff}}$ (BM)	Molar Conductance ( $\Omega^{-1}\text{cm}^2\text{mol}^{-1}$ )	Geometry
I3A2AT (LH)	Brown	70	227	120	-	60.41 (63.41)	3.90 (3.99)	16.79 (18.49)	13.43 (14.11)	-	-	-
[CrL(Ac) <sub>2</sub> (H <sub>2</sub> O) <sub>2</sub> ]	Black	55	433	>300	12.98 (12.01)	43.21 (45.63)	4.70 (4.73)	8.09 (9.39)	5.83 (7.17)	3.74	8.1	Octahedral
[MnL(Ac)(H <sub>2</sub> O) <sub>3</sub> ]	Brown	70	395	250	14.85 (13.92)	41.30 (42.64)	3.98 (4.35)	8.75 (10.66)	6.90 (8.13)	5.91	4.9	Octahedral
[NiLCl(H <sub>2</sub> O) <sub>3</sub> ]	Greenish red	80	376	180	14.75 (15.69)	36.46 (38.49)	3.45 (3.77)	11.01 (11.22)	8.22 (8.56)	3.04	6.6	Octahedral
[CuL(Ac)(H <sub>2</sub> O) <sub>3</sub> ]	Dark brown	80	404	290	15.03 (15.84)	40.09 (41.73)	3.56 (4.25)	8.13 (10.43)	6.54 (7.96)	1.97	3.1	Octahedral
[ZnL(Ac)(H <sub>2</sub> O)]	Creamish yellow	75	369	161	17.42 (17.61)	44.58 (45.6)	2.89 (3.55)	10.34 (11.4)	7.33 (8.7)	D	10.2	Tetrahedral
[ZrOL(NO <sub>3</sub> )(H <sub>2</sub> O)]	Flesh colour	90	414	>320	22.02 (21.98)	32.00 (34.85)	1.92 (2.44)	12.51 (13.55)	56.98 (7.75)	D	8.4	Square Pyramidal

**Table 1.19:** Characteristic infrared absorption frequencies ( $\text{cm}^{-1}$ ) of I3A2AT and its transition metal complexes

Complex	$\nu_{\text{H}_2\text{O}}$	$\nu_{\text{COOasy}}$	$\nu_{\text{C=N}}$	$\nu_{\text{COOsy}}$	$\nu_{\text{C=C}}$	$\nu_{\text{C-N}}$	$\nu_{\text{C-S}}$	$\nu_{\text{M-O}}$	$\nu_{\text{M-N}}$
I3A2AT (LH)	-	-	1627	-	1495	1241	1112	-	-
[CrL(Ac) <sub>2</sub> (H <sub>2</sub> O) <sub>2</sub> ]	3325	1695	1605	1550	1519	1242	1105	617	530
[MnL(Ac)(H <sub>2</sub> O) <sub>3</sub> ]	3324	1679	1620	1547	1495	1240	1101	607	491
[NiLCl(H <sub>2</sub> O) <sub>3</sub> ]	3166	-	1609	-	1520	1242	1125	640	430
[CuL(Ac)(H <sub>2</sub> O) <sub>3</sub> ]	3312	1683	1613	1543	1503	1237	1108	598	483
[ZnL(Ac)(H <sub>2</sub> O)]	3101	1698	1601	1573	1519	1241	1121	638	411
[ZrOL(NO <sub>3</sub> )(H <sub>2</sub> O)]	3241	1693	1623	1590	1511	1238	1107	607	450

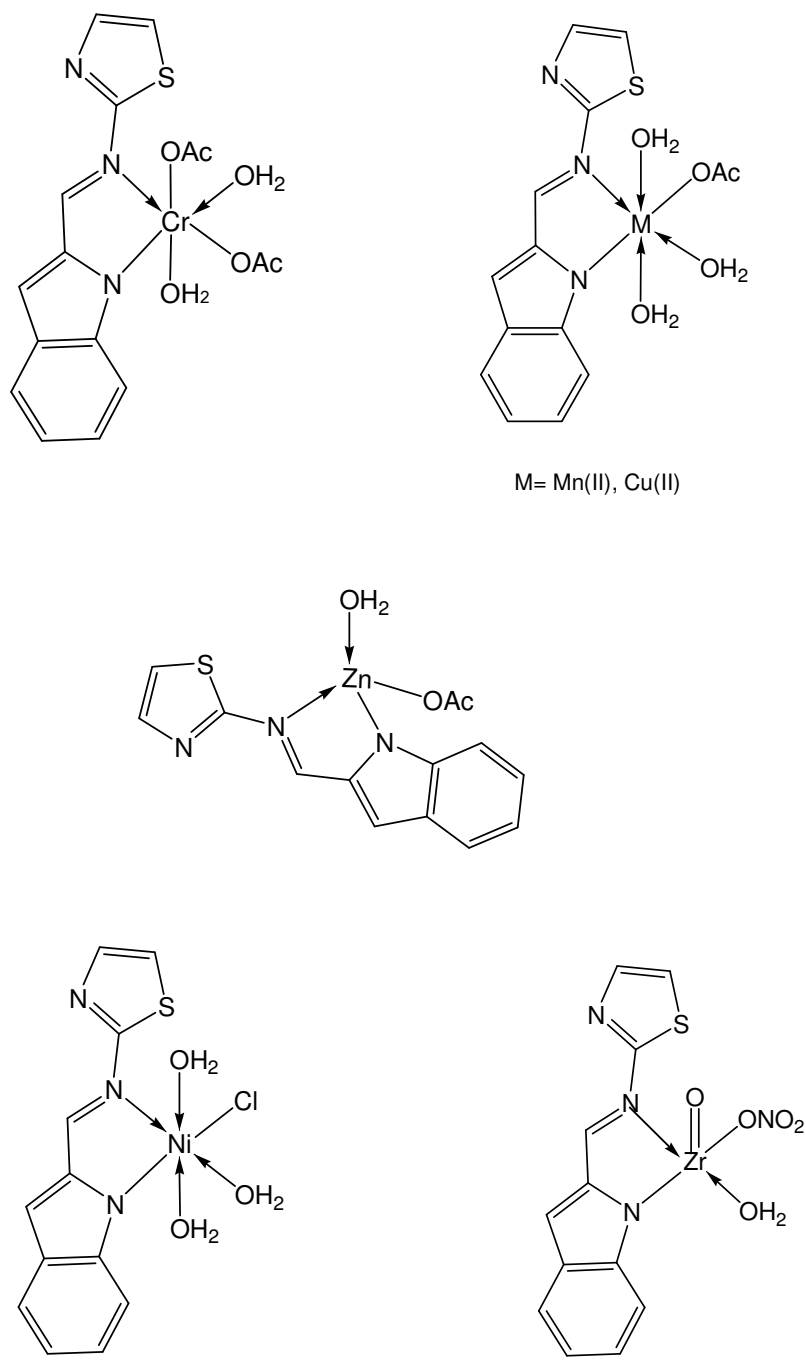


**Fig. 1.41:** Structures of transition metal complexes of I3A2AT

## SECTION II

### STUDIES ON SCHIFF BASE, (13E)-N1,N2-BIS((THIOPHENE-2-YL)METHYLENE) CYCLOHEXANE-1,2-DIAMINE (T2CDACH) AND ITS TRANSITION METAL COMPLEXES

Thiophene derivative of Schiff base, (13E)-N1,N2-bis((thiophen-2yl)methylene) cyclohexane -1,2-diamine (T2CDACH) which is a thiophene derivative, was synthesized and characterized by elemental analysis and various spectroscopic techniques. The structures of T2CDACH and its transition metal complexes with manganese, nickel, copper, zinc and zirconium of the ligand T2CDACH were established based on spectroscopic, magnetic and electrical studies. The detailed discussion on the synthesis and characterization of both the ligand and complexes are well depicted in this section.

#### Synthesis of T2CDACH

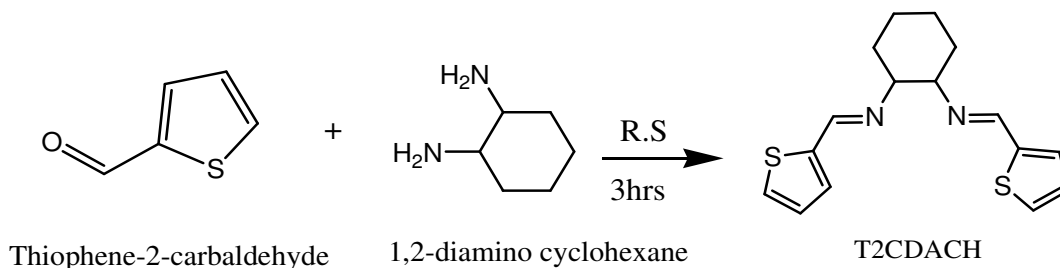


**Fig. 1.42:** Synthesis of T2CDACH

Heterocyclic Schiff base (13E)-N1,N2-bis((thiophen-2yl)methylene)cyclohexane -1,2-diamine (T2CDACH) was synthesized by the condensation of equimolar mixture of thiophene-2-carbaldehyde and 1,2-diaminocyclohexane, in ethanol medium and the reaction mixture was refluxed for 4 hours, concentrated, and cooled. The cream coloured solid formed was filtered, washed, and dried. Yield-90% (MP: 131<sup>0</sup>C)



## Characterization of T2CDACH

### *Elemental analysis*

Elemental analysis data of thiophene derived Schiff base T2CDACH is given in Table 1.22. The experimentally obtained percentages of elements like carbon, hydrogen, nitrogen and sulphur were in good agreement with the calculated values.

### *Electronic spectral analysis*

Thiophene derivative of Schiff base T2CDACH exhibited two important peaks in the UV-Visible spectrum. Peak at  $39525\text{cm}^{-1}$  corresponds to  $\pi \rightarrow \pi^*$  transitions while the peak at  $35971\text{cm}^{-1}$  assigned to  $n \rightarrow \pi^*$  transitions.

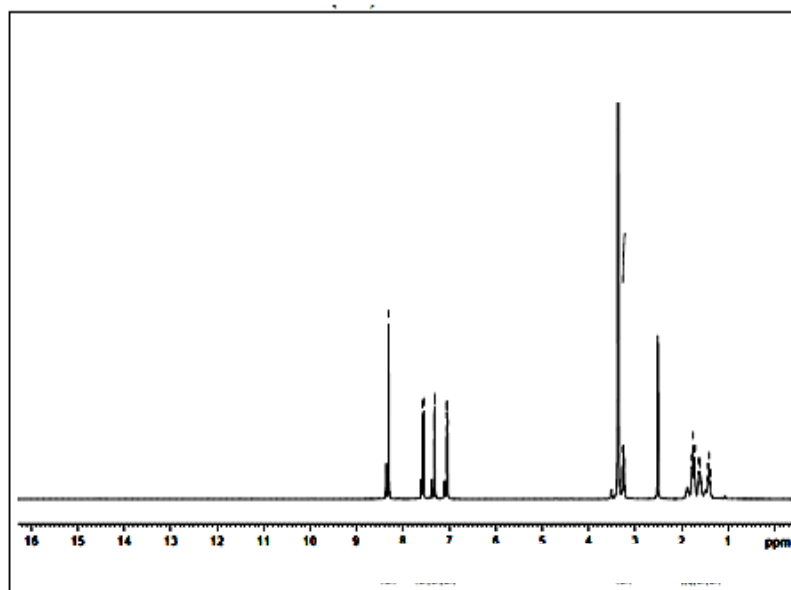
### *FTIR spectral analysis*

Characteristics stretching frequencies of different bonds of thiophene derivative of Schiff base T2CDACH were obtained in the infrared spectrum. The stretching vibration band displayed at  $1627\text{cm}^{-1}$  proved the formation of C=N linkage in the ligand. Aromatic C-H bond vibration and olefinic-H vibrations were observed at  $3070\text{cm}^{-1}$  and  $3008\text{cm}^{-1}$  respectively. The C-H stretching frequency in cyclohexane ring gave characteristics peaks at  $2924\text{cm}^{-1}$  and  $2829\text{cm}^{-1}$ . Aromatic C=C stretching frequency of thiophene moiety were observed at  $1508\text{cm}^{-1}$ . A signal at  $1211\text{cm}^{-1}$  was assignable to  $\nu_{\text{C-N}}$  and a peak corresponding to  $\nu_{\text{C-S}}$  was observed at  $1128\text{cm}^{-1}$ . In plane deformations were observed at  $1080\text{cm}^{-1}$  and  $1033\text{cm}^{-1}$ , while the out of plane deformations were observed at  $846$  and  $709\text{cm}^{-1}$ , respectively.

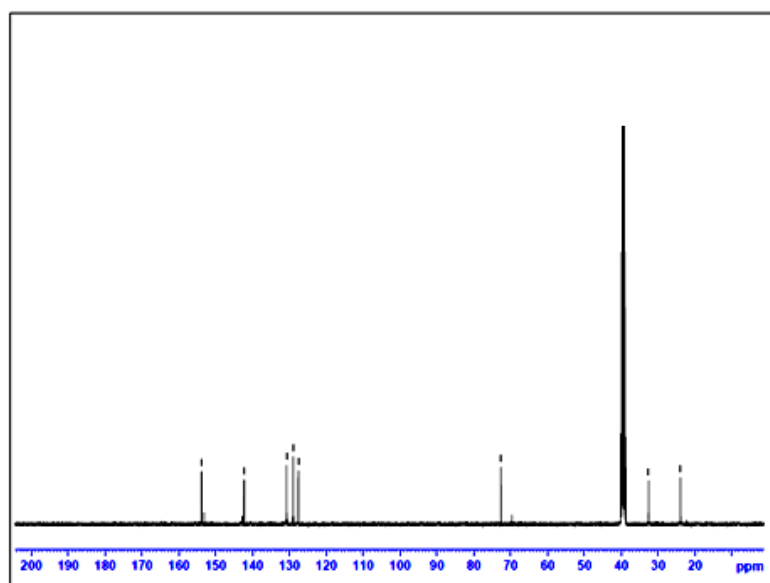
### *NMR spectral analysis*

In the proton NMR spectrum of T2CDACH, a singlet signal at  $8.30\delta$  corresponds to the proton present in the azomethine linkage. Protons of the thiophene ring and cyclohexane ring showed their respective signals in the range  $7.04-7.56\delta$  and  $1.40-3.25\delta$  respectively. Both upward and downward peaks were observed in DEPT 135 due to the

presence of CH and CH<sub>2</sub> groups in the molecule.



**Fig. 1.43:** <sup>1</sup>H NMR spectrum of T2CDACH

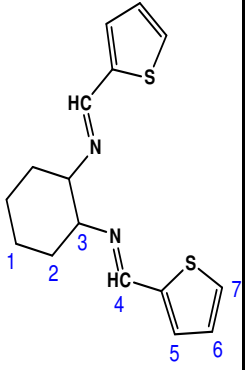


**Fig. 1.44:** <sup>13</sup>C NMR spectrum of T2CDACH

Eight different type carbon atoms showed 8 characteristic peaks in <sup>13</sup>C NMR spectrum of T2CDACH. Azomethine carbon displayed a peak at 153.83ppm and three different type sp<sup>3</sup> hybridised carbon atoms in cyclohexane ring exhibited three peaks between 23.93-72.61ppm. Five sp<sup>2</sup> carbons showed five peaks between 153.83-

127.58ppm.  $^1\text{H}$  and  $^{13}\text{C}$  NMR spectra of T2CDACH and the assignment signals are provided in Fig. 1.43, Fig. 1.44 and Table 1.20 respectively.

**Table 1.20:**  $^1\text{H}$  NMR and  $^{13}\text{C}$  NMR spectral data of T2CDACH

$^1\text{H}$ NMR			$^{13}\text{C}$ NMR		
	$\delta$ value	Labelled proton	$\delta$ value	Labelled carbon	
	1.40 (t,4H)	1	23.93	1	
	1.76 (m,4H)	2	32.57	2	
	3.25 (t,2H)	3	72.61	3	
	8.30 (s,2H)	4	153.8	4	
	7.56 (d,2H)	5	142.2	5	
	7.04 (t,2H)	6	128.9	6	
	7.31 (d,2H)	7	127.5	7	
				130.8	8

### Mass spectral analysis

Purity of the synthesized thiophene derivative T2CDACH was proved by the appearance of only one peak in the gas chromatogram. The molecular ion peak due to  $[\text{C}_{16}\text{H}_{18}\text{N}_2\text{S}_2]^+$  was appeared at  $m/z$  302 as a very weak signal. The base peak was shown at  $m/z$  193 due to the fragment  $[\text{C}_{11}\text{H}_{15}\text{NS}]^+$  and the appearance of peak at  $m/z$  219 was due to the loss of one thiophene moiety. Other peaks at  $m/z$  112, 110 and 97 were due to the fragments  $[\text{C}_5\text{H}_6\text{NS}]^+$ ,  $[\text{C}_5\text{H}_4\text{NS}]^+$  and  $[\text{C}_5\text{H}_5\text{S}]^+$  respectively. Mass spectrum of T2CDACH is shown in Fig. 1.45.

Above discussions, clearly establish the structure of thiophene derivative of Schiff base, T2CDACH as provided in Fig. 1.46.

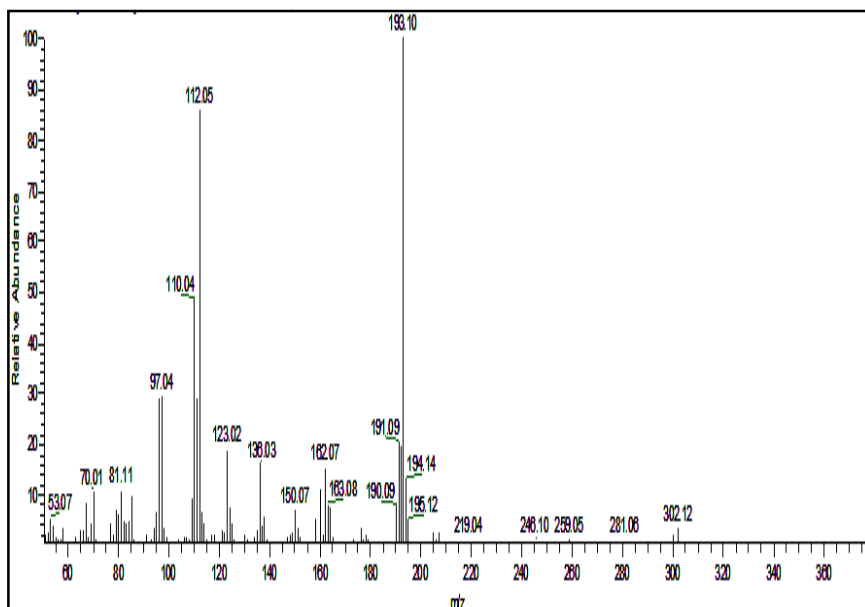


**Fig. 1.45:** Mass spectrum of T2CDACH

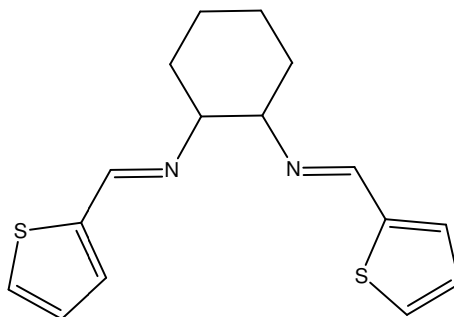


**Fig. 1.46:** Structure of T2CDACH

### Synthesis of Complexes

Complexes of T2CDACH were synthesized by adding hot ethanolic solution of corresponding metal salts to the refluxing solution of ligand in 1:1 ratio and further refluxed for 5h. Acetates of manganese, nickel, copper and zinc were used, while nitrate salt of zirconium was employed for this purpose. Then, the mixture was cooled and the separated complexes filtered, cleaned and dried. All complexes were coloured and their melting points were found to be greater than 300<sup>0</sup>C. Details of properties are reported in Table 1.22.

## Characterization of Complexes

### *Elemental analysis*

Microanalytical methods were employed for the estimation. The metal content in the chelates were derived by using pyrolytic, volumetric and gravimetric methods. CHNS analysis was used for determining carbon, hydrogen, nitrogen and sulphur content in the complexes. There is a good correlation between observed and calculated values of elemental analysis. The metal percentage data of the complexes obtained theoretically and experimentally are listed in Table 1.22. The results obtained are in match with theoretical explanations, which along with spectral data confirm 1:1 stoichiometry between metal and ligand in these complexes

### *Electronic spectral analysis*

In the case of complexes, bathochromic shift was occurred for these bands which was a clear evidence for the complex formation. The electronic spectra of all complexes of T2CDACH showed mainly two peaks, due to  $\pi \rightarrow \pi^*$  and  $n \rightarrow \pi^*$  transitions and they exhibited a downward shift in frequency in the spectra of chelates. This red shift confirms the extension of conjugation and hence the complexation.

**Table 1.21:** Electronic spectral data of Schiff base T2CDACH and its transition metal complexes

Compound	Electronic bands in $\text{cm}^{-1}$	
	$\pi \rightarrow \pi^*$	$n \rightarrow \pi^*$
T2CDACH	39525	35971
[MnL(Ac) <sub>2</sub> (H <sub>2</sub> O) <sub>2</sub> ]	38461	34602
[NiL(Ac) <sub>2</sub> (H <sub>2</sub> O) <sub>2</sub> ]	38759	35211
[CuL(Ac) <sub>2</sub> (H <sub>2</sub> O) <sub>2</sub> ]	38910	35087
[ZnL(Ac) <sub>2</sub> ]	38759	34602
[ZrOL(NO <sub>3</sub> ) <sub>2</sub> ]	38759	35460

The electronic bands of thiophene based Schiff base T2CDACH and its metal complexes are summarized in Table 1.21.

#### ***Magnetic moment analysis***

The magnetic moment values of the complexes T2CDACH are represented in Table 1.22. The observed magnetic moment value for the Mn(II) complex is 5.90BM which establishes its octahedral geometry. The effective magnetic moment values of Ni(II) complex was found to be 2.21BM, which may be due to the antiferromagnetic exchange. Cu-T2CDACH complex exhibited its magnetic moment value 1.18BM which is less than the value obtained from spin only formula. Diamagnetic character was found for Zn(II) and ZrO(II) complexes, which is quite justifiable with the absence of unpaired electron ( $d^{10}$  or  $d^0$ ) in its configuration.

#### ***Molar conductance analysis***

Molar conductance measurement was done in the complexes and the data is tabulated in Table 1.22. The molar conductance values of all complexes of T2CDACH were very low and appeared in the range of  $5-15\Omega^{-1}\text{cm}^2\text{mol}^{-1}$ . These values suggest the non-electrolytic behaviour of the chelates and absence of ionisable ions outside the coordination sphere of metal chelates

#### ***FTIR spectral analysis***

In T2CDACH complexes, the involvement of azomethine groups in coordination with metal was confirmed by shift of stretching frequency to lower values. The presence of new broad signals around  $3387\text{cm}^{-1}$ ,  $3442\text{cm}^{-1}$  and  $3233\text{cm}^{-1}$  in Mn(II), Ni(II) and Cu(II) complexes respectively confirmed the presence of coordinated water molecules in the complexes. Significant characteristic adsorption frequencies in the regions,  $1547-1590\text{cm}^{-1}$  and  $1681-1717\text{cm}^{-1}$  were accredited to the symmetric and asymmetric stretching vibrations of acetate groups respectively in complexes of T2CDACH except in

the case of Zr-T2CDACH complex. Also the appearance of stretching frequencies corresponding to M-O and M-N bonds confirmed the formation of complex. FTIR spectral informations of T2CDACH and its transition metal complexes are displayed in Table 1.23. The frequency separation between  $\nu_{\text{COO(asy)}}$  and  $\nu_{\text{COO(sy)}}$  was found to be above  $150\text{cm}^{-1}$ , which confirm the monodenticity of acetate group. Based on the spectral analysis it is established that the Schiff base T2CDACH act as bidentate ligand towards chelation with transition metal ions. Fig. 1.47 depicts the structures of transition metal complexes of T2CDACH.

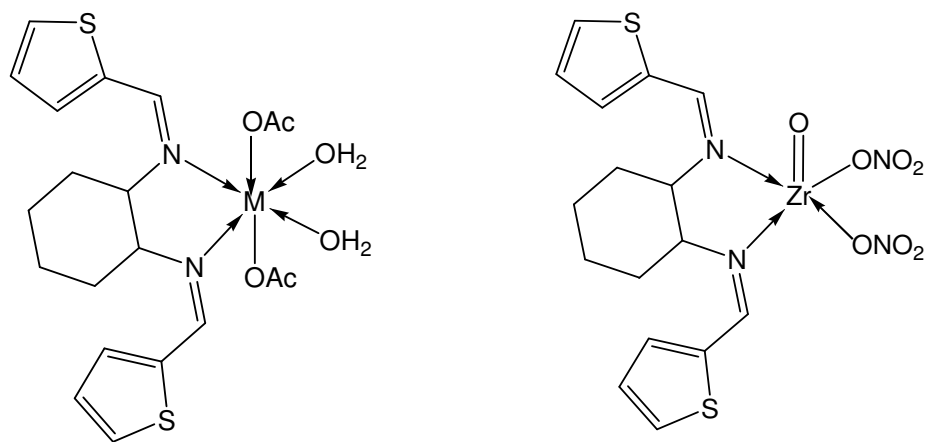
**Table 1.22:** Microanalytical, magnetic and conductance data of the ligand T2CDACH and its transition metal complexes

Complex	Colour	Yield (%)	Mol. Wt.	M.P (°C)	Metal% Found (Cald.)	C % Found (Cald.)	H % Found (Cald.)	N % Found (Cald.)	S % Found (Cald.)	$\mu_{\text{eff}}$ (BM)	Molar Conductance ( $\Omega^{-1}\text{cm}^2\text{mol}^{-1}$ )	Geometry
T2CDACH (L)	Cream	90	302	131	-	63.30 (63.54)	6.2 (6.0)	9.25 (9.26)	19.73 (21.20)	-	-	-
[MnL(Ac) <sub>2</sub> (H <sub>2</sub> O) <sub>2</sub> ]	Black	60	511	>300	10.72 (10.76)	45.23 (46.96)	5.47 (5.52)	4.92 (5.48)	12.18 (12.54)	5.90	5.0	Octahedral
[NiL(Ac) <sub>2</sub> (H <sub>2</sub> O) <sub>2</sub> ]	Light Green	40	515	>300	12.03 (11.46)	44.12 (46.62)	4.75 (5.48)	4.58 (5.44)	11.81 (12.45)	2.21	8.0	Octahedral
[CuL(Ac) <sub>2</sub> (H <sub>2</sub> O) <sub>2</sub> ]	Dark Violet	90	520	>310	11.88 (12.31)	43.74 (46.18)	5.58 (5.43)	4.98 (5.39)	11.54 (12.33)	1.18	15.0	Octahedral
[ZnL(Ac) <sub>2</sub> ]	Dark Brown	80	485	>310	12.94 (13.40)	53.34 (51.31)	4.93 (5.68)	4.67 (5.44)	12.31 (12.45)	D	10.0	Tetrahedral
[ZrOL(NO <sub>3</sub> ) <sub>2</sub> ]	Slight Green	80	533	280	17.91 (17.07)	36.42 (37.21)	3.52 (3.86)	9.88 (10.21)	10.99 (11.69)	D	11.0	Square Pyramidal



**Table 1.23:** Characteristic infrared absorption frequencies ( $\text{cm}^{-1}$ ) of T2CDACH and its transition metal complexes

Complex	$\nu_{\text{H}_2\text{O}}$	$\nu_{\text{COO(asy)}}$	$\nu_{\text{C=N}}$	$\nu_{\text{COO(sy)}}$	$\nu_{\text{C=C}}$	$\nu_{\text{C-S}}$	$\nu_{\text{M-O}}$	$\nu_{\text{M-N}}$
T2CDACH (L)	-	-	1627	-	1508	1128	-	-
[MnL(Ac) <sub>2</sub> (H <sub>2</sub> O) <sub>2</sub> ]	3387(br)	1715	1621	1588	1510	1127	698	521
[NiL(Ac) <sub>2</sub> (H <sub>2</sub> O) <sub>2</sub> ]	3442(br)	1698	1624	1547	1501	1126	653	513
[CuL(Ac) <sub>2</sub> (H <sub>2</sub> O) <sub>2</sub> ]	3233(br)	1681	1622	1554	1508	1135	706	474
[ZnL(Ac) <sub>2</sub> ]	-	1709	1621	1590	1506	1127	661	503
[ZrOL(NO <sub>3</sub> ) <sub>2</sub> ]	-	-	1624	-	1529	1132	650	480



M= Mn(II), Ni(II), Cu(II)

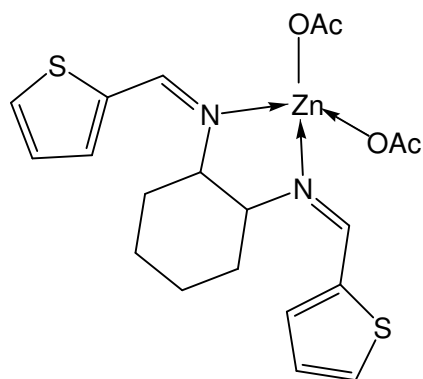


**Fig. 1.47:** Structures of transition metal complexes of T2CDACH

## SUMMARY

Seven novel sulphur containing Schiff bases were synthesized and characterized by different techniques like CHNS analysis and spectral studies such as UV-visible, FTIR, NMR and Mass spectroscopy. Five of them are thiadiazole based Schiff bases namely (E)-(N-anthracene-9-ylmethylene)-5-(4-nitrophenyl)-1,3,4-thiadiazol-2-amine (A9CNPTDA), N-(anthracen-9(10H)-ylidene)-5-(4-nitrophenyl)-1,3,4-thiadiazol-2-amine (ANNPTDA), (E)-5-(4-nitrophenyl)-N-((pyridine-2-yl)methylene)-1,3,4-thiadiazol-2-amine (P2CNPTDA), (E)-5-(4-nitrophenyl)-N-(1(pyridine-3-yl)ethylidene)-1,3,4-thiadiazol-2-amine (3APNPTDA) and (E)-5-(4-nitrophenyl)-N-(1(pyridin-2-yl)ethylidene)-1,3,4-thiadiazol-2-amine (2APNPTDA). Two of them are indole/ thiophene derivatives, N-((1H-indol-3-yl)methylene)thiazol-2-amine (I3A2AT) and (13E)-N1,N2-bis((thiophene-2-yl)methylene)cyclohexane-1,2-diamine (T2CDACH). Thiadiazole based Schiff bases were synthesized in two steps. First step is the synthesis of parent amine 5-(4-nitrophenyl)-1,3,4-thiadiazol-2-amine (NPTDA) followed by condensation reaction with corresponding carbonyl compounds. The chelating abilities of these 'S' containing Schiff bases were investigated by synthesizing a number of transition metal complexes. Then these complexes were also subjected to characterization studies by CHNS analysis, magnetic moment measurements, molar conductance studies different and spectral analysis. All the results are detailed and well discussed in this part.

Two polynuclear 'S' containing Schiff bases (E)-(N-anthracene-9-ylmethylene)-5-(4-nitrophenyl)-1,3,4-thiadiazol-2-amine (A9CNPTDA), N-(anthracen-9(10H)-ylidene)-5-(4-nitrophenyl)-1,3,4-thiadiazol-2-amine (ANNPTDA) were synthesized from 5-(4-nitrophenyl)-1,3,4-thiadiazole-2-amine (NPTDA) and polynuclear carbonyl compounds like anthracene-9-carbaldehyde and anthrone respectively. Transition metal

complexes of A9CNPTDA were prepared with Cr(III), Mn(II), Fe(III), Co(II), Ni(II), Cu(II), Zn(II) and ZrO(II) ions. 1:1 stoichiometry was found to exist between the metal and ligand in all the complexes of A9CNPTDA. The Cr(III) and Mn(II) chelates were found to have octahedral geometry. In the case of iron, cobalt, nickel and copper complexes a distorted octahedral geometry were fixed. Diamagnetic character was found for Zn(II) and ZrO(II) complexes in the magnetic studies and tetrahedral and square pyramidal geometry respectively were assigned for them. The studies establish that this polynuclear Schiff base A9CNPTDA is acting as a zerovalent bidentate ligand in the metal complexes having the active probes like highly polarisable 'S' atom of thiadiazole ring and azomethine nitrogen for coordination. The nonelectrolytic nature of these complexes was confirmed by molar conductance studies. The presence of coordinated water molecule was established from IR studies, by the presence of broad bands in the range 3340-3400cm<sup>-1</sup>.

The complexing ability of another polynuclear Schiff base ANNPTDA which is derived from NPTDA and anthrone is explored with transition metal ions like Cr(III), Ni(II), Cu(II), Zn(II) and ZrO(II) ions. Various analytical techniques were employed to establish the structure and geometry. The metal content and CHNS analysis showed that all the complexes except Zn(II) and ZrO(II) possess 1:2 stoichiometry between metal ligand. Magnetic moment values and electronic spectra studies revealed that all the complexes except Zn(II) and ZrO(II) have octahedral geometry. Zn(II) complex has tetrahedral geometry and ZrO(II) hold square pyramidal structure. Spectral data also confirmed the geometry of the complexes

Three pyridine based thiadiazole derivatives of Schiff bases P2CNPTDA, 2APNPTDA and 3APNPTDA were synthesized from the coupling reactions between NPTDA and pyridine-2-carbaldehyde or 2-acetyl pyridine or 3-acetyl pyridine. The

chelating efficacy of these pyridine derivatives of Schiff bases were explored by synthesizing transition metal complexes. All the complexes of these Schiff bases were found to have 1:1 stoichiometry between the metal and ligand. Various spectral techniques established the exact coordination probes of these ligands. These ligands were bidentate in nature coordinating through azomethine group and nitrogen atom of pyridine moiety. Molar conductance data suggested that all the compounds were non-electrolytic in nature.

For nickel(II) and copper(II) complexes of P2CNPTDA, octahedral geometry were assigned according to their magnetic behaviour. Iron(III) chelate of P2CNPTDA was exhibiting distorted octahedral geometry. Tetrahedral geometry was assigned for both the zinc(II) and cadmium(II) complexes. Zirconium complexes of P2CNPTDA exhibit square pyramidal geometry. Transition metal complexes of 3APNPTDA were synthesized with Cr(III), Mn(II), Fe(II), Ni(II), Cu(II), Zn(II) and ZrO(II) ions and characterized by different analytical techniques. It was concluded that all the complexes of 3APNPTDA were of 1:1 stoichiometry between the ligand and metal ion. Cr(III), Mn(II), Fe(III), Ni(II) and Cu(II) complexes of 3APNPTDA obeyed octahedral geometry whereas Zn(II) and ZrO(II) complexes showed tetrahedral and square pyramidal geometry respectively. This Schiff base acted as a nonovent bidentate ligand during complexation. Six transition metal complexes of Schiff base 2APNPTDA were synthesized and characterized. It is shown from the investigations that this Schiff base behaved as neutral bidentate ligand in all complexes. Spectral and magnetic studies revealed that complexes of Cr(III), Co(II), Ni(II) and Cu(II) possess octahedral nature. For the zinc and zirconium complexes, diamagnetic nature was observed and tetrahedral and square pyramidal geometry were assigned respectively for them.

The chelating efficiency of imine I3A2AT derived from 2-aminothiazole and

indole-3-carbaldehyde was fair and six transition metal complexes were synthesized with Cr(III), Mn(II), Ni(II), Cu(II), Zn(II) and ZrO(II) ions and characterized. Octahedral geometry was shown by chromium, manganese, nickel and copper complexes, while tetrahedral and square pyramidal geometry was followed by zinc and zirconium complexes. It was found that all complexes of 13A2AT were of 1:1 stoichiometry. N-H peak appeared in the IR spectrum of 13A2AT was disappeared in all complexes which indicated that the 'N' atom was coordinated to metal atom, after deprotonation. The 'N' atom of indole ring and azomethine linkage participated in complexation which was confirmed by spectral analysis especially FTIR studies.

The metal chelates of the thiophene derivative of Schiff base T2CDACH were prepared and characterized using various analytical techniques. Metal complexes of Mn(II), Ni(II), and Cu(II) exhibited octahedral geometry. But Zn(II) and ZrO(II) complexes showed tetrahedral and square pyramidal geometry respectively. All the complexes of T2CDACH were found to be non-electrolytic in nature. The presence of coordinated water molecule was established from IR studies by the presence of a broad band at about  $3300\text{cm}^{-1}$ . The results obtained from elemental and metal content analysis are in match with the theoretical expectations, which along with spectral data confirm 1:1 stoichiometry between metal and ligand in these complexes. Based on the spectral analysis it is established that the Schiff base T2CDACH act as bidentate ligand towards chelation with transition metal ions, coordinating through nitrogen atoms of two azomethine moiety.

In short, seven potential novel 'S'containing Schiff base ligands derived from primary amines namely, 5-(4-nitrophenyl)-1,3,4-thiadiazol-2-amine, 2-aminothiazole and 1,2-diaminocyclo hexane with different carbonyl compounds such as anthracene-9-carbaldehyde, anthrone, pyridine-2-carbaldehyde or 2-acetyl pyridine, 3-acetyl pyridine,

indole-3-carbaldehyde and thiophene-2-carbaldehyde and their forty three transition metal chelates were synthesized and characterized using most modern analytical tools, which are further employed for evaluating their applications in biological and corrosion inhibition fields and discussed in subsequent parts.

## REFERENCES

- [1] A.T. Balaban, D.C. Oniciu, A.R. Katritzky, Aromaticity as a cornerstone of heterocyclic chemistry, *Chem. Rev.* 104 (2004) 2777–2812.
- [2] T.Y. Fonkui, M.I. Ikhile, D.T. Ndinteh, P.B. Njobeh, Microbial activity of some heterocyclic Schiff bases and metal complexes: A review, *Trop. J. Pharm. Res.* 17 (2018) 2507–2518.
- [3] M. Taha, M.T. Javid, S. Imran, M. Selvaraj, S. Chigurupati, H. Ullah, F. Rahim, F. Khan, J.I. Mohammad, K.M. Khan, Synthesis and study of the  $\alpha$ -amylase inhibitory potential of thiadiazole quinoline derivatives, *Bioorganic Chem.* 74 (2017) 179–186.
- [4] N. Siddiqui, S.B. Andalip, R. Ali, O. Afzal, M.J. Akhtar, B. Azad, R. Kumar, Antidepressant potential of nitrogen-containing heterocyclic moieties: an updated review, *J. Pharm. Bioallied Sci.* 3 (2011) 194–205.
- [5] X.-H. Yang, L. Xiang, X. Li, T.-T. Zhao, H. Zhang, W.-P. Zhou, X.-M. Wang, H.-B. Gong, H.-L. Zhu, Synthesis, biological evaluation, and molecular docking studies of 1,3,4-thiadiazol-2-amide derivatives as novel anticancer agents, *Bioorg. Med. Chem.* 20 (2012) 2789–2795.
- [6] Y. Vaishnav, D. Dewangan, S. Verma, A. Mishra, A.S. Thakur, P. Kashyap, S.K. Verma, PPAR gamma targeted molecular docking and synthesis of some new amide and urea substituted 1,3,4-thiadiazole derivative as antidiabetic compound, *J. Heterocycl. Chem.* 57 (2020) 2213–2224.
- [7] M. Harfenist, D.J. Heuser, C.T. Joyner, J.F. Batchelor, H.L. White, Selective inhibitors of monoamine oxidase. 3. Structure- activity relationship of tricyclics bearing imidazoline, oxadiazole, or tetrazole groups, *J. Med. Chem.* 39 (1996) 1857–1863.
- [8] L. Dong, B. Song, J. Wu, Z. Wu, Y. Zhu, X. Chen, D. Hu, Synthesis and antiviral activity of novel thioether derivatives containing 1,3,4-oxadiazole/thiadiazole and emodin moieties, *Phosphorus Sulfur Silicon Relat. Elem.* 191 (2016) 904–907.
- [9] P. Li, D. Hu, D. Xie, J. Chen, L. Jin, B. Song, Design, synthesis, and evaluation of new sulfone derivatives containing a 1,3,4-oxadiazole moiety as active antibacterial agents, *J. Agric. Food Chem.* 66 (2018) 3093–3100.



- [10] N.N. Farshori, M.R. Banday, A. Ahmad, A.U. Khan, A. Rauf, Synthesis, characterization, and in vitro antimicrobial activities of 5-alkenyl/hydroxyalkenyl-2-phenylamine-1,3,4-oxadiazoles and thiadiazoles, *Bioorg. Med. Chem. Lett.* 20 (2010) 1933–1938.
- [11] E. Palaska, G. Şahin, P. Kelicen, N.T. Durlu, G. Altinok, Synthesis and anti-inflammatory activity of 1-acylthiosemicarbazides, 1,3,4-oxadiazoles, 1,3,4-thiadiazoles and 1,2,4-triazole-3-thiones, *J. Med. Farm.* 57 (2002) 101–107.
- [12] V. Jatav, P. Mishra, S. Kashaw, J. Stables, CNS depressant and anticonvulsant activities of some novel 3-[5-substituted 1,3,4-thiadiazole-2-yl]-2-styryl quinazoline-4(3H)-ones, *Eur. J. Med. Chem.* 43 (2008) 1945–1954.
- [13] E.E. Oruç, S. Rollas, F. Kandemirli, N. Shvets, A.S. Dimoglo, 1,3,4-thiadiazole derivatives. Synthesis, structure elucidation, and structure- antituberculosis activity relationship investigation, *J. Med. Chem.* 47 (2004) 6760–6767.
- [14] Y. Hu, C.-Y. Li, X.-M. Wang, Y.-H. Yang, H.-L. Zhu, 1,3,4-Thiadiazole: synthesis, reactions and applications in medicinal, agricultural, and materials chemistry, *Chem. Rev.* 114 (2014) 5572–5610.
- [15] D.R. Kumar, M.S. Sayed, M.L. Baynosa, J.-J. Shim, 5-Amino-2-mercapto-1,3,4-thiadiazole coated nitrogen-doped-carbon sphere composite for the determination of phenolic compounds, *Microchem. J.* 105023 (2020) 1-11.
- [16] D. Seeliger, B.L. de Groot, Ligand docking and binding site analysis with PyMOL and Autodock/Vina, *J. Comput. Aided Mol. Des.* 24 (2010) 417–422.
- [17] A. Asan, S. Soylu, T. Kiyak, F. Yıldırım, S. Öztaş, N. Ancın, M. Kabasakaloğlu, Investigation on some Schiff bases as corrosion inhibitors for mild steel, *Corros. Sci.* 48 (2006) 3933–3944.
- [18] M. Gholivand, F. Ahmadi, E. Rafiee, A Novel Al(III)-Selective Electrochemical sensor based on N,N'-Bis(salicylidene)-1,2-phenylenediamine complexes, *Electroanal. Int. J. Devoted Fundam. Pract. Asp. Electroanal.* 18 (2006) 1620–1626.
- [19] W. Wróblewski, Z. Brzózka, D.M. Rudkevich, D.N. Reinhoudt, Nitrite-selective ISE based on uranyl salophen derivatives, *Sens. Actuators B Chem.* 37 (1996) 151–155.
- [20] M.R. Ganjali, F. Mizani, M. Salavati-Niasari, Novel monohydrogenphosphate sensor based on vanadyl salophen, *Anal. Chim. Acta.* 481 (2003) 85–90.

- [21] M. Shamsipur, S. Ershad, N. Samadi, A.R. Esmailbeig, R. Kia, A. Abdolmaleki, Polymeric membrane lanthanum (III)-selective electrode based on N, N'-Adipylbis (5-phenylazo salicylaldehyde hydrazone), *Electroanal. Int. J. Devoted Fundam. Pract. Asp. Electroanal.* 17 (2005) 1828–1834.
- [22] S. Yamada, Advancement in stereochemical aspects of Schiff base metal complexes, *Coord. Chem. Rev.* 190 (1999) 537–555.
- [23] I. Kostova, L. Saso, Advances in research of Schiff-base metal complexes as potent antioxidants, *Curr. Med. Chem.* 20 (2013) 4609–4632.
- [24] K. Mohammed Yusuff, N. Sridevi, C. Pearly Sebastian, Characterization and catalytic activity of polymer supported ruthenium Schiff base complexes towards catechol oxidation, 105 (2007) 997-1002.
- [25] K.K.M. Yusuff, R. Sreekala, Mixed ligand five coordinate cobalt(II) complexes of a polymer-bound schiff base derived from 2-aminobenzimidazole, *J. Polym. Sci. Part Polym. Chem.* 30 (1992) 2595–2599.
- [26] M.M. Abd-Elzaher, A.A. Labib, H.A. Mousa, S.A. Moustafa, M.M. Ali, A.A. El-Rashedy, Synthesis, anticancer activity and molecular docking study of Schiff base complexes containing thiazole moiety, *Beni-Suef Univ. J. Basic Appl. Sci.* 5 (2016) 85–96.
- [27] Y.N. Belokon, A.G. Bulychev, V.I. Maleev, M. North, I.L. Malfanov, N.S. Ikonnikov, Asymmetric synthesis of cyanohydrins catalysed by a potassium  $\Delta$ -bis[N-salicylidene-(R)-tryptophanato]cobaltate complex, *Mendeleev Commun.* 14 (2004) 249–250.
- [28] H.L. Singh, A.K. Varshney, Synthetic, structural, and biochemical studies of organotin(IV) with Schiff bases having nitrogen and sulphur donor ligands, *Bioinorg. Chem. Appl.* 206 (2006) 1–7.
- [29] N.K. Rao, M.R. Reddy, Studies on the synthesis, characterisation and antimicrobial activity of new Co(II), Ni(II) and Zn(II) complexes of Schiff base derived from ninhydrin and glycine, *Biol. Met.* 3 (1990) 19–23.
- [30] N. Raman, J.D. Raja, A. Sakthivel, Synthesis, spectral characterization of Schiff base transition metal complexes: DNA cleavage and antimicrobial activity studies, *J. Chem. Sci.* 119 (2007) 303–310.
- [31] A. Mishra, M. Soni, Synthesis, structural, and biological studies of some Schiff bases and their metal complexes, *Met.-Based Drugs.* 7 (2008) 1-12.

- [32] V. Badwaik, R. Deshmukh, A. Aswar, Transition metal complexes of a Schiff base: synthesis, characterization, and antibacterial studies, *J. Coord. Chem.* 62 (2009) 2037–2047.
- [33] G. Ceyhan, C. Celik, S. Uruş, I. Demirtaş, M. Elmastaş, M. Tümer, Antioxidant, electrochemical, thermal, antimicrobial and alkane oxidation properties of tridentate Schiff base ligands and their metal complexes, *Spectrochim. Acta. A. Mol. Biomol. Spectrosc.* 81 (2011) 184–198.
- [34] X. Zhang, C. Jiao, J. Wang, Q. Liu, R. Li, P. Yang, M. Zhang, Removal of uranium (VI) from aqueous solutions by magnetic Schiff base: kinetic and thermodynamic investigation, *Chem. Eng. J.* 198 (2012) 412–419.
- [35] A. Nagajothi, A. Kiruthika, S. Chitra, K. Parameswari, Fe(III) complexes with Schiff base ligands: synthesis, characterization, antimicrobial studies, *Res. J. Chem. Sci.* 3 (2013) 606–613.
- [36] P. Subramanian, M. Sakunthala, Antibacterial activities of new Schiff base metal complexes synthesised from 2-hydroxy-1-naphthaldehyde and 5-amino-1-naphthol, *World J. Pharm. Pharm. Sci.* 2 (2013) 2753–2764.
- [37] K. Joshi, A. Rojivadiya, J. Pandya, Synthesis and spectroscopic and antimicrobial studies of schiff base metal complexes derived from 2-hydroxy-3-methoxy-5-nitrobenzaldehyde, *Int. J. Inorg. Chem.* 2014 (2014) 1–8.
- [38] A. Pradhan, A. Kumar, A review: an overview on synthesis of some Schiff bases and their metal complexes with anti-microbial activity, *Chem. Process Eng. Res.* 35 (2015) 84–86.
- [39] S.S. Tajudeen, G. Kannappan, Schiff base–copper(II) complexes: synthesis, spectral studies and anti-tubercular and antimicrobial activity, *Indian J. Adv. Chem. Sci.* 4 (2016) 40–48.
- [40] A. Hameed, M. Al-Rashida, M. Uroos, S. Abid Ali, K.M. Khan, Schiff bases in medicinal chemistry: a patent review (2010–2015), *Expert Opin. Ther. Pat.* 27 (2017) 63–79.
- [41] L. Zhu, N. Chen, H. Li, F. Song, X. Zhu, Synthesis, characterization and biological activities of Schiff bases of 2-amino-5-mercapto-1,3,4-thiadiazole and their Mo (VI) complexes, *Huazhong Shifan Daxue Xuebao Ziranxueban.* 37 (2003) 499–502.

- [42] D.A. Laidler, D.J. Milner, Asymmetric synthesis of cyclopropane carboxylates: catalysis of diazoacetate reactions by copper (II) Schiff base complexes derived from  $\alpha$ -amino acids, *J. Organomet. Chem.* 270 (1984) 121–129.
- [43] B. Dash, P. Mahapatra, D. Panda, J. Pattnaik, Fungicidal activities and mass spectral studies of some schiff bases derived from p-hydroxybenzaldehyde and their derivatives, *Chem. Informationsdienst.* 16 (1985) 163-172.
- [44] N. Rao, P. Rao, G. Reddy, M. Ganorkar, Metal-chelates of a new physiologically active tridentate schiff-base, Council Scientific Industrial Research Publ & Info Directorate, New delhi, 1987.
- [45] B. Garg, R. Dixit, I. Das, Studies on the complexation behaviour of dehydroacetic acid-4-methyl-2-quinolyhydrazone with bivalent metal ions, in: *Proc. Indian Acad. Sci.-Chem. Sci.*, (1990) 497–502.
- [46] M.A. Ali, M. Tarafdar, Metal complexes of sulphur and nitrogen-containing ligands: complexes of s-benzylthiocarbamate and a Schiff base formed by its condensation with pyridine-2-carboxaldehyde, *J. Inorg. Nucl. Chem.* 39 (1977) 1785–1791.
- [47] A. Mishra, M. Khare, S. Gautam, Synthesis, physico-chemical characterization, and antibacterial studies of some bioactive Schiff bases and their metal chelates, *Synth. React. Inorg. Met.-Org. Chem.* 32 (2002) 1485–1500.
- [48] A. Jha, Y. Murthy, U. Sanyal, G. Durga, Rapid synthesis, characterization, anticancer and antimicrobial activity studies of substituted thiadiazoles and their dinucleating ligand metal complexes, *Med. Chem. Res.* 21 (2012) 2548–2556.
- [49] M.N. Uddin, D.A. Chowdhury, M.M. Rony, M.E. Halim, Metal complexes of Schiff bases derived from 2-thiophenecarboxaldehyde and mono/diamine as the antibacterial agents, *Mod. Chem.* 2 (2014) 6–13.
- [50] A.S. Abu-Khadra, R.S. Farag, A.E.-D.M. Abdel-Hady, others, Synthesis, characterization and antimicrobial activity of Schiff base (E)-N-(4-(2-hydroxy benzylideneamino) phenylsulfonyl) acetamide metal complexes, *Am. J. Anal. Chem.* 7 (2016) 233-245.
- [51] S. Karabasannavar, P. Allolli, I.N. Shaikh, B.M. Kalshetty, Synthesis, characterization and antimicrobial activity of some metal complexes derived from thiazole Schiff bases with in-vitro cytotoxicity and DNA cleavage studies, *Indian J. Pharm. Educ. Res.* 51 (2017) 490–501.

- [52] E. Yousif, A. Majeed, K. Al-Sammarrae, N. Salih, J. Salimon, B. Abdullah, Metal complexes of Schiff base: preparation, characterization and antibacterial activity, *Arab. J. Chem.* 10 (2017) 1639–1644.
- [53] J. Thomas, G. Parameswaran, Structural, thermoanalytical and antitumour studies of metal chelates of anthracene-9-carboxaldehyde thiosemicarbazone, *Asian J. Chem.* 14 (2002) 1354-1364.
- [54] A. Prakash, S. Ahmad, Synthesis and characterisation of Schiff base complexes with Ti(III), Cr(III) and Ni(II), *Orient. J. Chem.* 25 (2009) 1035-1040.
- [55] G.I. Devi, P. Sabu, P. Geetha, Thermal decomposition Kinetics and mechanism of Co(II), Ni(II), and Cu(II) complexes derived from Anthracene carboxaldehyde L-Tyrosine, *Res. J. Chem. Sci.* 2231 (2013) 606-614.
- [56] K. Shaju, K. Joby Thomas, K. Vidhya Thomas, P.R. Vinod, Comparative cyclic voltammetric studies of (s)-2-(anthracen-9-(10H)-ylideneamino)-3-phenyl propanoic acid and its Cu(II) complex, *J. Chem. Sci.* 7 (2018) 73-84.
- [57] N. Raman, A. Kulandaisamy, C. Thangaraja, P. Manisankar, S. Viswanathan, C. Vedhi, Synthesis, structural characterisation and electrochemical and antibacterial studies of Schiff base copper complexes, *Transit. Met. Chem.* 29 (2004) 129–135.
- [58] Y. Gupta, S. Agarwal, S. Madnawat, Synthesis, characterization and antimicrobial studies of some transition metal complexes of Schiff bases, *Res. J. Chem. Sci.* ISSN. 2231 (2012) 606-617.
- [59] K. Pothiraj, T. Baskaran, N. Raman, DNA interaction studies of  $d^9$  and  $d^{10}$  metal complexes having Schiff base and polypyridyl ligands, *J. Coord. Chem.* 65 (2012) 2110–2126.
- [60] A.A.R. Despaigne, F.B. Da Costa, O.E. Piro, E.E. Castellano, S.R. Louro, H. Beraldo, Complexation of 2-acetylpyridine-and 2-benzoylpyridine-derived hydrazones to copper(II) as an effective strategy for antimicrobial activity improvement, *Polyhedron.* 38 (2012) 285–290.
- [61] N.S. Gwaram, H.M. Ali, H. Khaledi, M.A. Abdulla, A.H.A. Hadi, T.K. Lin, C.L. Ching, C.L. Ooi, Antibacterial evaluation of some Schiff bases derived from 2-acetylpyridine and their metal complexes, *Molecules.* 17 (2012) 5952–5971.
- [62] M.M. Ibrahim, H.M. Ali, M.A. Abdullah, P. Hassandarvish, Acute toxicity and gastroprotective effect of the Schiff base ligand 1H-indole-3-ethylene-5-nitro salicylaldimine and its nickel(II) complex on ethanol induced gastric lesions in rats, *Molecules.* 17 (2012) 12449–12459.

- [63] F. Rahaman, B. Mruthyunjayaswamy, Synthesis, spectral characterization and biological activity studies of transition metal complexes of Schiff base ligand containing indole moiety, *Complex Met.* 1 (2014) 88–95.
- [64] K.T. Tadele, T.W. Tsega, Schiff bases and their metal complexes as potential anticancer candidates: A review of recent works, *Anti-Cancer Agents Med. Chem. Former. Curr. Med. Chem.-Anti-Cancer Agents.* 19 (2019) 1786–1795.
- [65] O.A. EL-Gammal, H. Alshater, H.A. El-Boraey, Schiff base metal complexes of 4-methyl-1H-indol-3-carbaldehyde derivative as a series of potential antioxidants and antimicrobial: Synthesis, spectroscopic characterization and 3D molecular modeling, *J. Mol. Struct.* 1195 (2019) 220–230.
- [66] W. Wendlandt, C. Chou, The thermal decomposition of metal complexes—XI: The hexamminechromium (III) complexes, *J. Inorg. Nucl. Chem.* 26 (1964) 943–949.
- [67] E. Kohn, D. Venezky, R. Rice, F. Ross, G. Asbury Sr, A new electrochemical recorder paper, Naval Research Lab Washington DC, 1952.
- [68] L. Coury, Conductance measurements Part I: theory, *Curr.* 18 (1999) 91–96.
- [69] G. Maret, K. Dransfeld, Biomolecules and polymers in high steady magnetic fields, in strong ultrastrong magn. fields their Appl., (1985) 143–204.
- [70] E. Yousif, A. Majeed, K. Al-Sammarae, N. Salih, J. Salimon, B. Abdullah, Metal complexes of Schiff base: preparation, characterization and antibacterial activity, *Arab. J. Chem.* 10 (2017) 1639–1644.
- [71] M. Tunçel, S. Serin, Synthesis and characterization of new azo-linked Schiff bases and their cobalt(II), copper(II) and nickel(II) complexes, *Transit. Met. Chem.* 31 (2006) 805–812.
- [72] A. Paul, K. Joby Thomas, C. Sini Varghese, R. Johnson, Evaluation on Structural and Thermoanalytical Properties of a Novel Heterocyclic Schiff Base Derived from 3-Formylindole and its Metal Chelates, *Chem. Sci. Rev. Lett.* 4(2015), 278-284.
- [73] N.H. Al-Shaalan, Synthesis, characterization and biological activities of Cu(II), Co(II), Mn(II), Fe(II), and UO<sub>2</sub>(VI) complexes with a new Schiff base hydrazone: O-Hydroxyacetophenone-7-chloro-4-quinoline hydrazone, *Molecules.* 16 (2011) 8629–8645.
- [74] L. Racanè, V. Tralić-Kulenović, D.W. Boykin, G. Karminski-Zamola, Synthesis of new cyano-substituted bis-benzothiazolylarylfurans and arylthiophenes, *Molecules.* 8 (2003) 342–348.

- [75] C. Alarcón-Payer, T. Pivetta, D. Choquesillo-Lazarte, J.M. González-Pérez, G. Crisponi, A. Castiñeiras, J. Niclós-Gutiérrez, Thiodiacetato-copper (II) chelates with or without N-heterocyclic donor ligands: molecular and/or crystal structures of [Cu(tda)]<sub>n</sub>, [Cu(tda)(Him)<sub>2</sub>(H<sub>2</sub>O)] and [Cu(tda)(5Mphen)]·2H<sub>2</sub>O (Him= imidazole, 5Mphen= 5-methyl-1,10-phenanthroline), *Inorganica Chim. Acta.* 358 (2005) 1918–1926.
- [76] P.S. Deshmukh, A. Yaul, J.N. Bhojane, A. Aswar, Synthesis, characterization and thermogravimetric studies of some metal complexes with N 2 O 2 Schiff base ligand, *World Appl Sci J.* 9 (2010) 1301–1305.
- [77] G.L. Parrilha, R.P. Vieira, A.P. Rebolledo, I.C. Mendes, L.M. Lima, E.J. Barreiro, O.E. Piro, E.E. Castellano, H. Beraldo, Binuclear zinc (II) complexes with the anti-inflammatory compounds salicylaldehyde semicarbazone and salicylaldehyde-4-chlorobenzoyl hydrazone (H2LASSBio-1064), *Polyhedron.* 30 (2011) 1891–1898.
- [78] S. Erdemir, Synthesis of novel chiral Schiff base and amino alcohol derivatives of calix[4]arene and chiral recognition properties, *J. Mol. Struct.* 1007 (2012) 235–241.